

REPUBLIQUE ALGERIENNE DEMOCRATIQUE ET POPULAIRE  
MINISTERE DE L'ENSEIGNEMENT SUPERIEUR  
ET DE LA RECHERCHE SCIENTIFIQUE



UNIVERSITE MSBY - JIJEL  
Faculté des Sciences Exactes et Informatique  
Département de Physique



N° d'ordre :

Série :

**Mémoire**

présenté pour obtenir le diplôme de

**Master en physique**

Option : Physique Théorique

par

Bouzeraib Yassine

Production of heavy neutrinos in HNM and left right  
symmetric model : at NLO and parton shower approximations

Soutenu le : 15/07/2021

**Devant le Jury :**

Président :	Kh. Nouicer	Prof.	Univ. Jijel
Rapporteur :	M. S. Zidi	MCA	Univ. Jijel
Examineur :	T. Boudjedaa	Prof.	Univ. Jijel



## Acknowledgments

بِسْمِ اللَّهِ الرَّحْمَنِ الرَّحِيمِ

Praise be to **ALLAH**, Lord of the worlds, and prayers and peace be upon **Muhammad**, the Messenger of **ALLAH**.

First of all, I thank almighty **ALLAH** for giving me the courage, the will and the strength to carry out this work.

My thanks go next to my supervisor, **Mohamed Sadek Zidi** for his help, precious advice, patience and availability, and above all for trusting me on this subject, it was been an honor for me to work with him.

I also express my sincere gratitude to all the members of the jury, **T. Boudjedaa** and **Kh. Nouicer** for the careful reading of my manuscript and for their interesting suggestion and precious advises.

I thank everyone who contributed to my educational journey from primary school to university.

I would like to express my gratitude to the whole members of the LPTH members (Laboratory of Theoretical Physics) and especially the professors **S. Haouat**, **N.Ferkous**, **A. Bounames**, **Z. Belghobsi** and all my undergraduate professors.

## Dedication

I dedicate this work to my **Mother**, who is stayed up and worked hard until I reached this level. My **Mother** which the Books and Volumes are not enough for thanking her, so how with a line or two!!

To my late **Father**, may **ALLAH** have mercy on him.

To my Dear sister **Leyla Bouzeraib**, which is my companion in my journey.

To all my friends, especially **Zohair, Mohammed, Oussama, Abdelali** and **Abdelwahab**.

# Contents

<b>1</b>	<b>General Introduction</b>	<b>1</b>
<b>2</b>	<b>Standard Model</b>	<b>5</b>
2.1	SM Particles and Interactions . . . . .	5
2.2	SM Gauge Group and Lagrangian . . . . .	6
2.3	Higgs Mechanism and Particles Masses . . . . .	7
2.4	Lagrangian of Interaction . . . . .	10
2.5	Feynman's Rules . . . . .	10
2.6	SM Successes and Problems . . . . .	12
<b>3</b>	<b>Heavy Neutrino Model</b>	<b>13</b>
3.1	Why Heavy Neutrino Model ? . . . . .	13
3.2	Types of Fermions Fields in QFT . . . . .	13
3.2.1	Dirac fermions . . . . .	14
3.2.2	Weyl fermions . . . . .	15
3.2.3	Majorana fermions . . . . .	16
3.3	Physics of Neutrinos . . . . .	17
3.3.1	Properties of neutrinos . . . . .	17
3.3.2	Neutrinos, massless or massive! . . . . .	18
3.3.3	Active and Sterile neutrino . . . . .	20
3.3.4	Neutrinos, Dirac or Majorana type ? . . . . .	21
3.4	Heavy Neutrino Model . . . . .	22
3.4.1	Neutrino mass generation and seesaw mechanism type-I . . . . .	22
3.4.2	HNM lagrangian . . . . .	24
3.4.3	Feynman's Rules . . . . .	25
<b>4</b>	<b>Left-Right Symmetric Model</b>	<b>27</b>
4.1	Why Left-Right Symmetric Model ? . . . . .	27
4.2	Model Gauge Group . . . . .	27
4.3	Left-Right Symmetric Model Lagrangian . . . . .	28
4.3.1	Gauge field lagrangian . . . . .	29
4.3.2	Fermionic field lagrangian . . . . .	29
4.3.3	Yukawa interaction lagrangian . . . . .	29
4.3.4	Scalar field lagrangian . . . . .	30
4.4	Spontaneous Symmetry Breaking . . . . .	30
4.4.1	Charged gauge bosons masses . . . . .	31
4.4.2	Neutral gauge bosons masses . . . . .	33
4.4.3	Fermions masses and mixings . . . . .	34
4.4.4	Neutrinos masses . . . . .	34
4.5	Feynman's Rules . . . . .	36
<b>5</b>	<b>Production of a Heavy Neutrinos at LO Order</b>	<b>37</b>
5.1	Calculation Tools of the Hadronic Cross Section . . . . .	37
5.1.1	Cross sections . . . . .	37
5.1.2	Kinematics . . . . .	39
5.1.3	Tools of automatic calculations . . . . .	40
5.2	Charged Current Processes . . . . .	41
5.2.1	Heavy Neutrino Model (Dirac type) . . . . .	41

5.2.2	Heavy Neutrino Model (Majorana type)	47
5.2.3	Left-Right Symmetric Model	49
5.2.4	Variation of the Cross Section in Term of Heavy Neutrino Mass	50
5.3	Neutral Current Processes	52
5.3.1	Heavy Neutrino Model	52
5.3.2	Left Right Symmetric Model	54
5.3.3	Variation of the Cross Section in Term of Heavy Neutrino Mass	55
5.4	Main Differences Between the Two Models	57
5.4.1	Differences in decay modes and rates	57
5.4.2	Differences between HNM and LRSM models	59
5.4.3	Differences between Dirac and Majorana types of neutrino	59
<b>6</b>	<b>Production of Heavy Neutrino at Higher Perturbative Orders</b>	<b>61</b>
6.1	Hadronic Cross Section and Factorization Theorem	61
6.2	NLO Corrections and Parton Shower	62
6.2.1	Born contribution	63
6.2.2	Higher Order (HO) corrections	63
6.2.3	Subtraction method	65
6.2.4	Why NLO?	66
6.2.5	Fixed order and non Fixed order	74
6.2.6	Parton Shower; Why ?	74
6.3	Differential distribution at fixed order and parton shower	75
6.3.1	Charged current process	75
6.3.2	Neutral current process	80
<b>7</b>	<b>General Conclusion</b>	<b>85</b>
	<b>Bibliography</b>	<b>87</b>

# General Introduction

---

Origin of things, what are they made of ? How do they interact with each other ? These questions have always been the preoccupation of mankind. Civilizations throughout history have always tried to give answers to these questions. Beginning with the ancient Greek philosophers and the idea that the four elements: earth, water, air, and fire are the basis of everything, passing through the Periodic Table of Antoine Lavoisier in 1789 up to our modern age and after a huge cultural heritage of the most accurate theories so far: **Standard Model (SM)** of particle physics.

The Standard Model of particles, which looks like the periodic table for fundamental particles. On the left, there are twelve fermions: six quarks and six leptons divided into three generations which made all baryonic matter. On the right, there are four force mediators. If we want to learn all fundamental particle interactions we would first have to know that the world we live in is governed by four forces. The strong, weak, electromagnetic and gravitational forces. We have a successful quantum description for three of these forces except the gravitation. For the later one, there is no a complete quantum theory able to describe it yet, because it is so weak, so it doesn't have a significant effect at the quantum level. After almost a hundred years of scientific progress, we can very accurately describe the other forces in terms of quantum field theories. These theories explain how particles interact with each other via these three forces. Each force is mediated by a force carrier or mediator, called gauge boson. The electromagnetic force is mediated by the photon  $\gamma$ , the weak force is mediated by the  $W$  and  $Z$  bosons and the strong force is mediated by the gluons  $g$  (8 gluons). Also, do not forget the Higgs boson, which indicates the existence of the Higgs field, which gives to particles their masses by a mechanism called the spontaneous symmetry breaking. The Standard Model is a non-abelian gauge theory, based on the symmetry group  $SU_C(3) \times SU_L(2) \times U_Y(1)$ , i.e. the lagrangian of these theory, that describes the particles and their interactions, is invariant under the previous groupe. The calculation in this theory (and gauge theories in general) might be very complicated, but fortunately the american physicist Richard Feynman came up with an ingenious way to simplify the calculations, where the particles and their interactions are represented by some graphs called Feynman diagrams.

The SM is not the ultimate theory of elementary particles. Despite its successes it has fundamental problems like the arbitrary parameters which cannot be predicted by the theory, the non unification of the strong force with the electroweak force and the absence of a neutrinos masses ... etc. To solve these problems or some of them, many extensions of the Standard Model have been proposed, which are called also beyond the standard model models (BSM)" [1]. Some of them focus on unifying the three fundamental forces together, others focus on the inclusion of the neutrinos masses to solve the neutrino mass problem, other models focus on the asymmetry of the parity under the electroweak interaction and other are more ambitious since they try to solve all the problems at one time (like string theory!). The most important trends of the extensions of the Standard Model can be summarized in the following directions:

- **Extention of gauge symmetry:** by adding a new sub-gauge groups to the SM gauge group (as LR Symmetric Model) or finding a theory based on larger gauge group which is broken spontaneously to the SM gauge group (as grand unification theories  $SO(10)$  and  $SU(5)$ ).
- **Extension of the Higgs sector:** There are many theoretical reasons to support the idea that SM with a simple Higgs sector is not the end of the story. SM has difficulty in explaining

the relatively light higgs mass (hierarchy problem and quadratic divergences). Therefore, theoretical physicists have suggested extensions of the Higgs sector to include at least two Higgs doublets, and perhaps singlets and/or triplet and other representations (like the Two Higgs Doublets model) [2].

- **Extention of matter content:** by adding new hypothetical fermions or gauge bosons as the Heavy Neutrinos or adding a new generation and so one.
- **Extention with flavor symmetry:** the main purpose of these theories is to solve the hierarchy problem and giving an explanation for the free parameters of SM (as Technicolor and models with Leptoquarks).
- **Extention of space time dimention (Extra-dimention):** by adding a new dimension or more to the space-time that we are living in as the Kaluza-Klein inspired theories and Randall-Sundrum model.
- **Extention of Lorentz Symmetriy:** These are the theories that we know as supersymmetric theories (as MSSM and NMSSM theories).
- **One dimension object:** like superstring theory.

We are interested in this study by the problem of absence of the neutrino mass in SM. Our understanding of the neutrino is essential and the fact that the neutrinos are massives providing the first experimental evidence for new physics beyond the SM. There are many theories that try to solve this problem among of them the two models that we will discuss in this work. (i) The Heavy Neutrino Model which is an effective theory based on adding three heavy neutrino to the standard model. (ii) The Left Right Symmetric Model which is an extension of SM by enlarging its gauge groupe to be CP symmetric. Heavy Neutrino Model belongs to the matter content extension category, we just add three right-handed chiral neutrinos terms to the SM lagrangian. This model is based on the SM gauge groupe wich is one of the simplest extentions of SM. LR Symmetric Model belongs to the gauge symmetry extension category, it is based on  $SU_L(2) \times SU_R(2) \times U_{B-L}(1) \times P$  gauge groupe and this kind of theories has more fundamental gauge structure than the other kinds of BSM theories, where it solves the problem of the parity asymmetry in weak interactions, their gauge groupe generators are physically meaningful compared to SM [3].

To compare experimental results with the prediction of the theoretical models, one needs to calculate the physical observable like the total cross section and deferential distribution the most precisely as possible. In this work, we focus on the Next to Leading Order (NLO) calculations matched (or not) to parton shower. The NLO calculation includes the quantum corrections to the physical observables by entering an extra factor of  $\alpha_s$  (the coupling constant of the strong force) to the hadronic cross sections. This requires to take all Feynman diagrams beyond the LO, which are classified as follows:

- Virtual corrections: include one-loop to the Born diagrams
- Real emission: are introduced to cancel the soft and collinear divergences of the one-loop diagrams. A real emission diagram is obtained by emitting an extra parton from the Born diagram.

The squared amplitude of the virtaul correction is obtained by interfacing the Born diagrams with one-loop diagrams. The calculation of the one-loop integral leads to ultraviolet and infrared divergences. The ultraviolet divergences can be handled by carrying out the renormalisation procedure which consist of the redefinition of the parameters and the field of the model to eliminate these divergences. The infrared divergences (soft and collinear) cancel with the real contribution, the



---

remaining are absorbed in the PDFs. We remind that the real contribution is obtained by squaring the sum of all the real emission amplitudes. Parton Shower (PS) is another method of higher order correction, it approximates higher-order real-emission corrections to the hard scattering by simulating the branching of a single external parton into two partons with high energy, each of these partons may either split into two partons with less energy. At very low energy, the emission of partons stops due to the confinement phenomenon and hadronization begins. Hadronization is the process of forming hadrons from quarks and gluons, this occurs when low energy partons confine themselves to form hadrons which are not stable so they decay in general. This approach (PS) gives a good simulation for what's happening on detectors. All computational simulations have been completed automatically by using some programs and calculation tools. Results, computational steps and the numerical simulations with the calculation tools that we used are explained in details in chapter 5.

We start this work in chapter 2 by providing a brief introduction for the most important points in SM. Also, we summarise the successes and failures of this theory, therefore the necessity of the BSM physics. In chapter 3, we discuss in general the neutrinos physics and we present the effective theory of Heavy Neutrino Model, where we study two classes of this model. In the first one, the neutrino are of Dirac type and in the second one the neutrinos are of Majorana type. In chapter 4, we present the Left Right Symmetric Model. In order to know the difference between the two models and which one of them gives the best description for nature, and also what the neutrino spinors should be Dirac or Majorana type? We study two types of interactions the charged and neutral current processes in all models in chapters 5 and 6. In chapter 5 we study those processes at the leading order (LO) on the three cases: HNM where the neutrino is Dirac type or Majorana type and LR Symmetric Model where the neutrino is Majorana type. In chapter 6, we study the processes for the same models at next-to-leading order (NLO) matched (or not) to parton shower (PS).



# Standard Model

The Standard Model (SM) of particle physics is a renormalisable quantum field theory which combines the Glashow-Weinberg-Salam theory of ElectroWeak interactions with QCD in one theory. It unifies two fundamental forces EM and Weak and describes the interaction of all elementary particles known in nature. We follow in this chapter the notation of the ref. [1].

## 2.1 SM Particles and Interactions

The SM describes the interaction of all known quarks, leptons and gauge bosons. The left-handed fermions are organised in doublets of the  $SU_L(2)$  gauge group, while the right-handed fermions being singlets:

$$\text{Quarks} \sim \begin{pmatrix} u \\ d \end{pmatrix}_L \quad \begin{pmatrix} c \\ s \end{pmatrix}_L \quad \begin{pmatrix} t \\ b \end{pmatrix}_L \quad u_R, d_R, c_R, \dots \quad (2.1)$$

$$\text{Leptons} \sim \begin{pmatrix} e \\ \nu_e \end{pmatrix}_L \quad \begin{pmatrix} \mu \\ \nu_\mu \end{pmatrix}_L \quad \begin{pmatrix} \tau \\ \nu_\tau \end{pmatrix}_L \quad e_R, \mu_R, \tau_R \quad (2.2)$$

the gauge bosons are :

- $\gamma$  is the EM mediator, it is massless.
- $W^\pm, Z$  are the weak interaction mediators, they are massive.
- $g$  the is the gluons, they are the strong force mediators, they are massless.
- $H$  is the Higgs boson, it is responsible for the generation of particle masses, it is massive.

Here's some quantum numbers associated to the SM particles:

particles	$Q$	$I$	$I_3$	$Y$	$L_e$	$L_\mu$	$L_\tau$	$B$
$e^-(e^+)$	$-1(+1)$	$1/2$	$-1/2(1/2)$	$-1(1)$	$1(-1)$	$0$	$0$	$0$
$\mu^-(\mu^+)$	$-1(1)$	$1/2$	$-1/2(1/2)$	$-1(1)$	$0$	$1(-1)$	$0$	$0$
$\tau^-(\tau^+)$	$-1(1)$	$1/2$	$-1/2(1/2)$	$-1$	$0$	$0$	$1(-1)$	$0$
$u(\bar{u})$	$2/3(-2/3)$	$1/2$	$1/2(-1/2)$	$1/3(-1/3)$	$0$	$0$	$0$	$1/3(-1/3)$
$d(\bar{d})$	$-1/3(1/3)$	$1/2$	$-1/2(1/2)$	$-1/3(1/3)$	$0$	$0$	$0$	$1/3(-1/3)$
$c(\bar{c})$	$2/3(-2/3)$	$1/2$	$1/2(-1/2)$	$1/3(-1/3)$	$0$	$0$	$0$	$1/3(-1/3)$
$s(\bar{s})$	$-1/3(1/3)$	$1/2$	$-1/2(1/2)$	$-1/3(1/3)$	$0$	$0$	$0$	$1/3(-1/3)$
$t(\bar{t})$	$2/3(-2/3)$	$1/2$	$1/2(-1/2)$	$1/3(-1/3)$	$0$	$0$	$0$	$1/3(-1/3)$
$b(\bar{b})$	$-1/3(1/3)$	$1/2$	$-1/2(1/2)$	$-1/3(1/3)$	$0$	$0$	$0$	$1/3(-1/3)$

Table 2.1: Some quantum numbers of SM fermions.

leptons	$Q$	$I$	$I_3$	$Y$
$e_L$	-1	1/2	-1/2	-1
$\nu_{eL}$	0	1/2	1/2	-1
$e_R$	-1	0	0	-2

Table 2.2: Left and right lepton fields quantum numbers.

quarks	$Q$	$I$	$I_3$	$Y$
$u_L$	2/3	1/2	1/2	1/3
$d_L$	-1/3	1/2	-1/2	1/3
$u_R$	2/3	0	0	4/3
$d_R$	-1/3	0	0	-2/3

Table 2.3: Left and right quark fields quantum numbers.

## 2.2 SM Gauge Group and Lagrangian

The Standard Model is a non-Abelian gauge theory based on the symmetry group  $SU_C(3) \times SU_L(2) \times U_Y(1)$ , where

- $SU_C(3)$  is the color group (strong interaction). There are 8 generators of this group which corresponds to Gell-Mann matrices. The quarks are embedded on the fundamental representation of this group (called  $\mathbf{3}$ ), while the eight gluons are embedded on a joint representation (called  $\mathbf{8}$ ).
- $SU_L(2) \times U_Y(1)$  is the electroweak interaction group.
  - $SU_L(2)$  is the isospin group (weak isospin). There are 3 generators of the group called isospin  $I_i$  with  $I_i = \frac{\sigma_i}{2}$  (where  $\sigma_i$  are the Pauli matrices). The gauge coupling associated to this group is denoted  $g$ .
  - $U_Y(1)$  is the hypercharge group. There are one generator of this group which is  $Y$ , the gauge coupling of this group is  $g'$ .
- The electric charge, the isospin and the hypercharge are related by the Nishijima relation:  $Q = I_3 + \frac{Y}{2}$ .

Because the color group  $SU_C(3)$  is added by hand to electroweak group  $SU_L(2) \times U_Y(1)$ , therefore the SM group does not unify the electromagnetism and weak force with the strong force, so in this chapter we will focus more on Glashow-Weinberg-Salam theory or "the Standard Model of ElectroWeak interaction".

The total lagrangian of the GWS contains the following terms:

$$\mathcal{L} = \mathcal{L}_F + \mathcal{L}_G + \mathcal{L}_\phi + \mathcal{L}_Y \quad (2.3)$$

with:

$$\begin{aligned} \mathcal{L}_F &= \bar{L}i\gamma_\mu D_\mu L + \bar{R}i\gamma_\mu D_\mu R & \mathcal{L}_G &= -\frac{1}{4}W_{\mu\nu}^i W_i^{\mu\nu} - \frac{1}{4}B_{\mu\nu}B^{\mu\nu} \\ \mathcal{L}_\phi &= (D_\mu\phi)^\dagger(D^\mu\phi) - \mathcal{V}(|\phi|^2) & \mathcal{L}_Y &= -G_e(\bar{L}\phi R + \bar{R}\bar{\phi}L + h.c.) \end{aligned} \quad (2.4)$$

where:

- $\mathcal{L}_F$  is the fermionic lagrangian.
- $\mathcal{L}_G$  is the gauge lagrangian.
- $\mathcal{L}_\phi$  is the scalar field lagrangian.
- $\mathcal{L}_Y$  is the Yukawa term.

and

- $W_i^{\mu\nu} = \partial_\mu W_\nu^i - \partial_\nu W_\mu^i + g\varepsilon_{ijk}W_\mu^iW_\nu^k$ .  $W_i^\mu$  are the 3 massless gauge fields of  $SU_L(2)$
- $B_{\mu\nu} = \partial_\mu B_\nu - \partial_\nu B_\mu$ .  $B_\mu$  is the massless gauge field of  $U_Y(1)$
- Covariant derivative acting on  $L$ :  $D_\mu = \partial_\mu - ig\frac{\vec{\sigma}}{2} \cdot \vec{W} + \frac{i}{2}g'B_\mu$
- Covariant derivative acting on  $R$ :  $D_\mu = \partial_\mu + ig'B_\mu$

We notice that those terms are invariant under the gauge group  $SU_L(2) \times U_Y(1)$ . We remaind that all the fermions and bosons fields masses are absent in the lagrangian (2.3), since adding such terms will violate gauge invariance (this called the weak bases). To go to the real world we need a mechanism which gives the particles their masses, that is the Higgs Mechanism.

## 2.3 Higgs Mechanism and Particles Masses

Since the process of generating particles masses in the two models that we will take in the next two chapters (Heavy Neutrino Model in chp.(3) and Left-Right symmetric Model in chp.(4)) is the same in the Standard Model. Therefore, we will discuss spontaneous symmetry breaking (SSB) extensively and the principle will remain the same in the rest models with some differences.

The Higgs mechanism is one of spontaneous symmetry breaking mechanisms in SM. It is the process by which particles and gauge bosons acquire masses. Prior to SSB, leptons, quarks and bosons are massless because their mass terms are not gauge invariant. This is solved by introducing a scalar complex field  $\phi$  in doublets form of group  $SU_L(2)$  with a non-zero vacuum expectation value vev, to gives the particles their mass.

$$\phi = \begin{pmatrix} \phi^+ \\ \phi^0 \end{pmatrix} = \frac{1}{\sqrt{2}} \begin{pmatrix} \phi^1 + i\phi^2 \\ \phi^3 - i\phi^4 \end{pmatrix} \quad (2.5)$$

where, the Higgs lagrangian is given by:

$$\mathcal{L}_\phi = (D_\mu\phi)^\dagger(D^\mu\phi) - \mathcal{V}(|\phi|^2) \quad (2.6)$$

with

$$D_\mu = \partial_\mu - ig\frac{\vec{\sigma}}{2} \cdot \vec{W}_\mu - ig'\frac{Y}{2}B_\mu \quad (2.7)$$

The Higgs potential takes the following form :

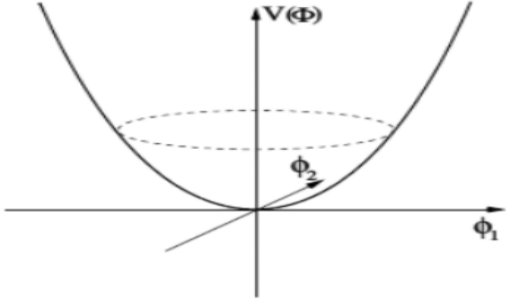
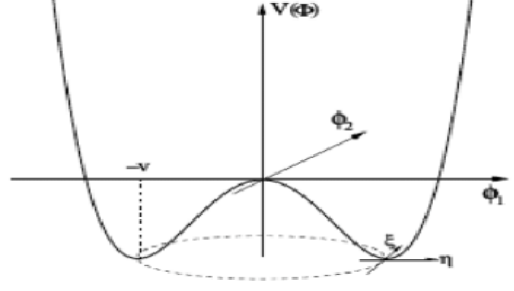
$$\mathcal{V}(|\phi|^2) = -\mu^2\phi^\dagger\phi + \lambda(\phi^\dagger\phi)^2 \quad (2.8)$$

where  $\mu, \lambda$  are real.

The lowest energy state is called vacuum expectation value (vev). It corresponds to the minimum of the potential  $\mathcal{V}$ , we can distinguish two cases:

- $\lambda > 0, \mu^2 > 0$   
in this case the solution which minimizes the potential is unique  $|\phi| = 0$ , therefore, there is no spontaneous symmetry breaking (see fig.(2.1)).
- $\lambda > 0, \mu^2 < 0$   
the solution that minimizes the potential is not unique (fig.(2.2)), it is given by

$$\phi^\dagger\phi = |\phi|^2 = \frac{v^2}{2} = -\frac{\mu^2}{2\lambda} \quad (2.9)$$

Figure 2.1: For  $\mu^2 > 0$ , no SSB (Wigner phase).Figure 2.2: For  $\mu^2 < 0$ , SSB (Nambu-Goldstone phase).

so, the mean value in the field is  $|\phi| = \frac{v}{\sqrt{2}} \Rightarrow \langle \phi \rangle_0 = \begin{pmatrix} 0 \\ \frac{v}{\sqrt{2}} \end{pmatrix}$ .

Now it is more convenient to write the scalar doublet in the form:

$$\phi = \begin{pmatrix} \phi^+ \\ \phi^0 \end{pmatrix} = \frac{1}{\sqrt{2}} \exp\left(\frac{i\sigma_i \xi_i}{2v}\right) \begin{pmatrix} 0 \\ v + H \end{pmatrix} \quad (2.10)$$

The fields  $\xi_i$  (for  $i = 1, 2, 3$ ) are the Goldstone bosons and  $H$  is the physical Higgs boson,  $v$  is the vev ( $v = 246 \text{ GeV}$ ). The mean values on the vacuum of the fields  $\xi_i$  and  $H$  are zero. The Goldstone bosons  $\xi_i$  will absorb the longitudinal components of the gauge bosons  $W$  and  $Z$ .

For going to the real world (mass bases), we introduce the following unitary gauge transformation:

$$\phi \rightarrow \phi' = \frac{1}{\sqrt{2}} \exp\left(\frac{-i\sigma_i \xi_i}{2v}\right) \exp\left(\frac{i\sigma_i \xi_i}{2v}\right) \begin{pmatrix} 0 \\ v + H \end{pmatrix} = \frac{1}{\sqrt{2}} \begin{pmatrix} 0 \\ v + H \end{pmatrix} \quad (2.11)$$

so we write now

$$(D^\mu \phi)' = \left[ \partial_\mu - ig \frac{\vec{\sigma}}{2} \cdot \vec{W}_\mu - ig' \frac{Y}{2} B_\mu \right] \frac{1}{\sqrt{2}} \begin{pmatrix} 0 \\ v + H \end{pmatrix} \quad (2.12)$$

but we have

$$\vec{\sigma} \cdot \vec{W}_\mu = \begin{pmatrix} W_\mu^3 & W_\mu^1 - iW_\mu^2 \\ W_\mu^1 + iW_\mu^2 & -W_\mu^3 \end{pmatrix} \quad (2.13)$$

so

$$(D^\mu \phi)' = \frac{1}{\sqrt{2}} \left( \partial_\mu - ig \frac{\sigma_3}{2} W_\mu^3 - ig' \frac{Y}{2} B_\mu \right) (v + H) \quad (2.14)$$

the kinetic term of the Higgs lagrangian is then:

$$\begin{aligned} (D_\mu \phi)'^+ (D^\mu \phi)' &= \frac{1}{2} (\partial_\mu H) (\partial^\mu H) + \frac{g^2}{8} (v + H)^2 (W_\mu^1 - iW_\mu^2) (W_\mu^1 + iW_\mu^2) \\ &\quad + \frac{g^2}{8} (v + H)^2 (g' B_\mu - W_\mu^3)^2 \end{aligned} \quad (2.15)$$

and the mass term for  $W_\mu^i$  bosons, is:

$$\frac{g^2}{8} v^2 (W_\mu^1 - iW_\mu^2) (W_\mu^1 + iW_\mu^2) + \frac{g^2}{8} v^2 (g' B_\mu - W_\mu^3)^2 \quad (2.16)$$

the charged gauge bosons are defined by:

$$W_{\mu}^{-} = \frac{W_{\mu}^1 + iW_{\mu}^2}{\sqrt{2}} \quad W_{\mu}^{+} = \frac{W_{\mu}^1 - iW_{\mu}^2}{\sqrt{2}} \quad (2.17)$$

we replace  $W^{\pm}$  in the equation (2.15) we get:

$$\left(\frac{g}{2}v\right)^2 W_{\mu}^{+} W_{\mu}^{-} + \frac{v^2}{8} (gW_{\mu}^3 - g'B_{\mu})^2 \quad (2.18)$$

the first term of the equation (2.18) gives the **mass of the charged bosons**:

$$m_{W^{\pm}} = \frac{g}{2}v. \quad (2.19)$$

The last term of equation (2.18) can be written as follows:

$$\frac{v^2}{8} (gW_{\mu}^3 - g'B_{\mu})^2 = \frac{1}{8}v^2 \begin{pmatrix} W_{\mu}^3 & B_{\mu} \end{pmatrix} \cdot \underbrace{\begin{pmatrix} g^2 & -gg' \\ -gg' & -g'^2 \end{pmatrix}}_M \cdot \begin{pmatrix} W_{\mu}^3 \\ B_{\mu} \end{pmatrix} \quad (2.20)$$

we can diagonalise this term by the following transformation:

$$\begin{pmatrix} Z_{\mu} \\ A_{\mu} \end{pmatrix} = \begin{pmatrix} \cos \theta_w & -\sin \theta_w \\ \sin \theta_w & \cos \theta_w \end{pmatrix} \cdot \begin{pmatrix} W_{\mu}^3 \\ B_{\mu} \end{pmatrix} \quad (2.21)$$

- where  $\theta_w$  is the Weinberg angle.

We get

$$\begin{aligned} \frac{v^2}{8} (gW_{\mu}^3 - g'B_{\mu})^2 &= \frac{1}{8}v^2 \begin{pmatrix} Z_{\mu} & A_{\mu} \end{pmatrix} \cdot \begin{pmatrix} g^2 + g'^2 & 0 \\ 0 & 0 \end{pmatrix} \cdot \begin{pmatrix} Z_{\mu} \\ A_{\mu} \end{pmatrix} \\ &= \frac{v^2}{8} (g^2 + g'^2) Z_{\mu} Z^{\mu} + 0 \times A_{\mu} A^{\mu} \end{aligned} \quad (2.22)$$

with

$$\cos \theta_w = \frac{g'}{\sqrt{g^2 + g'^2}} \quad \sin \theta_w = \frac{g}{\sqrt{g^2 + g'^2}} \quad \tan \theta_w = \frac{g'}{g} \quad (2.23)$$

therefore, the **mass of the photon**  $A_{\mu}$  remains **zero** and the **mass of the neutral gauge boson**  $Z_{\mu}$  is:

$$m_Z = \frac{1}{2}v\sqrt{g^2 + g'^2} \quad (2.24)$$

and the relation between the charged and the neutral gauge boson masses and the Weinberg angle is:

$$m_Z = \frac{m_{W^{\pm}}}{\cos \theta_w}. \quad (2.25)$$

The Higgs potential after spontaneous symmetry breaking gives the Higgs mass:

$$\mathcal{V}(\phi^{\dagger}\phi) \rightarrow -\frac{\mu^2 v}{4} + \frac{1}{2}(2\mu^2)H^2 + \lambda v H^3 + \frac{\lambda}{4}H^4 \quad (2.26)$$

so the **Higgs boson mass** is:

$$m_H = \sqrt{2\mu^2} \quad (2.27)$$

and the same thing for the fermions, when we break the symmetry spontaneously we get from Yukawa lagrangian their masses:

$$m_e = \frac{G_e v}{\sqrt{2}}. \quad (2.28)$$

## 2.4 Lagrangian of Interaction

When we break the symmetry spontaneously as we did in the previous section, in addition to the mass terms that we got, we get interaction of physical particles. There are two kinds of interactions of the fermions with the gauge bosons. The charged current and the neutral current interactions.

- **The charged current interaction:**

$$\mathcal{L}_{CC} = \frac{g}{\sqrt{2}}(J_\mu^- W^{-\mu} + J_\mu^+ W^{+\mu}) \quad (2.29)$$

where

$$\begin{aligned} - J_\mu^+ &= J_\mu^1 + iJ_\mu^2 = \frac{1}{2}\bar{\nu}_e\gamma_\mu(1 - \gamma_5)e \\ - J_\mu^- &= J_\mu^1 - iJ_\mu^2 = \frac{1}{2}\bar{e}\gamma_\mu(1 - \gamma_5)\nu_e \end{aligned}$$

- **The neutral current interaction:**

$$\begin{aligned} \mathcal{L}_{NC} &= g' \cos \theta_w J_\mu^{EM} A^\mu + \frac{g}{\cos \theta_w} (J_\mu^3 - \sin^2 \theta_w J_\mu^{EM}) \\ &= g' \cos \theta_w J_\mu^{EM} A^\mu + \frac{g}{\cos \theta_w} J_\mu^Z \end{aligned} \quad (2.30)$$

– where  $J_\mu^Z$  is explicitly written

$$J_\mu^Z = a_L^f \bar{f}_L \gamma_\mu f_L + a_R^f \bar{f}_R \gamma_\mu f_R + a_L^{f'} \bar{f}'_L \gamma_\mu f'_L + a_R^{f'} \bar{f}'_R \gamma_\mu f'_R \quad (2.31)$$

where

$$a_L^f = \frac{1}{2} - Q_f \sin^2 \theta_w \quad a_L^{f'} = -\frac{1}{2} - Q_{f'} \sin^2 \theta_w \quad (2.32)$$

$$a_R^f = -Q_f \sin^2 \theta_w \quad a_R^{f'} = -Q_{f'} \sin^2 \theta_w \quad (2.33)$$

where  $Q_f$ ,  $Q_{f'}$ , are electric charges of  $f$ ,  $f'$  (in the unit of  $e$ ), respectively, and  $J_\mu^{EM}$  given by:

$$J_\mu^{EM} = -\bar{e}_L \gamma_\mu e_L - \bar{e}_R \gamma_\mu e_R \quad (2.34)$$

## 2.5 Feynman's Rules

- **External fermions propagators**

External fermions propagators are given by:

entering fermion  $f$

$$\begin{array}{c} \longrightarrow \bullet \\ \text{p} \end{array} \quad u_l(p)$$

going out fermion  $f$

$$\begin{array}{c} \bullet \longrightarrow \\ \text{p} \end{array} \quad \bar{u}_l(p)$$



entering anti-fermion  $\bar{f}$


 $\bar{v}_l(p)$

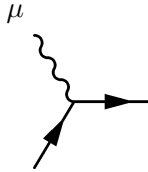
going out anti-fermion  $\bar{f}$


 $v_l(p)$

### • Feynman vertices

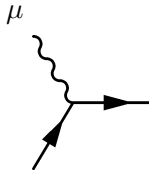
Since our focus was only on the ElectroWeak theory ( $GW_S$ ), we just give their vertices:

$l - \nu_l - W$  vertex



$$-i \frac{g}{\sqrt{2}} \gamma_\mu \frac{1 - \gamma_5}{2}$$

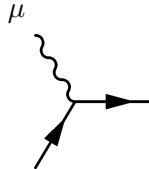
$u - d - W$  vertex (same generation)



$$-i \frac{g}{\sqrt{2}} \cos(\theta_C) \gamma_\mu \frac{1 - \gamma_5}{2}$$

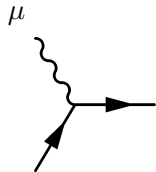
where  $\theta_C$  are Cabibo angeles.

$u - d - W$  vertex (different generations)



$$\mp i \frac{g}{\sqrt{2}} \sin(\theta_C) \gamma_\mu \frac{1 - \gamma_5}{2}$$

$f - f - Z$  vertex



$$\frac{-ie}{\sin(\theta_W) \cos(\theta_W)} \gamma_\mu \left[ a_L^f \frac{1 - \gamma_5}{2} + a_R^f \frac{1 + \gamma_5}{2} \right]$$

with

$$\begin{cases} a_L^f = -\frac{1}{2} + \sin^2(\theta_W) & a_R^f = \sin^2(\theta_W) & \text{For } f = e^-, \mu^-, \tau^- \\ a_L^f = \frac{1}{2} - \frac{2}{3} \sin^2(\theta_W) & a_R^f = -\frac{2}{3} \sin^2(\theta_W) & \text{For } f = u, c, t \\ a_L^f = -\frac{1}{2} + \frac{1}{3} \sin^2(\theta_W) & a_R^f = \frac{1}{3} \sin^2(\theta_W) & \text{For } f = d, s, b \end{cases}$$

$f - f - H$  vertex



$$-\frac{ie}{2 \sin(\theta_W)} \frac{m_f}{M_W}$$

incoming  $V = W, Z$  bosons

$$\underbrace{\text{~~~~~}}_k \bullet \text{ a, } \mu \quad \varepsilon_\mu^a(k)$$

## 2.6 SM Successes and Problems

Due to its experimental success, the SM is one of the most important theories in quantum physics. It predicts the presence of many particles before they are detected in many experiments like the Higgs boson, the  $W$  and  $Z$  bosons and the top quarks. It explains how the two forces Electromagnetism and Weak are unified ...etc. Here are some of it's successes:

- Unifies the weak force and Electromagnetic force in one of the most accurate theories, **ElectroWeak theories**.
- It predicted the existence of the  $W$  and  $Z$  bosons (discovered in 1983).
- Predicted the existence of the top quark. It was discovered in 1995. Its properties were experimented with the collider detector at Fermilab (CDF) and (Do).
- It predicted the existence of the **Higgs boson**  $H$  and it was discovered at LHC in 2012.

Despite the success of the SM, there are serious problems for which the SM does not give an answer to, we summarize it in several points:

- **Dark matter:** SM is not able to propose a candidate for dark matter.
- **The hierarchy problem:** SM can not explain the large difference between weak force and gravitational force.
- **Free parameters in the Standard Model:** there are 19 free parameters that we need to put in by hand.
- **Unification of fundamental forces:** SM does not unify all fundamental forces (it unifies only two fondamental forces from four (EM and Weak)).
- **Mass of Neutrinos:** Neutrinos in the SM are massless, but experiments show that neutrinos are massive [4].

This is what motivate us to search for models beyond the standard model which tries to give answers for these questions.

# Heavy Neutrino Model

In this chapter, we extend the SM by including three heavy neutrinos  $N_i$  (for  $i = 1, 2, 3$ ) where their masses are generated via the seesaw mechanics: type- $I$ . We will begin this chapter by giving some motivations for Heavy Neutrino Models (HNM). Then, we will discuss the inclusion of different fermion fields types in QFT. At next, we will give a brief review about neutrinos and their masses where we give the mass part of Lagrangian that will give for neutrinos their possible mass terms (Dirac or Majorana). Finally we give the new vertices that describe the interaction between the standard model particles (and bosons) and heavy neutrinos.

## 3.1 Why Heavy Neutrino Model ?

In the previous chapter, we discussed the success and failures of the SM and the necessity of having a model beyond it, to solve its problems. Among them is the absence of the neutrino mass. One of the simplest models that tries to solve this problem is Heavy Neutrino Model. Our motivation for this model can be summarized in the following three points:

- Their Lagrangian is one of the simplest extensions for the SM Lagrangian, we have just to add a Lagrangian for new right handed neutrinos that are singlet under the SM gauge group.
- It is based on the seesaw mechanism type- $I$ , which is one of the simplest and most popular ways to give to the neutrinos their masses.
- It explains the smallness of the neutrino mass even if we compared it with the electron mass.

### Overview of the model particles and interactions:

Fermions in HNM are organized as in the case of the Standard Model. However, because the neutrinos have masses we have to add three right-chiral singlets to the fields of the SM. So the fields in this model are given by:

$$Quarks \sim \begin{pmatrix} u \\ d \end{pmatrix}_L \quad \begin{pmatrix} c \\ s \end{pmatrix}_L \quad \begin{pmatrix} t \\ b \end{pmatrix}_L \quad u_R, d_R, c_R \dots \quad (3.1)$$

$$Leptons \sim \begin{pmatrix} e \\ \nu_e \end{pmatrix}_L \quad \begin{pmatrix} \mu \\ \nu_\mu \end{pmatrix}_L \quad \begin{pmatrix} \tau \\ \nu_\tau \end{pmatrix}_L \quad e_R, \mu_R, \tau_R, \nu_{eR}, \nu_{\mu R}, \nu_{\tau R} \quad (3.2)$$

where the gauge bosons are the same of the Standard Model. We mention that the new right-chiral singlets are massive. They are half-integer spin particles and they participate only in the weak interactions. In the following tables, we give the isospin, the electric charge and hypercharge of the particles of HNM.

## 3.2 Types of Fermions Fields in QFT

Fermions are particles which follow the Fermi-Dirac statistics and generally has half-integer spin and obey the Pauli exclusion principle, they can be massive or massless. Mathematically, fermions fields come in three types (Dirac, Weyl and Majorana). We give a brief definition for this types, because we will need it later when we discuss the possible neutrinos types.

leptons	$Q$	$I$	$I_3$	$Y$
$e_L$	-1	1/2	-1/2	-1
$\nu_{eL}$	0	1/2	1/2	-1
$e_R$	-1	0	0	-2
$\nu_{eR}$	0	0	0	0

Table 3.1: Right and left leptons quantum numbers.

quarks	$Q$	$I$	$I_3$	$Y$
$u_L$	2/3	1/2	1/2	1/3
$d_L$	-1/3	1/2	-1/2	1/3
$u_R$	2/3	0	0	4/3
$d_R$	-1/3	0	0	-2/3

Table 3.2: Right and left quarks quantum numbers.

### 3.2.1 Dirac fermions

Dirac fermions can be massive (like the electron in SM) and massless (like neutrino in SM). All fermions in the standard model have distinct antiparticles, where the signs of additive quantum numbers (like  $Q$ ,  $I_3$ , ...) are opposite, hence all of them are Dirac fermions. The evolution of the Dirac fermions is controlled by the Dirac equation, which is given by:

$$(i\gamma^\mu \partial_\mu - m)\psi = 0. \quad (3.3)$$

where the free fermions wave function is a superposition of a plane waves, it is expressed in terms of Dirac spinor as follows:

$$\psi(x) = \int \frac{d^3p}{(2\pi)^3 2E_p} \sum_{s=1}^2 [u(p, s)a(p, s)e^{-ip \cdot x} + v(p, s)b^\dagger(p, s)e^{+ip \cdot x}] \quad (3.4)$$

where  $a(\vec{p}, s)$  and  $b^\dagger(\vec{p}, s)$  are the creation and annihilation operators of fermion (anti-fermion) states, which satisfy respectively:

$$\begin{aligned} a(p, s)|e^-(p, s) \rangle &= |0 \rangle & b(p, s)|e^+(p, s) \rangle &= |0 \rangle \\ a^\dagger(p, s)|0 \rangle &= |e^-(p, s) \rangle & b^\dagger(p, s)|0 \rangle &= |e^+(p, s) \rangle \end{aligned} \quad (3.5)$$

Here  $u(p, s)$  and  $v(p, s)$  are the Dirac spinors with four-momentum  $p$  in the spin state  $s$ . If we substitute the fermions wave function  $\psi$  into the Dirac equation, we get:

$$(\not{p} - m)u(p, s) = 0 \quad (\not{p} + m)v(p, s) = 0 \quad (3.6)$$

those spinors satisfied the projections:

$$\sum_s u(p, s)\bar{u}(p, s) = \not{p} + m \quad \sum_s v(p, s)\bar{v}(p, s) = \not{p} - m \quad (3.7)$$

from the equation (3.45) and the spinors sum (3.7), we obtains the Feynman propagator for the free Dirac field:

$$\langle 0|\mathcal{T}(\psi(x), \bar{\psi}(x'))|0 \rangle = i \int \frac{d^4k}{(2\pi)^4} \exp(-ik \cdot (x - x'))S_F(k) \quad (3.8)$$

where  $S_F(k)$  is the momentum space propagator, which is:

$$S_F(k) = \frac{1}{\not{k} - m + i\varepsilon} \quad (3.9)$$

for a particle at rest  $\vec{p} = 0$  we find

$$\left( i\gamma^0 \partial_t - m \right) \psi = (\gamma^0 E - m)\psi = 0 \quad (3.10)$$

the solutions are the four eigenspinors:

$$u = \begin{pmatrix} 1 \\ 0 \\ 0 \\ 0 \end{pmatrix} \quad \bar{u} = \begin{pmatrix} 0 \\ 1 \\ 0 \\ 0 \end{pmatrix} \quad v = \begin{pmatrix} 0 \\ 0 \\ 1 \\ 0 \end{pmatrix} \quad \bar{v} = \begin{pmatrix} 0 \\ 0 \\ 0 \\ 1 \end{pmatrix} \quad (3.11)$$

Then, the wave function of the four fermions are given by:

$$\psi_1 = \exp(-imt)u \quad \psi_2 = \exp(-imt)\bar{u} \quad \psi_3 = \exp(+imt)v \quad \psi_4 = \exp(+imt)\bar{v} \quad (3.12)$$

- There are four possible states, we would expect only two spin states for a spin 1/2 fermion (the other are associated to anti-fermions).
- Note also that the change of the sign in the exponents of the plane waves in the states  $\psi_3$  and  $\psi_4$  has an important physical meaning, the four solutions in the following equations describe two different spinstates with  $E = m$  (which represent the fermions), and two spin states with  $E = -m$  (which represent the anti-fermions).

Each Dirac fermion, has two chiralities:

$$\psi_L = P_L\psi \quad \psi_R = P_R\psi \quad (3.13)$$

with

$$P_L = \frac{1 - \gamma_5}{2} \quad P_R = \frac{1 + \gamma_5}{2} \quad (3.14)$$

where  $P_{L,R}^2 = P_{L,R}$ ,  $P_L.P_R = P_R.P_L = 0$  and  $P_{L,R}^\dagger = P_{R,L}$ . One can see  $\psi_L$  and  $\psi_R$  as two degrees of freedom with  $\psi = \psi_L + \psi_R$  [5].

We remind that, in the absence of interaction, the Dirac field lagrangian density is given by:

$$\mathcal{L}_D = \bar{\psi}(i \not{\partial} - m)\psi \quad (3.15)$$

where one can get the Dirac equation (the equation of evolution of the fermion field) from this lagrangian density by applying the Euler-Lagrange equations.

### 3.2.2 Weyl fermions

Weyl fermions are massless half odd integer spin particles, they are modeled by Weyl equation. When Dirac published his equation in 1928, a German mathematical physicist, Hermann Weyl published his equation in 1929 as a simplified version of the Dirac equation:

$$\sigma^\mu \partial_\mu \psi = 0 \quad \mu = 0, 1, 2, 3. \quad (3.16)$$

where  $\sigma^\mu = (I_2, \sigma_x, \sigma_y, \sigma_z)$  is a vector whose components are the  $2 \times 2$  identity matrix and the Pauli matrices and  $\psi$  is the wave-function of the Weyl spinors. It is clear that this equation (3.16) corresponds to a massless fermions.

The solutions of Weyl equation are the left- and right-chiral handed spinors, which are described by 2-component complex spinors that we give in the previous section. In the chiral representation, one can write

$$\psi = \begin{pmatrix} \psi_L \\ \psi_R \end{pmatrix} \Rightarrow \quad P_L\psi = \begin{pmatrix} \psi_L \\ 0 \end{pmatrix} \quad P_R\psi = \begin{pmatrix} 0 \\ \psi_R \end{pmatrix} \quad (3.17)$$

with

$$P_L = \frac{1 - \gamma_5}{2} = \begin{pmatrix} I & 0 \\ 0 & 0 \end{pmatrix} \quad P_R = \frac{1 + \gamma_5}{2} = \begin{pmatrix} 0 & 0 \\ 0 & I \end{pmatrix} \quad (3.18)$$

where  $\psi_{L,R}$  are the Weyl two-component fields.

Because of Weyl fermions are massless the  $L$  and the  $R$ -chiral component correspond to particles with negative and positive helicity ( $h = \pm\frac{1}{2}$ ). Which means that a single Weyl  $L$  field, for example, can be introduced independently of the other chirality, where its free lagrangian density is

$$\mathcal{L}_0 = \psi_L^\dagger i\bar{\sigma}^\mu \partial_\mu \psi_L \quad \bar{\sigma}^\mu = (I, -\vec{\sigma}) \quad (3.19)$$

which describes the physics of a free massless negative helicity particle and a positive helicity antiparticle.

- **Remark:** a Dirac fermion is equivalent to two Weyl fermions. The Lagrangian density for the free Dirac field can be written in terms of the Weyl fields as:

$$\mathcal{L}_D = \psi_L^\dagger i\bar{\sigma}^\mu \partial_\mu \psi_L + \psi_R^\dagger i\sigma^\mu \partial_\mu \psi_R - m(\psi_L^\dagger \psi_R + \psi_R^\dagger \psi_L) \quad (3.20)$$

and the free Dirac equation becomes,

$$i\bar{\sigma}^\mu \partial_\mu \psi_L - m\psi_R = 0 \quad i\sigma^\mu \partial_\mu \psi_R - m\psi_L = 0 \quad (3.21)$$

This tells us that a general field can be described by two Weyl fields: one left-chiral and one right-chiral, therefore, they can be seen as the building blocks for any fermion field [5].

### 3.2.3 Majorana fermions

In his famous 1937 article Majorana begins by refusing the hypothesis of the "Dirac sea", and more specifically the idea that any particle must have an antiparticle different from itself, which can be problematic, precisely, for neutral particles such as neutrino. Majorana immediately remarks on the fundamental law of Dirac's approach saying that "Dirac forgot a basic symmetry, the symmetry of the particle in relation with itself". The very elegant Majorana point of view consists in showing that one can deduce the Dirac equation from a more fundamental principle which is the **variational principle**. (For more details see the reference [6]).

In the modern form of Majorana equation we start from the Dirac equation, where we define complex Dirac-like matrices as the following:

$$\bar{\gamma}^0 = \sigma_2 \quad \bar{\gamma}^1 = \sigma_1 \otimes I_2 \quad \bar{\gamma}^2 = i\sigma_3 \otimes I_2 \quad \bar{\gamma}^3 = i\sigma_2 \otimes I_2 \quad (3.22)$$

here's the explicit form of those matrices:

$$\bar{\gamma}^0 = \begin{pmatrix} 0 & 0 & 0 & -i \\ 0 & 0 & -i & 0 \\ 0 & i & 0 & 0 \\ i & 0 & 0 & 0 \end{pmatrix} \quad \bar{\gamma}^1 = \begin{pmatrix} 0 & 0 & i & 0 \\ 0 & 0 & 0 & i \\ i & 0 & 0 & 0 \\ 0 & i & 0 & 0 \end{pmatrix} \quad (3.23)$$

$$\bar{\gamma}^2 = \begin{pmatrix} i & 0 & 0 & 0 \\ 0 & i & 0 & 0 \\ 0 & 0 & -i & 0 \\ i & 0 & 0 & -i \end{pmatrix} \quad \bar{\gamma}^3 = \begin{pmatrix} 0 & 0 & 0 & -i \\ 0 & 0 & i & 0 \\ 0 & i & 0 & 0 \\ -i & 0 & 0 & 0 \end{pmatrix} \quad (3.24)$$

Let's rewrite the Dirac equation in (3.3) in terms of the new matrices, we get

$$(i\bar{\gamma}^\mu \partial_\mu - m)\psi = 0 \quad \Rightarrow \quad (i\bar{\partial}_\mu - m)\psi = 0 \quad (3.25)$$

this equation becomes real and only admits real solutions, which corresponds to particles which are their own antiparticles, and the spinors of **the fermions in this case are the same for their own antiparticles**  $u = v$  and  $\bar{u} = \bar{v}$ . It should therefore be noted that the leptonic number has

been violated in processes in which Majorana fermions are involved because of the property that the particles are their own antiparticles, so a process like  $n \rightarrow p + e^- + \nu_{e^-}$  is allowed.

We remind that, in the absence of interaction, the Majorana field lagrangian density is given

$$\begin{aligned} \mathcal{L}_M &= \bar{\psi}(i\bar{\gamma}^\mu\partial_\mu - m)\psi \\ \Rightarrow \mathcal{L}_M &= \bar{\psi}(i\partial_\mu - m)\psi \quad \text{or} \quad \mathcal{L}_M = \bar{\psi}_L(i\partial_\mu)\psi_L - \frac{1}{2}(m\bar{\psi}_L^c\psi_L + h.c) \end{aligned} \quad (3.26)$$

with  $\psi = \psi_L + C\bar{\psi}_L^T$  and  $\psi^c = \psi_L + \psi_L^c$ , where one can get the Majorana equation (the equation of evolution of the fermion field) from this lagrangian density by applying the Euler-Lagrange equations.

### Propagator for Majorana fermions

For free Dirac fields the leptonic numbers are conserved, therefore there is only a single type of propagator. But for Majorana neutrinos, the leptonic numbers are not conserved, so there are three non-zero propagators:

$$\begin{aligned} \langle 0|\mathcal{T}(\psi(x), \bar{\psi}(x'))|0\rangle &= i \int \frac{d^4k}{(2\pi)^4} \exp(-ik \cdot (x - x')) S_F(k) \\ \langle 0|\mathcal{T}(\psi(x), \bar{\psi}(x'))|0\rangle &= i \int \frac{d^4k}{(2\pi)^4} \exp(-ik \cdot (x - x')) C^\dagger S_F(k) \end{aligned} \quad (3.27)$$

$$\langle 0|\mathcal{T}(\psi(x), \bar{\psi}(x'))|0\rangle = i \int \frac{d^4k}{(2\pi)^4} \exp(-ik \cdot (x - x')) S_F(k)(-C) \quad (3.28)$$

where  $S_F(k) = \frac{1}{\not{k} - m + i\epsilon}$  is the momentum space propagator.

- The first Majorana propagator is analogous to the Dirac case.
- The second and third can be thought of as annihilating or creating two neutrinos, respectively [5]. So, we can find processes where the leptonic number is violated by  $\Delta l = \pm 2$ .

## 3.3 Physics of Neutrinos

### 3.3.1 Properties of neutrinos

Neutrinos are spin-half, electrically neutral particles. They participate only in gravitational and weak interactions. They are introduced by Pauli in 1930 to explain the energy crisis that had plagued the understanding of *beta*-decay process since the time of their discovery. Soon after Pauli's suggestion, Fermi wrote down the Hamiltonian describing the interactions of the neutrino with other elementary particles required to explain the nuclear *beta*-decay observations (Fermi theory). After that, physics of neutrino became an active domain of research. Today we are sure that neutrinos exist, they are produced everywhere naturally: in stars, supernovae, coming from Big Bang, generated in gamma ray bursts and in cosmic ray interactions in the atmosphere. After development of technology, we can now easily produce and detect neutrinos in the laboratory and particles accelerators in huge numbers. Also, we know that neutrinos are massive (Super-Kamiokanda Neutrino Detection Experiment" [7]).

Finally, we must remark that the neutrinos comes in three different types or generations according to the lepton they are produced with, so if the neutrino produced with an electron  $e^-$  the neutrino is an "electron-neutrino  $\nu_{e^-}$ " ( $\dots + \nu_{e^-} \rightarrow e^- + \dots$ ), if the neutrino produced with a muon  $\mu^-$  the neutrino is a "muon-neutrino  $\nu_{\mu^-}$ " ( $\dots + \nu_{\mu^-} \rightarrow \mu^- + \dots$ ), and the same for  $\tau^-$  the neutrino that produced with it is a "tau-neutrino  $\nu_{\tau^-}$ " ( $\dots + \tau^- \rightarrow \dots + \nu_{\tau^-}$ ).

### 3.3.2 Neutrinos, massless or massive!

At the time when Pauli postulated the neutrino existence and for almost half a century after that, most people believed that neutrinos were massless particles. This feature was embodied in the construction of the SM of the electroweak interactions. However, recent neutrino experiments and neutrino oscillations data strongly suggest that neutrinos have finite mass, much smaller than any known fermion even the electron (see fig.(5.1)). The neutrino mass searches can be divided into two categories:

- **Direct laboratory searches:**

We give one direct research experiment which predicts that the neutrino has a mass. It is the process of neutrinoless double *beta*-decay (denoted  $\beta\beta 0\nu$ )<sup>1</sup>. In this process a nucleus  $X_Z^A$  decays into a daughter nucleus  $X_{Z+2}^A + 2e^-$  without any accompanying neutrinos and can go only if the neutrino is its own anti-particle (the case of Majorana fermion). This stringent limit on a parameter, which we call (effective electron neutrino mass)  $m_{\nu_e}$  is  $0.2eV$ . The experimental value of this parameter has been found by the Heidelberg-Moscow collaboration using enriched Germanium  $Ge$  in an underground experiment at Gran Sasso, Italy.

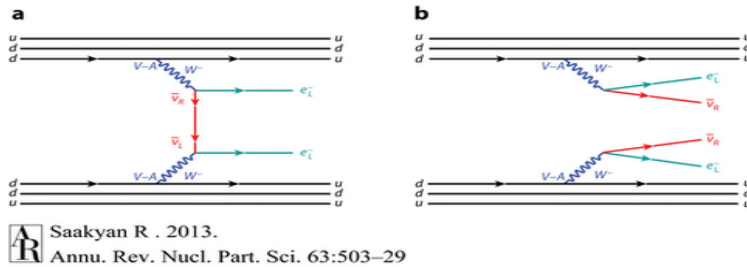


Figure 3.1: Double beta decay with and without neutrinos: (a)  $2n \rightarrow 2p + 2e^-$  and (b)  $2n \rightarrow 2p + 2e^- + 2\bar{\nu}$

- **Indirect searches involving neutrinos oscillations:**

The best way to look for neutrino mass until now is to realize that a neutrino produced in a weak-interaction process is actually superposition of several states (at least two of the mass states are not zero). We know from quantum mechanics that a particle changing its state must have a mass. We will call the state produced in a weak process (the types that we measure or generations) a weak eigenstate,  $\nu_l$  with  $l = e^-, \mu^-, \tau^-$ . If we denote a mass eigenstate as  $\nu_i$  with mass  $m_i$  ( $i = 1, 2, 3$ ), then the state  $\nu_l$  produced in the weak process at  $t = 0$  is

$$|\nu_l\rangle = \sum_i U_{li} |\nu_i\rangle \quad (3.29)$$

where  $U$  is a unitary matrix similar to the quark mixing matrices.

We assume that the 3-momentum  $p$  of the different components in the beam are the same. However, we consider their masses are different, the energies of all these components cannot be equal for the component  $\nu_i$ , the energy is given by the relativistic energy-momentum relation  $E_i = \sqrt{p^2 + m_i^2}$ , after a time  $t$ , the evolution of the initial state is given by:

$$|\nu_l(t)\rangle = \sum_i \exp(-i E_i t) U_{li} |\nu_{l0}\rangle \quad (3.30)$$

<sup>1</sup>The double beta decay is the decay of two neutrons simultaneously. In the standard model, this process must be accompanied with the emission of two anti-neutrinos (denoted  $\beta\beta 2\nu$ ), which was observed in many experiments. Many physicists suggest that the double beta decay might happen without the emission of neutrinos which implies somehow that neutrinos are of Majorana type.



By writing this we are assuming that the neutrino state  $\nu_i$  are stable. Since all  $E$ 's are not equal if the masses are not, the last equation represent a different superposition of the physical eigenstates  $\nu_i$  compared to equation (3.30). In general, this state has the properties of a  $\nu_l$  and other flavor states. The amplitude of finding  $\nu_{l'}$  in the original  $\nu_l$  beam is :

$$\begin{aligned} \langle \nu_{l'} | \nu_l(t) \rangle &= \sum_{i,j} \langle \nu_j | U_{jl'}^\dagger \exp(-i E_i t) U_{li} | \nu_i \rangle \\ &= \sum_i \exp(-i E_i t) U_{li} U_{l'i}^* \end{aligned} \quad (3.31)$$

If we use the fact that the mass eigenstates are orthonormal. The probability of finding a  $\nu_{l'}$  in an originally  $\nu_l$  beam at time =  $t$  is:

$$P_{\nu_{l'}\nu_l}(t) = | \langle \nu_{l'} | \nu_l(t) \rangle |^2 = \sum_{i,j} U_{li} U_{l'i}^* U_{lj} U_{l'j}^* \exp(-i(E_i - E_j)t). \quad (3.32)$$

To simplified this equation, we use the exponential representation for a complex numbers:  $z = |z| \exp(i \text{Arg}(z))$

$$P_{\nu_{l'}\nu_l}(t) = \sum_{i,j} U_{li} U_{l'i}^* U_{lj} U_{l'j}^* \exp(-i(E_i - E_j)t) \quad (3.33)$$

$$\begin{aligned} &= |U_{li} U_{l'i}^* U_{lj} U_{l'j}^*| \exp(i \text{Arg}(U_{li} U_{l'i}^* U_{lj} U_{l'j}^*)) \exp(-i(E_i - E_j)t) \\ P_{\nu_{l'}\nu_l}(t) &= \sum_{i,j} \overbrace{|U_{li} U_{l'i}^* U_{lj} U_{l'j}^*|}^{\text{Arg}(U_{li} U_{l'i}^* U_{lj} U_{l'j}^*)} \exp(-i(E_i - E_j)t) \\ &= \sum_{i,j} |U_{li} U_{l'i}^* U_{lj} U_{l'j}^*| \exp(i \text{Arg}(U_{li} U_{l'i}^* U_{lj} U_{l'j}^*)) \exp(-i(E_i - E_j)t) \\ &= \sum_{i,j} |U_{li} U_{l'i}^* U_{lj} U_{l'j}^*| (\cos((E_i - E_j)t) - \varphi_{ll'ij}) \end{aligned} \quad (3.34)$$

$$(3.35)$$

where  $\varphi_{ll'ij} = \text{Arg}(U_{li} U_{l'i}^* U_{lj} U_{l'j}^*)$ . But neutrinos are extremely relativistic, then, we can approximate the energy-momentum relation as:

$$E_i = \sqrt{p^2 + m_i^2} = |p| \sqrt{1 + \frac{m_i^2}{p^2}} = |p| + \frac{m_i^2}{2p} \quad (3.36)$$

because  $m_i \ll p$ . If we replace  $t$  by the distance  $x$  traveled by the beam, and  $E_{i,j}$  by the last relation we get:

$$(E_i - E_j)t \simeq \left( \frac{m_i^2 - m_j^2}{2p} \right) x \quad \Rightarrow \quad \frac{2\pi (m_i^2 - m_j^2)x}{2\pi 2p} = \frac{2\pi (m_i^2 - m_j^2)x}{4p} = \frac{2\pi x}{L_{ij}} \quad (3.37)$$

where we put  $E = p$  and  $L_{ij} = \frac{4\pi E}{(m_i^2 - m_j^2)}$ , so

$$P_{\nu_{l'}\nu_l}(x) = | \langle \nu_{l'} | \nu_l(t) \rangle |^2 = \sum_{i,j} |U_{li} U_{l'i}^* U_{lj} U_{l'j}^*| \cos \left[ \frac{2\pi x}{L_{ij}} - \varphi_{ll'ij} \right]. \quad (3.38)$$

The quantities  $L_{ij}$  are called the oscillation lengths, which gives a distance scale over which the oscillation effects can be appreciable.

- Notice that if the distance  $x$  is an integral multiple of all  $L_{ij}$ , we obtain  $P_{\nu_{l'}\nu_l} = \delta_{ll'}$ , as in the original beam. But at distances where this condition is not fulfilled, we can see non-intuitive effects, which are searched for in experiments.

- An important point to note is that these experiments provide information only about squares of the mass difference and not about absolute masses. Therefore, we still need direct search experiments to complete the oscillation experiments.

Usually we use a simplified version of the formula (3.38), for two-neutrino case, it is given by:

$$P_{\nu_l \nu_l}(x) = \sin^2(2\theta) \sin^2\left(\frac{1.27\Delta m^2(eV^2) L(\text{meter})}{E(\text{MeV})}\right) \quad (3.39)$$

this formula provides a simple way to read off the mass differences squared's probed in a given experiment [3].

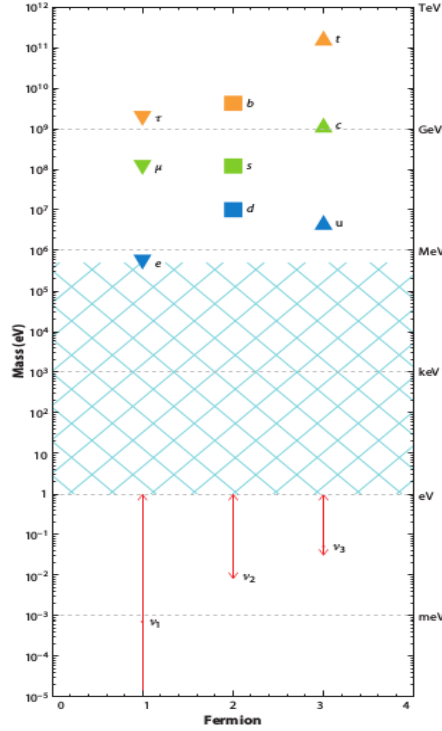


Figure 3.2: The Standard Model fermion masses. There are no known fermions in the blue-hatched mass region. The neutrino masses are not known; only the mass-squared differences are. The arrows indicate the allowed ranges for the neutrino masses, assuming a so-called normal mass ordering:  $m_3^2 > m_2^2 > m_1^2$ . [8]

### 3.3.3 Active and Sterile neutrino

Active neutrinos are the left-chiral doublet Weyl neutrinos, which transform as  $SU(2)$  doublets with a charged lepton partner. It is have normal weak interactions. So, the left electron doublet and its right-chiral partner are related by following CP transformation:

$$l_L = \begin{pmatrix} \nu_{eL} \\ e_L^- \end{pmatrix} \xrightarrow{CP} l_R = \begin{pmatrix} e_R^+ \\ \nu_{eR}^c \end{pmatrix} \quad (3.40)$$

where  $\psi_R^c = C\bar{\psi}_L^T$  is a field related by  $CP$  to  $\psi_L$

Sterile neutrinos are right-chiral singlet Weyl fermions under  $SU(2)$  gauge group. Those neutrinos do not interact in SM normal weak interactions, its interact except by mixing, Yukawa interactions, or beyond the SM (BSM) interactions [5]. So, the right-chiral electron singlet and its left-chiral partner are related by following CP transformation:

$$\nu_{eR} \xrightarrow{CP} \nu_{eL}^c \quad (3.41)$$

### 3.3.4 Neutrinos, Dirac or Majorana type ?

In this part, we will discuss the difference between Dirac and Majorana types of neutrinos. A Majorana neutrino is its own anti-particle, whereas a Dirac neutrino is not. This apparently simple difference between them which leads to a large number of profounds and distinguishing physical implications which can be used to test whether which the neutrino is, a Majorana or a Dirac fermion. Let's start from the fact that a particle has a mass must have a right-hand chiral part, so we take  $\nu$  as a four-component spinor and  $\nu_{L,R}$  as its left and right chiral projections. We can write the Dirac mass  $\mathcal{L}_{\mathcal{D}}$  term and the Majorana mass  $\mathcal{L}_{\mathcal{M}}$  term as follows (we had consider only one neutrino species for simplicity) [1]:

- The Dirac mass term:

$$\begin{aligned}\mathcal{L}_{\mathcal{D}} &= -m_D \bar{\nu} \nu \\ &= -m_D (\bar{\nu}_R \nu_L + \bar{\nu}_L \nu_R)\end{aligned}\quad (3.42)$$

- The Majoran mass term:

$$\mathcal{L}_{\mathcal{M}} = -\frac{1}{2} m_R \bar{\nu}_R^c \nu_R - \frac{1}{2} m_L \bar{\nu}_L^c \nu_L + h.c. \quad (3.43)$$

where  $m_D$  and  $m_{L,R}$  are arbitrary complex numbers (in general), and  $\bar{\nu}_{L,R}^c = \nu_{L,R}^T C^{-1}$  with  $C$  is the generalized charge conjugation operator.

We should pay attention to several points here:

- The first point is to remark that  $\mathcal{L}_{\mathcal{D}}$  is invariant under a global  $U(1)$  symmetry. This  $U(1)$  symmetry may be identified with the lepton number  $l$ , with  $L(\nu) = L(\bar{\nu}) = 1$ .
- On the other hand,  $\mathcal{L}_{\mathcal{M}}$  in the Lagrangian, it breaks the lepton number by two units ( $\Delta l = 2$ ). Therefore, in the presence of  $\mathcal{L}_{\mathcal{M}}$ , it should consist of monitoring processes in which the lepton number is violated, such as double  $\beta$  decay. So, observation of any such process will constitute strong evidence for the Majorana type of the neutrino.
- One can write the free field Majorana neutrino lagrangian density as:

$$\mathcal{L}_0 = \frac{1}{2} (\bar{\nu} i \not{\partial} \nu) + \mathcal{L}_{\mathcal{M}} \quad (3.44)$$

where the Majorana neutrino field is expressed as:

$$\nu_M(x) = \int \frac{d^3 p}{(2\pi)^3 2E_p} \sum_{s=1}^2 [u(p, s) a(p, s) e^{-ip \cdot x} + v(p, s) a^\dagger(p, s) e^{+ip \cdot x}] \quad (3.45)$$

So we conclude that: in process where the type of the neutrino is a Dirac type, the mass term of lagrangia conserved the leptonic number, but if it is violated, the type is a Majorana one.

In general, one can consider a model where both active and sterile neutrino are present. In this case, both Dirac and Majorana mass term should be taken into account. We write,

$$\mathcal{L}_{\nu_{mass}} = -\frac{1}{2} m_R \bar{\nu}_R^c \nu_R - \frac{1}{2} m_L \bar{\nu}_L^c \nu_L - m_D \bar{\nu}_R \nu_L + h.c. \quad (3.46)$$

In the matrix form, the previous equation can be written as,

$$\mathcal{L}_{\nu_{mass}} = -\frac{1}{2} \begin{pmatrix} \bar{\nu}_L^c & \nu_R \end{pmatrix} \cdot \underbrace{\begin{pmatrix} m_L & m_D \\ m_D & m_R \end{pmatrix}}_M \cdot \begin{pmatrix} \nu_L \\ \nu_R^c \end{pmatrix} + h.c. \quad (3.47)$$

where the property  $\overline{\nu_L}\nu_R = \overline{\nu_R^c}\nu_L^c$  has been used. (In this case,  $m_D$  can be chosen real by some redefining of phases). In general case, this matrix is a complex symmetric matrix (to be denoted henceforth by  $M$ ). There are several important special cases of the mixed model in equation (3.47):

- (i) **Dirac:** if  $m_L = m_R = 0$  and  $m_D \neq 0$  the mass of neutrino is a **Dirac mas**. There are two Dirac mass eigenstates, with the eigenvalues  $m^- = m_D$  and  $m^+ = -m_D$ .
- (ii) **Majoran:** if either  $m_L$  or  $m_R$  or both nonzero and  $m_D$  arbitrary, the mass of neutrino is **Majoran mass** case. The mass matrix  $M$  is diagonal  $m^- = m_L$  and  $m^+ = m_R$ .
- (iii) **Pseudo-Dirac:** there is a third case for mass called **Pseudo-Dirac** if  $m_D \neq 0$  and  $m_L = m_R \ll m_D$ . The mass term of Lagrangian in equation (3.30) becomes in this case:

$$\begin{aligned}\mathcal{L}_{\nu_{mass}} &= -\frac{1}{2}m_{L,R}(\overline{\nu_R^c}\nu_R + \overline{\nu_L^c}\nu_L) - m_D\overline{\nu_R}\nu_L + h.c. \\ &= -\frac{1}{2}m_{L,R}(\overline{\nu_L}\nu_R + \overline{\nu_R}\nu_L) - m_D\overline{\nu_R}\nu_L + h.c. \\ &= -m_R\overline{\nu_R}\nu_L - m_D\overline{\nu_R}\nu_L + h.c.\end{aligned}\quad (3.48)$$

where  $\nu_R^c = \nu_L$ , which seems like Dirac treme of mass [3].

- (iv) **Seesaw:** when the condition  $m_R \gg m_D$ ,  $m_L$  is satisfied (e.g  $m_L = 0$  and  $m_D = \Theta(m_u, m_e, m_d)$  and  $m_R = \Theta(M_X)$  where  $M_X \sim 14$  TeV). This is what known as the seesaw where the eigenstates and eigenvalues in the seesaw limit are:

$$\nu_{1L} \sim \nu_L - \frac{m_D}{m_R}\nu_L^c \Rightarrow \nu_{1L} \sim \nu_L - \frac{m_D}{m_R}\nu_R \quad (3.49)$$

$$\nu_{2L} \sim \frac{m_D}{m_R}\nu_L + \nu_L^c \Rightarrow \nu_{2L} \sim \frac{m_D}{m_R}\nu_L + \nu_R \quad (3.50)$$

$$(3.51)$$

and the mass eigenstate are:

$$m_1 \sim m_L - \frac{m_D^2}{m_R} \quad m_2 \sim m_R \quad (3.52)$$

we remark that  $m^- \ll m_D$  for  $m_L = 0$  and  $m^+ = m_R \gg m^-$  and this what suggests the terminology seesaw. Namely, when one eigenstate  $m^+$  gets heavy another eigenstate  $m^-$  becomes lighter.

- (iv) **Mixing:** In general case in which  $m_D$  and  $m_T$  (and/or  $m_R$ ) are both small and comparable leads to non-degenerate Majorana mass eigenvalues and significant ordinary-sterile ( $\nu_L$ - $\nu_R$ ) mixing [5].

## 3.4 Heavy Neutrino Model

### 3.4.1 Neutrino mass generation and seesaw mechanism type-I

The seesaw mechanism type  $I$  (inverse or linear) is the simplest mechanism for generating tiny neutrino masses. In this mechanism, we extend the Standard Model by assuming two or more additional right-handed neutrino fields  $\nu_{Ri}$ . While the neutrino type can be Dirac or Majorana we can write the most general formula of the seesaw type  $I$  Lagrangian [26] which contain the two possibilities as follow:

$$\mathcal{L}_{type-I} = \frac{i}{2}\overline{N_i^R}\not{\partial} - y_{i\alpha}\overline{N_i^R}\bar{\phi}^\dagger L_\alpha - \frac{1}{2}\overline{N_i^R}m_{Rij}(N_j^R)^c + h.c. \quad (3.53)$$

where  $L_\alpha = (\nu_\alpha, l_\alpha)$ ,  $y_{i\alpha}$  is Yukawa matrix, we used a more convenient notation ( $\nu_{Ri} = N_{Ri}$  which is the new heavy neutrino eigenstates to clarify the difference between them and the light eigenstates ones as we will discuss soon). We choose the case where  $N_{Ri}$  ( $i = 1, 2, 3$ ).

When we break the symmetry spontaneously as we did in the SM model, the seesaw mechanism type I lagrangian give us the following result:

$$\mathcal{L}_{type-I} \xrightarrow{SSB} \frac{i}{2} \overline{N_i^R} \not{\partial} \left[ (m_D)_{i\alpha} + y_{i\alpha} \phi_0 \right] N_i^R + y_{i\alpha} \phi + \overline{N_i^R} l_\alpha^L - \frac{1}{2} \overline{N_i^R} m_{Rij} (N_j^R)^c + h.c \quad (3.54)$$

where  $(m_D)_{i\alpha}$  is a matrix of complex masses and  $\phi_0$  contains the real SM Higgs boson. The Dirac and Majorana mass terms in the neutrino Lagrangian can be organized as follows by Autonne-Takagi factorization:

$$\mathcal{L}_{type-I} \rightarrow -\frac{1}{2} \left( \overline{(\nu_\alpha^L)^c} \quad \overline{(N_i^R)} \right)^T \cdot \underbrace{\begin{pmatrix} 0_{\alpha\beta} & (m_D^T)_{\alpha j} \\ (m_D)_{\beta i} & (m_R)_{ij} \end{pmatrix}}_M \cdot \begin{pmatrix} \nu_\beta^L \\ (N_j^R)^c \end{pmatrix} + h.c. \quad (3.55)$$

The total neutrino mass matrix therefore corresponds to a complex symmetric  $M$ :

$$M = \begin{pmatrix} 0_{\alpha\beta} & (m_D^T)_{\alpha j} \\ (m_D)_{\beta i} & (m_R)_{ij} \end{pmatrix} \quad \text{with two eigenvalues} \quad m_\pm = \frac{m_R \pm \sqrt{M_M^2 + 4m_D^2}}{2}$$

where we diagonalized the mass matrix by one unitary transformation:

$$L^\dagger \cdot \begin{pmatrix} 0_{\alpha\beta} & (m_D^T)_{\alpha j} \\ (m_D)_{\beta i} & (m_R)_{ij} \end{pmatrix} \cdot L = \begin{pmatrix} m^- & 0 \\ 0 & m^+ \end{pmatrix} \quad (3.56)$$

The eigenvalues of this mass matrix are (for  $m_R \gg m_D$ , this condition will satisfy the seesaw limit which gives us heavy right-handed neutrinos and light left-handed ones):

$$\begin{aligned} m^- &= \delta_{ij} m_i^\nu = -\frac{m_{Dik} (m_{Dkj})^T}{m_{Ri}} \Rightarrow m^- = -\frac{m_D^2}{m_R} \\ m^+ &= \delta_{\beta\alpha} m_{R\alpha} \Rightarrow m^+ = m_R \end{aligned} \quad (3.57)$$

where  $m^-$  are the **light neutrino mass eigenstates** and  $m^+$  are the **heavy neutrino mass eigenstates**.

- $M$  is the neutrinos mass matrix,  $M_D$  are the Dirac mass and  $M_R$  are the Majorana mass.
- The Majorana component  $M_R$  is order of GUT scale and its violates lepton number.
- The Dirac component  $M_D$  is very small and conserves lepton number.
- This mechanism explains the smallness of the active neutrino mass (Dirac type) and predict the existence of heavy neutrino of Majorana type, where the relation  $m^- \cdot m^+ = -m_D^2$  suggests the terminology seesaw. Namely, when one eigenstate  $m^+$  gets heavy another eigenstate  $m^-$  becomes lighter[1].

$L$  is a  $(3+3) \times (3+3)$  unitary matrix and can be parameterized as:

$$\begin{pmatrix} U_{3 \times 3} & V_{3 \times 3} \\ X_{3 \times 3} & Y_{3 \times 3} \end{pmatrix} \quad (3.58)$$

the relation between the gauge interaction eigenstates and the mass eigenstates are given by:

$$\begin{pmatrix} \nu_L \\ N_L^c \end{pmatrix} = L \cdot \begin{pmatrix} \nu_L \\ N_L^c \end{pmatrix}_m \quad (3.59)$$

with the mass eigenstates  $\nu_m = (m = 1, 2, 3)$ ,  $N_{m'}^c (m' = 1, 2, 3)$ , and the mixing relations between the gauge and mass eigenstates are:

$$\nu_{aL} = \sum_1^3 U_{am} \nu_{mL} + \sum_4^6 V_{am'} N_{m'L}^c \quad N_{bL}^c = \sum_1^3 X_{bm} \nu_{mL} + \sum_4^6 Y_{bm'} N_{m'L}^c \quad (3.60)$$

$$\nu_{aR}^c = \sum_1^3 U_{am}^* \nu_{mR}^c + \sum_4^6 V_{am'}^* N_{mR}^c \quad N_{bR}^c = \sum_1^3 X_{bm}^* \nu_{mR}^c + \sum_4^6 Y_{bm'}^* N_{mR}^c \quad (3.61)$$

- Note that the unitarity condition for  $L$  leads to the relations:

$$UU^\dagger + VV^\dagger = U^\dagger U + V^\dagger V = I_{3 \times 3} \quad XX^\dagger + YY^\dagger = X^\dagger X + Y^\dagger Y = I_{3 \times 3} \quad (3.62)$$

Parametrically:  $UU^\dagger, Y^\dagger Y \sim \Theta(1)$  and  $VV^\dagger, X^\dagger X \sim \Theta(m_\nu/m_N)$ [9].

### 3.4.2 HNM lagrangian

Heavy neutrino model based originally on seesaw mechanism type  $I$  (inverse or linear) which generated the neutrinos mass and explain their smallness as we discussed in the previous section. So this model based on the same gauge group of the Standard Model ( $SU(3)_C \times SU(2)_L \times U(1)_Y$ ), the Lagrangian in this model is: the Lagrangian of the Standard Model plus Lagrangian of the new right handed neutrinos that are singlet under the SM gauge group as we mentioned above.

Total Lagrangian is given in following:

$$\mathcal{L}_{HNM} = \mathcal{L}_{SM} + \mathcal{L}_N. \quad (3.63)$$

The lagrangian  $\mathcal{L}_N$  is the heavy neutrino lagrangian, it contains three parts,

$$\mathcal{L}_{HNM} = \mathcal{L}_{Kin} + \mathcal{L}_{mass} + \mathcal{L}_{Int} \quad (3.64)$$

where

- $\mathcal{L}_{Kin} = \bar{N}(i\bar{\gamma}^\mu D_\mu - m)N$  is the kinetic energy term.
- $\mathcal{L}_{mass}$  is the mass term (the eq.(3.46)).
- $\mathcal{L}_{Int}$  describes the interaction of heavy neutrino with weak gauge bosons and higgs boson.

This lagrangian is obtained after SSB of a theory based on groupe larger than SM gauge group (LR symmetric model for example). In this chapter we just focus on the heavy neutrino part. We focus on the Lagrangian part of interaction because it is the important in our phenomenological study in the next chapters (5, 6). The leptonically universal gauge interactions involving neutrinos are of the form:

$$\mathcal{L} = - \left[ \frac{g}{\sqrt{2}} W_\mu^+ \sum_{a=1}^3 \bar{\nu}_{aL} \gamma^\mu l_{aL} + h.c. \right] - \left[ \frac{g}{2 \cos \theta_W} Z_\mu \sum_{a=1}^3 \bar{\nu}_{aL} \gamma^\mu \nu_{aL} + h.c. \right] \quad (3.65)$$

In terms of the mass eigenstates (we use the relations 3.60 and 3.65), the gauge interaction lagrangian (3.65) can be written as:

$$\begin{aligned} \mathcal{L} = & -\frac{g}{2} W_\mu^+ \left( \sum_{l=e}^{\tau} \sum_{m=1}^3 \bar{\nu}_m (U^\dagger O_L)_{lm} \gamma^\mu P_L l^- + \sum_{l=e}^{\tau} \sum_{m'=4}^6 \bar{N}_{m'}^c (V^\dagger O_L)_{m'l} \gamma^\mu P_L l^- \right) + h.c. \\ & - \frac{g}{2 \cos \theta_W} Z_\mu \left( \sum_{m_1, m_2=1}^3 \bar{\nu}_{m_1} U^\dagger U \right)_{m_1 m_2} \gamma^\mu P_L \nu_{m_2} + \sum_{m'_1, m'_2=4}^6 \bar{N}_{m'_1}^c V^\dagger V \right)_{m'_1 m'_2} \gamma^\mu P_L N_{m'_2}^c \\ & - \frac{g}{2 \cos \theta_W} Z_\mu \left( \sum_{m_1=1}^3 \sum_{m'_2=4}^6 \bar{\nu}_{m_1} (U^\dagger V)_{m_1 m'_2} \gamma^\mu P_L N_{m'_2}^c + h.c. \right) \end{aligned} \quad (3.66)$$

we define the combination matrices to make the couplings more intuitive by:

$$U^{l\nu} = O_L^\dagger U \quad V^{lN} = O_L^\dagger N \quad U^{\nu N} = U^\dagger V \quad U^{\nu\nu} = U^\dagger U \quad V^{NN} = V^\dagger V \quad (3.67)$$

We thus rewrite the gauge interaction lagrangian by one mixing matrix for each term as in following:

$$\begin{aligned} \mathcal{L} = & -\frac{g}{2} W_\mu^+ \left( \sum_{l=e}^{\tau} \sum_{m=1}^3 \overline{\nu}_m U_{lm}^{l\nu*} \gamma^\mu P_L l^- + \sum_{l=e}^{\tau} \sum_{m'=4}^6 \overline{N}_{m'}^c V_l^{lN*} m' \gamma^\mu P_L l^- \right) + h.c. \\ & - \frac{g}{2 \cos \theta_W} Z_\mu \left( \sum_{m_1, m_2=1}^3 \overline{\nu}_{m_1} U_{m_1 m_2}^{\nu\nu} \gamma^\mu P_L \nu_{m_2} + \sum_{m'_1, m'_2=4}^6 \overline{N}_{m'_1}^c V_{m'_1 m'_2}^{NN} \gamma^\mu P_L N_{m'_2}^c \right) \\ & - \frac{g}{2 \cos \theta_W} Z_\mu \left( \sum_{m_1=1}^3 \sum_{m'_2=4}^6 \overline{\nu}_{m_1} U_{m_1 m'_2}^{\nu N} \gamma^\mu P_L N_{m'_2}^c + h.c. \right) \end{aligned} \quad (3.68)$$

It may be convenient in certain practical calculations to rewrite the current interactions in terms of their flavor eigenstates where we do not forget to the interaction part of neutrinos with the Higgs boson [9]. We need in our phenomenological study to care about the first generation of the heavy neutrino particle where the explicit form of the interaction lagrangian is given by [12]:

$$\mathcal{L}_{Int} = \mathcal{L}_{SM-int} + \mathcal{L}_{N-int} \quad (3.69)$$

$$\begin{aligned} \mathcal{L}_{Int} = & -\frac{g}{2} W_\mu^+ \sum_{l=e}^{\tau} \sum_{m=1}^3 \overline{\nu}_m U_{lm}^* \gamma^\mu P_L l^- - \frac{g}{2} W_\mu^+ \sum_{l=e}^{\tau} \overline{N}_{lN}^c V_{lN}^* \gamma^\mu P_L l^- \\ & - \frac{g}{2 \cos \theta_W} Z_\mu \sum_{l=e}^{\tau} \sum_{m=1}^3 \overline{\nu}_m U_{lm}^* \gamma^\mu P_L \nu_l - \frac{g}{2 \cos \theta_W} Z_\mu \sum_{l=e}^{\tau} \overline{N}_{lN}^c V_{lN}^* \gamma^\mu P_L \nu_l \\ & - \frac{gm_N}{2m_W} h \sum_{l=e}^{\tau} \overline{N}_{lN}^c V_{lN}^* \gamma^\mu P_L \nu_l + h.c. \end{aligned} \quad (3.70)$$

where  $P_L = \frac{1-\gamma_5}{2}$  and  $U_{lm}^*$  is the light neutrino mixing matrix and  $V_{lN}^*$  is the parameterizes active-heavy mixing.

The precise values of  $V_{lN}^*$  are model-dependent and are constrained by the neutrino oscillation and collider experiments, tests of lepton universality, and double  $\beta$  decay.

- **Remark:** the fact that  $V_{lN}^*$  are model-dependent allow us to destinguiche enables between BSM which include HNM and LR-symmetric Model. we will discuss this point expandly in chp.(5).
- We notice that this model is implemented on `FeynRules` where all the verteces and counter terms at one-loop in QCD are generated. In chapters 5 and 6 we employ the UFO-The Universal FeynRules Output model generated by `FeynRules` [24] to do phenomenological studies at NLO order by `Madgraph` [25].

### 3.4.3 Feynman's Rules

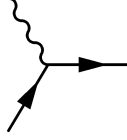
#### External Heavy Neutrino propagators

External heavy neutrino propagators are the same one of the fermions( see the section (2.5)).

#### Feynman vertices [12]

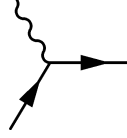
This is the new vertices in this model

- vertex  $W - \bar{\nu}_l - l$



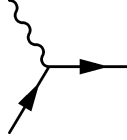
$$- \frac{ig}{\sqrt{2}} U_{lm}^* \gamma^\mu P_L$$

- vertex  $W - \bar{N}^c - l$



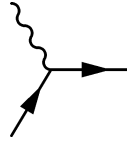
$$- \frac{ig}{\sqrt{2}} V_{lm}^* \gamma^\mu P_L$$

- vertex  $Z - \bar{\nu}_l - \nu_l$



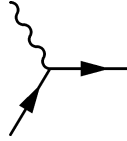
$$- \frac{ig}{2 \cos \theta_W} U_{lm}^* \gamma^\mu P_L$$

- vertex  $Z - \bar{N}^c - \nu_l$



$$- \frac{ig}{2 \cos \theta_W} V_{lm}^* \gamma^\mu P_L$$

- vertex  $h - \bar{N}^c - \nu_l$



$$- \frac{ig m_N}{2 m_W} V_{lm}^* \gamma^\mu P_L$$

where

$$P_L = \frac{1 - \gamma_5}{2}$$

$$P_R = \frac{1 + \gamma_5}{2}$$



# Left-Right Symmetric Model

---

Left-Right Symmetric Model was first suggested by the physicists Josef Pati and Abdus Salam [11], after that this idea it was developed by Mohapatra and others in an attempt to unify leptons and quarks. The model is attractive to study because it removes the left-right asymmetry which occurs in the standard model. Actually, there is no obvious reason why the left-handed and right-handed fields should obey different physics, and the LRSM takes care of this. Since symmetry is important in physics, adding the right handed  $SU_R(2)$  group to SM (with other differences, we will discuss it later) is a promising extension of the standard model (because it might explain CP violation). We follow in this chapter the notation of ref. [3].

## 4.1 Why Left-Right Symmetric Model ?

This model has many advantages over the SM and solves several problems, we can summarize it in the following points:

- It solves the problems of parity violation at low energy weak interaction, while all other forces in nature are parity conserving. The basic premise of the left-right symmetric models is that the fundamental weak interaction Lagrangian is invariant under parity symmetry at energy scales much above the standard model scale ( $100 \text{ GeV}$ ), the parity symmetry observed in nature arise from vacuum being non invariant under parity symmetry. An immediate consequence of this hypothesis is that there must be right-handed neutrinos in nature, as a consequence, neutrinos must be massive.
- In this model, neutrinos have masses and there is an explanation for the smallness of neutrinos mass.
- Up to energies above weak scale new effects associated with parity invariance of the Lagrangian appear (heavy right handed neutrino and new right handed weak mediators ( $W_R^\pm$  and  $Z_R$  bosons)), thus we can check the model validity by looking for the presence of these hypothetical particles at experiments.
- The fundamental planck scale theories such as string theories (and string duality) more easily lead to a LRSM gauge structure an not to the SM gauge structure.

## 4.2 Model Gauge Group

The LRSM is symmetric under parity transformations, which effectively switch the left- and right-handed fields. The gauge group defining our LRSM is given by:

$$SU_L(2) \times SU_R(2) \times U_{B-L}(1) \times P \quad (4.1)$$

we note that one of the deficiencies of the standard model is the absence of any physical meaning of the hypercharge  $U_Y(1)$  generator, which is arbitrarily adjusted to give the correct electric charges for the particles. But, in the left-right symmetric models  $U_{B-L}(1)$  generator can be identified as

the  $B-L$  quantum number so that all of the weak-interaction symmetry generators have a physical meaning. With the following assignment of fermions to the gauge group, denoting:

$$Q = \begin{pmatrix} u \\ d \end{pmatrix} \quad L = \begin{pmatrix} e^- \\ \nu_{e^-} \end{pmatrix} \quad (4.2)$$

so we have

$$Q_L = \left(\frac{1}{2} \quad 0 \quad \frac{1}{3}\right) \quad Q_R = \left(0 \quad \frac{1}{2} \quad \frac{1}{3}\right) \quad (4.3)$$

$$L_L = \left(\frac{1}{2} \quad 0 \quad -1\right) \quad L_R = \left(0 \quad \frac{1}{2} \quad -1\right) \quad (4.4)$$

where the left handed particles are doublets on  $SU_L(2)$  and singlets on  $SU_R(2)$  (the opposite for the right handed particles). The electric charge, isospin and B-L quantum number are related by:

$$Q = I_{3L} + I_{3R} + \frac{B-L}{2} \quad (4.5)$$

where

- $I_{3L}$  is the third component of isospin of the left handed particles. Where  $g_{2L}$  is the gauge coupling associated to  $SU_L(2)$ .
- $I_{3R}$  is the third component of isospin of the right handed particles. Where  $g_{2R}$  is the gauge coupling associated to  $SU_R(2)$ .

Due to the parity symmetry, the model have only two gauge couplings before spontaneous symmetry breaking ( $g_2 = g_{2L} = g_{2R}$  and  $g'$ ), as in SM, we can define  $\sin \theta_w = \frac{e}{g_{2L}}$  and the mixing angle  $\theta_w$  can be used to parametrise the neutral current hamiltonian.

The LRSM gauge group must be broken to SM gauge group, after that, to electromagnetism gauge group  $U_{EM}(1)$ . In the first spontaneous symmetry breaking the parity symmetry is lost and we get the right gauge bosons with masses  $m_{W_R}, (m_{Z_R})$ , respectively. In the second symmetry breaking we get the left gauge bosons with masses  $m_{W_L}, (m_{Z_L})$ , respectively (the later are the gauge bosons of the standard model). The SSB stages are summarised as follows:

$$\begin{aligned} & SU_L(2) \times SU_R(2) \times U_{B-L}(1) \times P \\ & \quad \downarrow \downarrow \\ & SU_L(2) \times U_Y(1) \quad \longrightarrow \quad m_{W_R}, m_{Z_R} \\ & \quad \downarrow \downarrow \\ & U_{EM}(1) \quad \longrightarrow \quad m_{W_L}, m_{Z_L} \end{aligned} \quad (4.6)$$

### 4.3 Left-Right Symmetric Model Lagrangian

The LRSM Lagrangian is given by:

$$\mathcal{L}_{LRSM} = \mathcal{L}_G + \mathcal{L}_F + \mathcal{L}_Y + \mathcal{L}_S \quad (4.7)$$

where

- $\mathcal{L}_G$  is the gauge fields lagrangian.

- $\mathcal{L}_F$  is the fermionic fields lagrangian.
- $\mathcal{L}_Y$  is the Yukawa interaction lagrangian.
- $\mathcal{L}_S = (D_\mu\phi)^\dagger(D^\mu\phi) + (D_\mu\Delta_L)^\dagger(D^\mu\Delta_L) + (D_\mu\Delta_R)^\dagger(D^\mu\Delta_R) - \mathcal{V}(|\Delta_L|^2, |\Delta_R|^2, |\phi|^2)$  is the scalar fields lagrangian needed for SSB, with
  - $(D_\mu\phi)^\dagger(D^\mu\phi) + (D_\mu\Delta_L)^\dagger(D^\mu\Delta_L) + (D_\mu\Delta_R)^\dagger(D^\mu\Delta_R)$  is the kinetic term,
  - $\mathcal{V}(|\Delta_L|^2, |\Delta_R|^2, |\phi|^2)$  is the higgs potential.
 where  $\phi$  is doublet under  $SU_L(2)$  and  $SU_R(2)$  gauge groups,  $\Delta_L$  is triplet under  $SU_L(2)$  and singlet under  $SU_R(2)$ ,  $\Delta_R$  is triplet under  $SU_R(2)$  and singlet under  $SU_L(2)$ .

In following we give more detail about the structure of the lagrangian.

#### 4.3.1 Gauge field lagrangian

$\mathcal{L}_G$  describes the kinetic terms for the gauge fields and their self interactions. It is given by:

$$\mathcal{L}_G = -\frac{1}{4}F_{L\mu\nu}^i F_{iL}^{\mu\nu} - \frac{1}{4}F_{R\mu\nu}^i F_{iR}^{\mu\nu} - \frac{1}{4}B_{\mu\nu}B^{\mu\nu} \quad (4.8)$$

where

- The abelian field strength of  $U(1)$  is  $B_{\mu\nu} = \partial_\mu B_\nu - \partial_\nu B_\mu$ .
- The non-abelian field strengths of  $SU_L(2)$ ,  $SU_R(2)$  have the form

$$F_{L\mu\nu}^i = \partial_\mu W_{L,R\nu}^i - \partial_\nu W_{L,R\mu}^i - if_{ik}^j W_{L,R\mu}^j W_{L,R\nu}^k$$

with  $f_{ik}^j$  are the structure constants of the group.

#### 4.3.2 Fermionic field lagrangian

$\mathcal{L}_F$  describes the fermionic kinetic terms and the interactions term between fermions and gauge fields. Summing over all fermions doublets ( $Q$  for quarks and  $L$  for leptons) we get:

$$\mathcal{L}_f = \sum_{\psi=Q,L} (\bar{\psi}_L i\gamma^\mu D_\mu \psi_L + \bar{\psi}_R i\gamma^\mu D_\mu \psi_R) \quad (4.9)$$

where the covariant derivatives are given by:

$$D_\mu = \begin{cases} \partial_\mu + ig_L \frac{\vec{\sigma}}{2} \cdot \vec{W}_{L\mu}^i + ig' \frac{B-L}{2} B_\mu \\ \partial_\mu + ig_R \frac{\vec{\sigma}}{2} \cdot \vec{W}_{R\mu}^i + ig' \frac{B-L}{2} B_\mu \end{cases} \quad (4.10)$$

the gauge field corresponding to  $U_{B-L}(1)$  transformations is  $B_\mu$ , with the gauge coupling  $g'$ , and the fields corresponding to  $SU_{L,R}(2)$  transformations are  $W_{L,R}$  with gauge couplings  $g_L = g_R = g$  (as we suggested earlier).

#### 4.3.3 Yukawa interaction lagrangian

The interaction of fermions with the scalar fields is given by Yukawa's Lagrangian, it is given by:

$$\begin{aligned} \mathcal{L}_Y = & \sum_{\psi=Q,L} \sum_{i,j} (h_{ij}^f \bar{\psi}_{iL} \phi \psi_{jR} + \bar{h}_{ij}^f \bar{\psi}_{iL} \bar{\phi} \psi_{jR}) \\ & + \sum_{i,j} f_{ij} (\bar{L}_{iL}^c \Delta_L L_{jL} + \bar{L}_{iR}^c \Delta_R L_{jR}) + h.c. \end{aligned} \quad (4.11)$$

If the scalar field has a non-zero vev, then when we substitute it into the Yukawa Lagrangian, we get the mass terms for fermions.

### 4.3.4 Scalar field lagrangian

It consists of two parts as presented in the beginning of this section, the unique minimal set required to break the symmetry down to the  $U_{EM}(1)$  is:

- $\Delta_L(1, 0, +2) + \Delta_R(0, 1, +2)$ , Where  $\Delta_L(1, 0, +2)$  is triplet on  $SU_L(2)$  and singlet on  $SU_R(2)$ , while  $\Delta_R(1, 0, +2)$  is singlet on  $SU_L(2)$  and triplet on  $SU_R(2)$ .
- $\phi(\frac{1}{2}, \frac{1}{2}, 0)$  is doublet on  $SU_L(2)$  and  $SU_R(2)$ .

And we have under left-right symmetry  $\Delta_L \leftrightarrow \Delta_R$  and  $\phi \leftrightarrow \phi^+$ . We choose these fields  $\Delta_L + \Delta_R$  to break the gauge group of LRSM to the gauge group of SM  $SU_L(2) \times U_Y(1)$ , then we use  $\phi$  to break this gauge group to  $U_{EM}(1)$ .

Higgs potential composed of two parts  $\mathcal{V}(|\Delta_L|^2, |\Delta_R|^2, |\phi|^2) = \mathcal{V}(|\Delta_L|^2, |\Delta_R|^2) + \mathcal{V}(|\phi|^2)$ , We give the general formula and discuss the symmetry breaking in the next section.

## 4.4 Spontaneous Symmetry Breaking

We now show that, for a range of parameters, an exactly left-right symmetric potential would lead to parity-violating that will breaks the gauge symmetry. Let's start with  $\mathcal{V}(|\Delta_L|^2, |\Delta_R|^2)$ , the most general potential formula involving  $\Delta_{L,R}$  which conserve parity and gauge invariance is:

$$\begin{aligned}
\mathcal{V}(|\Delta_L|^2, |\Delta_R|^2) = & -\mu^2 \text{Tr}[\Delta_L^\dagger \Delta_L + \Delta_R^\dagger \Delta_R] \\
& + \rho_1 \left[ (\text{Tr}[\Delta_L^\dagger \Delta_L])^2 + (\text{Tr}[\Delta_R^\dagger \Delta_R])^2 \right] \\
& + \rho_2 \left[ \text{Tr}[\Delta_L^\dagger \Delta_L \Delta_L^\dagger \Delta_L] + \text{Tr}[\Delta_R^\dagger \Delta_R \Delta_R^\dagger \Delta_R] \right] \\
& + \rho_3 \left[ \text{Tr}[\Delta_L^\dagger \Delta_L] + \text{Tr}[\Delta_R^\dagger \Delta_R] \right] \\
& + \rho_4 \left[ \text{Tr}[\Delta_L^\dagger \Delta_L^\dagger] \text{Tr}[\Delta_L \Delta_L] + \text{Tr}[\Delta_R^\dagger \Delta_R^\dagger] \text{Tr}[\Delta_R \Delta_R] \right]
\end{aligned} \tag{4.12}$$

where the scalar fields  $\Delta_L$  and  $\Delta_R$  can be parametrised as:

$$\Delta_{L,R} = \frac{1}{2} \vec{\sigma} \cdot \vec{\delta}_{L,R} \begin{pmatrix} \frac{\delta^+}{2} & \delta^{++} \\ \delta^0 & -\frac{\delta^+}{2} \end{pmatrix}_{L,R} \tag{4.13}$$

by following the same steps in the SM we can choose the vev of  $\Delta_{L,R}$  (which minimises the potential) as follows:

$$\begin{pmatrix} 0 & 0 \\ v_{L,R} & 0 \end{pmatrix} \tag{4.14}$$

The potential  $\mathcal{V}$  then becomes,

$$\mathcal{V}(v_L, v_R) = -\mu^2(v_L^2 + v_R^2) + (\rho_1 + \rho_2) + (v_L^4 + v_R^4) + \rho_3 v_L^2 v_R^2 \tag{4.15}$$

Putting  $v_L = v \sin \alpha$  and  $v_R = v \cos \alpha$  and differentiating  $\mathcal{V}(v_L, v_R)$  with respect to  $\alpha$  we get the condition:

$$\left[ \rho_3 - 2(\rho_1 + \rho_2) \right] v \sin 2\alpha \cos 2\alpha = 0 \tag{4.16}$$

- For  $\rho_3 \neq 2(\rho_1 + \rho_2)$  the solutions of eq.(4.17) are  $\alpha = 0, \frac{\pi}{2}, \frac{\pi}{4} \dots$   
so  $\alpha = 0$  corresponds to  $v_L = 0$  and  $v_R \neq 0$ , whereas  $\alpha = \frac{\pi}{4}$  corresponds to  $v_R = 0$  and  $v_L \neq 0$ . So we conclude that if  $\alpha = 0$  ( $v_R \neq 0$ ), this choice corresponds to parity violation.

Taking the second derivative of  $\mathcal{V}(v_L, v_R)$  with respect to  $\alpha$ , we get:

$$2v \cdot \left[ \rho_3 - 2(\rho_1 + \rho_2) \right] \cdot \left[ \cos^2 2\alpha - \sin^2 2\alpha \right] = 0 \quad (4.17)$$

- For  $\rho_3 > 2(\rho_1 + \rho_2)$ ,  $\alpha = 0, \frac{\pi}{2}$  corresponds to the maximum,  $\alpha = \frac{\pi}{4}$  corresponds to the minimum.

Thus, for a range of parameters, we get the correct unbroken symmetry group of the SM (we will discuss how we choose the parameters in the next sections when we talk about the generation of bosons and neutrino masses).

If we include the  $\phi$  multiplet, we get the total potential:

$$\begin{aligned} \mathcal{V}(|\Delta_L|^2, |\Delta_R|^2, |\phi|^2) &= \mathcal{V}(|\Delta_L|^2, |\Delta_R|^2) - \sum_{ij} \text{Tr}[\phi_i^\dagger \phi_j] \\ &+ \sum_{ijkl} \lambda_{ijkl} \text{Tr}[\phi_i^\dagger \phi_j] \text{Tr}[\phi_k^\dagger \phi_l] \\ &+ \sum_{ijkl} \lambda'_{ijkl} \text{Tr}[\phi_i^\dagger \phi_j \phi_k^\dagger \phi_l] \\ &+ \sum \alpha_{ij} \text{Tr}[\phi_i^\dagger \phi_j] \text{Tr}[\Delta_L^\dagger \Delta_L + \Delta_R^\dagger \Delta_R] \\ &+ \sum \beta_{ij} \text{Tr}[\phi_i \phi_j^\dagger \Delta_L^\dagger \Delta_L + p h i_i^\dagger \phi_j \Delta_R^\dagger \Delta_R] \\ &+ \sum \gamma_{ij} \text{Tr}[\Delta_L^\dagger \phi_i \Delta_R \phi_j^\dagger] \end{aligned} \quad (4.18)$$

where

$$\phi_1 = \begin{pmatrix} \phi_1^0 & \phi_1^\dagger \\ \phi_2^- & \phi_2^0 \end{pmatrix} \quad \phi_2 = \sigma_2 \phi_1^* \sigma_2 = \begin{pmatrix} \phi_2^{0*} & -\phi_2^\dagger \\ -\phi_1^- & \phi_2^{0*} \end{pmatrix} \quad (4.19)$$

the equation(4.18) is a very complicated potential. To study the minimum of this potential, we assume that  $\langle \Delta_L \rangle, \langle \Delta_R \rangle, \langle \phi \rangle$ , have the following form:

$$\langle \Delta_{L,R} \rangle = \begin{pmatrix} 0 & 0 \\ v_{L,R} & 0 \end{pmatrix} \quad \langle \phi \rangle = \begin{pmatrix} k & 0 \\ 0 & k' \end{pmatrix} \exp(i\alpha). \quad (4.20)$$

- We mention that  $k$  and  $k'$  are nonzero and  $v_L$  can be written as:

$$v_L = \frac{\gamma_{12}}{2(\rho_1 + \rho_2) - \rho_3} \cdot \frac{k^2}{v_R} \quad (4.21)$$

we assume for simplicity that  $k' \ll k$ , since  $k \ll v_R$  we get  $v_L \ll k$ . This is a seesaw-like formula for vacuum expectation values, it is useful to understand, in the gauge theory context, why some physical parameters are small compared to others.

Now let us study the effect of symmetry breaking on the particles masses of LRSM theory:

#### 4.4.1 Charged gauge bosons masses

Now, we show how the symmetry breaking generate the mass of the heavy vector bosons. It is easy to show, by expanding the kinetic term of  $\mathcal{L}_\phi$ , that the  $W_L^\dagger - W_R^\dagger$  mass matrix is given by :

$$\begin{pmatrix} \frac{1}{2} g^2 (k^2 + k'^2 + 2v_L) & g^2 k k' \\ g^2 k k' & \frac{1}{2} g^2 (k^2 + k'^2 + 2v_R) \end{pmatrix} \quad (4.22)$$

The eigenstates of this matrix denote the physical  $W_{1,2}$  bosons

$$\begin{cases} W_1 = W_L \cos \xi + W_R \sin \xi \\ W_2 = -W_L \sin \xi + W_R \cos \xi \end{cases} \quad (4.23)$$

then their masses are given by:

$$\begin{cases} m_{W_1}^2 \simeq \frac{1}{2} g^2 (k^2 + k'^2) \\ m_{W_2}^2 \simeq \frac{1}{2} g^2 (k^2 + k'^2 + 2v_R) \end{cases} \quad (4.24)$$

$$\Rightarrow \begin{cases} m_{W_1} \simeq \frac{1}{\sqrt{2}} g \sqrt{(k^2 + k'^2)} \\ m_{W_2} \simeq \frac{1}{\sqrt{2}} g \sqrt{(k^2 + k'^2 + 2v_R)} \end{cases} \quad (4.25)$$

with

$$\tan 2\xi = \frac{2kk'}{v_R^2 - v_L^2}. \quad (4.26)$$

$$(4.27)$$

The charged current weak interactions can now be written as

$$\begin{aligned} \mathcal{L}_{CC} = & \frac{g}{2} (\bar{u}_L \gamma_\mu d_L + \bar{\nu}_L \gamma_\mu e_L) (W_1^{\dagger\mu} \cos \xi + W_2^{\dagger\mu} \sin \xi) \\ & + \frac{g}{2} (\bar{u}_R \gamma_\mu d_R + \bar{\nu}_R \gamma_\mu e_R) (W_2^{\dagger\mu} \cos \xi - W_1^{\dagger\mu} \sin \xi) + h.c. \end{aligned} \quad (4.28)$$

We have suppressed the generation index in eq.(4.28).

- We note that presence of quark mixings, the weak quark- and lepton-currents will include mixing angles as well as  $CP$ -violating phases  $\alpha$ .
- If we use the constraints that we discussed earlier ( $k', v_L \ll k$  and  $k \ll v_R$ ) we get from (4.26) that  $\xi \simeq 0$ , so if we replace this value in equation (4.23) we get the physical charged bosons:

$$W_1 \simeq W_L \qquad W_2 \simeq W_R \quad (4.29)$$

and the charged gauge bosons masses becomes:

$$\Rightarrow \begin{cases} m_{W_L} \simeq \frac{1}{\sqrt{2}} g \sqrt{(k^2 + k'^2)} \\ m_{W_R} \simeq \frac{1}{\sqrt{2}} g \sqrt{(k^2 + k'^2 + 2v_R)} \end{cases} \quad (4.30)$$

we can note from the condition ( $k', v_L \ll k$  and  $k \ll v_R$ ) that the mass of  $m_{W_L} \ll m_{W_R}$ , where  $m_{W_L}$  comes when we break the left gauge group  $SU_L(2)$  and  $m_{W_R}$  comes when we break the right gauge group  $SU_R(2)$ . So  $W_L$  is the SM charge gauge boson that we know and  $W_R$  is a new heavy charge gauge boson comes from the right part of the gauge group.

### 4.4.2 Neutral gauge bosons masses

The mass matrix of the three neutral gauge bosons  $W_{3L}, W_{3R}$  and  $B$ , given by:

$$\begin{pmatrix} \frac{1}{2} g^2(k^2 + k'^2 + 4v_L^2) & -\frac{1}{2} g^2(k^2 + k'^2) & -2gg'v_R^2 \\ -\frac{1}{2} g^2(k^2 + k'^2) & \frac{1}{2} g^2(k^2 + k'^2 + 4v_R^2) & -2gg'v_R^2 \\ -2gg'v_L^2 & 2gg'v_R^2 & 2g'^2(v_L^2 + v_R^2) \end{pmatrix} \quad (4.31)$$

To obtain the eigenstates of this matrix, we diagonalise it by a bi-unitary transformation (as we did in the SM), we get the new basis (define  $\sin \theta_w = e/g$ )

$$\begin{cases} A = \sin \theta_w (W_{3L} + W_{3R}) + \sqrt{\cos 2\theta_w} B \\ Z_L = \cos \theta_w W_{3L} - \sin \theta_w \tan \theta_w W_{3R} - \tan \theta_w \sqrt{\cos 2\theta_w} B \\ Z_R = \frac{\sqrt{\cos 2\theta_w}}{\cos \theta_w} W_{3R} - \tan \theta_w B \end{cases} \quad (4.32)$$

$A$  is the photon that remains massless after symmetry breaking and is an exact eigenstate. The remaining physical neutral gauge bosons are given by:

$$\begin{cases} Z_1 = Z_L \cos \xi + Z_R \sin \xi \\ Z_2 = -Z_L \sin \xi + Z_R \cos \xi \end{cases} \quad (4.33)$$

where

$$\begin{cases} \tan 2\xi \simeq 2\sqrt{\cos 2\theta_w} \frac{m_{Z_L}^2}{m_{Z_R}^2} \\ m_{Z_L}^2 \simeq \frac{g^2}{2\cos^2 \theta_w} (k^2 + k'^2 + 4v_L^4) \\ m_{Z_R}^2 \simeq \frac{g^2}{2\cos^2 \theta_w \cos 2\theta_w} [4v_R^2 \cos^4 \theta_w + (k^2 + k'^2) \cos^2 2\theta_w + 4v_L^2 \sin^4 \theta_w] \end{cases} \quad (4.34)$$

- If we use the constraints ( $k', v_L \ll k$  and  $k \ll v_R$ ) we get the physical neutral bosons like:

$$Z_1 \simeq Z_L \quad Z_2 \simeq Z_R \quad (4.35)$$

and the neutral gauge bosons masses becomes:

$$\begin{cases} m_{Z_L} \simeq \frac{g}{\sqrt{2\cos^2 \theta_w}} \sqrt{(k^2 + k'^2 + 4v_L^4)} \\ m_{Z_R} \simeq \frac{g}{\sqrt{2\cos^2 \theta_w \cos 2\theta_w}} \sqrt{[4v_R^2 \cos^4 \theta_w + (k^2 + k'^2) \cos^2 2\theta_w + 4v_L^2 \sin^4 \theta_w]} \end{cases} \quad (4.36)$$

as we did with the charge gauge bosons, we can note from the condition ( $k', v_L \ll k$  and  $k \ll v_R$ ) that the mass of  $m_{Z_L} \ll m_{Z_R}$ , where  $m_{Z_L}$  comes when we break the left gauge group  $SU_L(2)$  and  $m_{Z_R}$  comes when we break the right gauge group  $SU_R(2)$ . So  $Z_L$  is the SM neutral gauge boson that we know and  $Z_R$  is a new heavy neutral gauge boson comes from the right part of the gauge group.

The neutral current is given by:

$$\begin{aligned} \mathcal{L}_{NC} = & \frac{g}{\cos \theta_w} \left[ \left( J_L^\mu - \frac{\xi}{\sqrt{\cos 2\theta_w}} (\sin^2 \theta_w J_L^\mu + \cos^2 \theta_w J_R^\mu) \right) Z_{1\mu} \right. \\ & \left. + \frac{1}{\sqrt{\cos 2\theta_w}} (\sin^2 \theta_w J_L^\mu + \cos^2 \theta_w J_R^\mu) \right] \end{aligned} \quad (4.37)$$

where

$$J_{LR}^\mu = \sum_f \bar{f} \gamma^\mu (I_{3L,R} - Q \sin^2 \theta_w) f \quad (4.38)$$

### 4.4.3 Fermions masses and mixings

Fermion masses in the LRSM are as in the SM, arise from the Yukawa coupling between quarks, leptons, and the Higgs bosons responsible for gauge symmetry breaking. The most general gauge-invariant Yukawa coupling as we mentioned in eq.(4.11) is:

$$\begin{aligned} \mathcal{L}_Y = & \sum_{\psi=Q,L} \sum_{i,j} (h_{ij}^f \bar{\psi}_{iL} \phi \psi_{jR} + \bar{h}_{ij}^f \bar{\psi}_{iL} \bar{\phi} \psi_{jR}) \\ & + \sum_{i,j} f_{ij} (\bar{L}_{iL}^c \Delta_L L_{jL} + \bar{L}_{iR}^c \Delta_R L_{jR}) + h.c. \end{aligned} \quad (4.39)$$

when we substituting the vacuum expectation values from eq.(4.20), we get for charged fermions the following mass matrices:

$$\begin{cases} m_{ij}^u = h_{ij}^q k \exp^{i\alpha} + \bar{h}_{ij}^q k' \exp^{-i\alpha} \\ m_{ij}^d = h_{ij}^q k \exp^{-i\alpha} + \bar{h}_{ij}^q k' \exp^{i\alpha} \\ m_{ij}^e = h_{ij}^l k \exp^{-i\alpha} + \bar{h}_{ij}^l k' \exp^{i\alpha} \end{cases} \quad (4.40)$$

We will discuss the neutrino masses in the next section.

The invariance of the Yukawa coupling under parity symmetry requires that:

$$h_{ij}^a = h_{ji}^{*a} \quad (4.41)$$

where  $a$  goes over all the Yukawa couplings involving  $\phi$  and  $\bar{\phi}$ . This property leads to interesting constraints on the mass matrices, which are:

- $h$  complex,  $\alpha = 0$  (manifest left-right symmetry):

In the literature, this is called "manifest left-right symmetry" when the mixing angles in the left- and right-handed quark sectors are identical, which implies that:

$$m^a = m^{a\dagger} \quad a = u, d, e \quad (4.42)$$

and the hermitian matrices are diagonalized by unitary transformations  $Um^aU^\dagger = D^a$ .

- $h$  real,  $\alpha \neq 0$  (pseudo-manifest left-right symmetry):

In this case reality of  $h$  is caused by the invariance of  $CP$  prior to symmetry breaking. In this case, eq.(4.40) implies that the mass matrices are complex and symmetric, they are diagonalized by  $Um^aU^TK = D^a$ , where  $K$  is a diagonal unitary matrix. As a result, the left- and right-handed mixing angles are equal but the corresponding phases are different.

### 4.4.4 Neutrinos masses

When  $V-A$  theory was proposed by Sudarshan and Marshak, Feynman and Gell-Mann built their argument on the assumption that neutrinos are massless. If  $m_\nu = 0$ , then the neutrino spinor obeys the Weyl equation, which is invariant under  $\gamma_5$  transformations ( $\nu \rightarrow \gamma_5\nu$ ), then Marshak and Sudarshan argued that neutrinos participate only in weak interactions, the weak Hamiltonian  $H_{we}$  should be invariant under separate  $\gamma_5$  transformations, and this leads to the successful  $V-A$  theory of charged-current weak interactions. Therefore from this point, the existence of neutrinos mass should be connected with the existence of  $V + A$  theory.

As we discussed in the previous chapter (3) (section 3.4.1) there are two possibilities of neutrino type (Dirac or Majorana), and the general formula of the mass term is given in (3.46) by:

$$\mathcal{L}_{\nu_{mass}} = -\frac{1}{2}m_R\bar{\nu}_R^c\nu_R - \frac{1}{2}m_L\bar{\nu}_L^c\nu_L - m_D\bar{\nu}_R\nu_L + h.c. \quad (4.43)$$



we get the mass matrix  $M$  as before:

$$\begin{pmatrix} 0_{\alpha\beta} & (m_D^T)_{\alpha j} \\ (m_D)_{\beta i} & (m_R)_{ij} \end{pmatrix} \quad (4.44)$$

The mechanism which we use to obtain and explain smallness of the neutrino masses is the seesaw mechanism type  $I$  like in the previous section.

Whene we diagonalize it we get eigenvalues of this mass matrix, we get  $m_i^\nu$  which are the **light neutrino eigenstates** and  $m_\alpha^N$  which are the **heavy neutrino eigenstates**

$$\begin{aligned} m_i^\nu &= -\frac{m_D^2}{m_{Ri}} \\ m_\alpha^N &= m_{R\alpha}. \end{aligned} \quad (4.45)$$

Now we want to see the connection between the mass mixing matrix  $M$  with the vev parameters and some knowing parameters and how to naturally deduce the mass of the light  $\nu$  and heavy neutrino  $N$  when we break the symmetry! By using the same higgs fields that we given before  $[\Delta_L(1, 0, +2) + \Delta_R(0, 1, +2), \phi(\frac{1}{2}, \frac{1}{2}, 0)]$ . Shematically, the masses of neutrinos are generated as follows:

$$\begin{array}{ccc} & SU_L(2) \times SU_R(2) \times U_{B-L}(1) \times P & \\ & \downarrow & \\ \Delta_L \simeq 0 & \Delta_R = v_R \neq 0 & M_\nu = \begin{pmatrix} 0 & 0 \\ 0 & v_R \end{pmatrix} \end{array} \quad (4.46)$$

$$\begin{array}{ccc} & \downarrow & \\ & SU_L(2) \times U_Y(1) & \\ & \downarrow & \\ \langle \phi \rangle = \begin{pmatrix} k & 0 \\ 0 & k' \end{pmatrix} & & M_\nu = \begin{pmatrix} 0 & \frac{1}{2}hk \\ \frac{1}{2}hk & fv_R \end{pmatrix} \end{array} \quad (4.47)$$

$$\begin{array}{ccc} & \downarrow & \\ & U_{EM}(1) & \end{array}$$

By diagonalizing the above  $M_\nu$  we obtain the following eigenstates and masses :

$$\nu = \nu_L \cos \xi + \nu_R \sin \xi \quad m_\nu \simeq \frac{h^2 k^2}{2fv_R} \quad (4.48)$$

$$N = -\nu_L \sin \xi + \nu_R \cos \xi \quad m_N \simeq 2fv_R \quad (4.49)$$

where  $\tan \xi (m_\nu/m_N)^2$  as claimed before :  $v_R \rightarrow \infty \Rightarrow m_\nu \rightarrow 0$ , and the leptonic charged currents now look as:

$$\begin{pmatrix} \nu \cos \xi + N \sin \xi \\ e^- \end{pmatrix}_L \quad \begin{pmatrix} -\nu \sin \xi + N \cos \xi \\ e^- \end{pmatrix}_R \quad (4.50)$$

if we reparametrize the  $m_\nu$  and  $m_N$  in terms of  $m_e$  and  $m_{W_R}$ , we get :

$$\begin{cases} m_\nu \simeq \frac{r^2}{\beta} \cdot \frac{m_e^2}{m_{W_R}} \\ m_N \simeq \beta m_{W_R} \end{cases} \quad (4.51)$$

where  $r$  and  $\beta$  are dimensionless parameters,  $m_e$  is the electron mass and  $m_{W_R}$  are the right- and the left-handed charged gauge boson mass.

## 4.5 Feynman's Rules

### External Heavy Neutrino propagators

External heavy neutrino propagators are the same one of the fermions ( they are the same rules in the  $SM$  chapter (see the section (2.5) ).

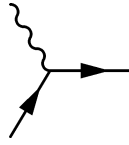
### Internal Propagators

$W_R, Z_R$  propagators have the same form of  $W, Z$  in  $SM$ .

### Feynman vertices [25]

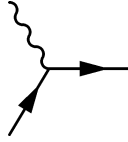
In addition to the vertices in the previous chapter ( see the section (3.4.3) ), we have new vertices arising from the interaction between the new right-handed gauge boson  $W_L, W_R, Z_R$  and the fermions, we give this vertices below:

- vertex  $W_R - q - q'$



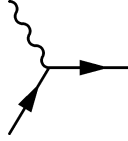
$$-\frac{igk_R^q}{\sqrt{2}} V_{ij}^{CKM} \gamma^\mu P_R$$

- vertex  $W_R - l - \nu$



$$-\frac{igk_R^l}{\sqrt{2}} X_{lm} \gamma^\mu P_R$$

- vertex  $W_R - l - N$



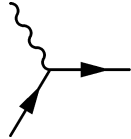
$$-\frac{igk_R^l}{\sqrt{2}} Y_{lm'} \gamma^\mu P_R$$

The matrix  $Y_{lm'}$  ( $X_{lm}$ ) quantifies the mixing between the heavy (light) neutrino mass eigenstate  $m_N$  ( $m_\nu$ ) and the right-handed chiral state with corresponding lepton flavor  $l$ . The mixing scale as

$$|Y_{lm'}|^2 \sim \Theta(1) \quad |X_{lm}|^2 \sim 1 - |Y_{lm'}|^2 \sim \Theta\left(\frac{m_\nu^2}{m_{N'm}^2}\right) \quad (4.52)$$

The mixing scale as  $|Y_{li}| \sim \Theta(1)$ , and  $K_R^q \in \mathfrak{R}$  independently normalizes the  $W_R$  coupling strength to leptons. At TeV collider scales, both light neutrino masses and light neutrino mixing can be taken to zero, so for simplicity, we take  $Y_{lm'}$  to be diagonal with unit entries  $|Y_{e^- N_1}| = |Y_{\mu^- N_2}| = |Y_{\tau^- N_3}| = 1$  and  $|Y_{others}| = 0$ .

- vertex  $Z_R - f - f$



$$\frac{-iK_R^f g \delta_{ij}}{\sqrt{1 - \frac{\tan^2 \theta_w}{(K_R^f g)^2}}} \gamma^\mu \left( g_L^{Z_R, f} P_L + g_R^{Z_R, f} P_R \right)$$

where

$$P_L = \frac{1 - \gamma_5}{2} \quad P_R = \frac{1 + \gamma_5}{2}$$

and

$$g_L^{Z_R, f} = (I_L^{3, f} - Q^f) \frac{1}{(K_R^f)^2} \cdot \tan^2 \theta_w \quad g_R^{Z_R, f} = I_R^{3, f} - \frac{1}{(K_R^f)^2} \cdot \tan^2 \theta_w Q^f.$$

# Production of a Heavy Neutrinos at LO Order

In this chapter we study the production of heavy neutrinos for many processes in the Leading Order (LO) approximation at the LHC in the BSM models presented in chapter 3 and chapter 4. We leave the higher order corrections to the next chapter, where we will study the same processes in more details at Next to Leading Order (NLO) approximation. All the processes studied in this work are proton-proton collision, we can classify them in two types according to the nature of the current responsible for the interaction:

- Charged current processes (CC), where the weak force is mediated by the  $W^\pm$  or  $W_r^\pm$  gauge bosons.
- Neutral current processes (NC), where the weak force is mediated by  $Z$  or  $Z_r$  gauge bosons.

The aim of this study is to find the differences between these models which allows us to know the correct one by comparing our results with the experimental results that are looking for the presence of a heavy neutrino  $N$ . In both models, the neutrinos can be of Dirac or Majorana types. In HNM model, we considered the two types of neutrinos, however in the LRSM we considered only the Majorana type of neutrinos.

## 5.1 Calculation Tools of the Hadronic Cross Section

Here are some physical quantities and kinematics that we need to study our processes:

### 5.1.1 Cross sections

#### Partonic cross section $\hat{\sigma}$

The cross section is a physical quantity related to the probability of producing particles in a collision  $1 + 2 \rightarrow 3 + 4 + \dots + N$ . The unit of the cross section is the the unit of area, the *barn* where  $1 \text{ barn} = 10^{-24} \text{ cm}^2$ . The partonic cross section normalised by the incident flux is defined by:

$$\hat{\sigma} = \frac{1}{4 \sqrt{(p_1 \cdot p_2)^2 - m_1^2 m_2^2}} \frac{1}{(2\pi)^2} \int \delta^4(p_1 + p_2 - \sum_{i=1}^n p_i) \frac{d^3 \vec{p}_3}{2 E_3} \dots \frac{d^3 \vec{p}_n}{2 E_n} \overline{\sum} |M|^2 \quad (5.1)$$

where  $p_i$  are the momentum of particles,  $m_i$  are the particle masses,  $M$  is the amplitude and  $\delta$  is the Dirac delta function of the particle's four-momentum, which ensures that the energy and momentum are conserved during an interaction.

#### Hadronic cross section $\sigma^H$

According to the parton model (proposed by Feynman), the proton is made up of elementary particles called partons. Partons are point-like particles of negligible mass. If we consider the collision between 2 hadrons (2 protons for example), we note the momentum of the hadrons is  $P_1$  and  $P_2$  and the momentum of the 2 partons  $p_1$  and  $p_2$ . Partons will carry a fraction of hadrons

momentum, then  $p_1 = x_1 P_1$ ,  $p_2 = x_2 P_2$ . We define the hadronic cross section  $\sigma^H$  as a convolution of the partonic cross section  $\hat{\sigma}^{ij \rightarrow k+l+X}$  of the sub processes  $ij \rightarrow k+l+X$  and the parton distribution functions  $\mathcal{F}_i^{H^1}(x_1, \mu_F^2)$ ,  $\mathcal{F}_j^{H^2}(x_2, \mu_F^2)$  (or PDFs). The general form of  $\sigma^H$  for hadron-hadron collision is:

$$\hat{\sigma}^H = \sum_{i,j} \int dx_1 dx_2 \mathcal{F}_i^{H^1}(x_1, \mu_F^2) \mathcal{F}_j^{H^2}(x_2, \mu_F^2) \hat{\sigma}^{ij \rightarrow k+l+X}(p_1, p_2, \mu_F^2, \mu_R^2) \quad (5.2)$$

with  $i, j = q, \bar{q}, g$ , where  $q = u, d, s, c$  in the four flavour scheme (4FS) and  $q = u, d, s, c, b$  the five flavour scheme (5FS) <sup>1</sup>.

- $\mathcal{F}_i^{H^1}(x_i, \mu_F^2)$  is the partonic distribution function, it represents the distribution of the parton  $i$  inside the hadron  $H$ , it encodes the physics at low energy.
- $\hat{\sigma}^{ij \rightarrow k+l+X}$  is the partonic cross section, it encodes the physics at high energy and gives the probability transition from de initial state  $i + j$  to the final state  $k + l + X$ .
- $\mu_F^2$  is the factorisation scale, which factorise the physics of short and long distances.
- $\mu_R^2$  is the renormalisation scale introduced by the renormalisation procedure to eliminate the UV divergences.

### Differential cross section

We now define the differential cross section. This quantity is obtained by keeping one or more variable of integration of the total cross section non-integrated. For example, if we keep the variable  $\cos(\theta)$  we denote the differential cross section  $d\hat{\sigma}/d\cos(\theta)$ , which gives us information about the distribution of the probability in term the angle  $\theta$ . Many differential cross sections are needed to compare theory and experiment, in the following we give some of them:

- $d\hat{\sigma}/dt$  with  $t$  is the MandelStam variable  $t = (p_1 - p_3)^2 = (p_2 - p_4)^2$ .
- $d\hat{\sigma}/d\cos(\theta)$  where  $\theta$  is the angle between the direction of the incident particle and one of the outgoing particles.
- $d\hat{\sigma}/dm_T$  where  $m_T$  is the transverse mass.
- $d\hat{\sigma}/dp_T$  where  $p_T$  is the transverse momentum.
- $d\hat{\sigma}/dy$  where  $y$  is the rapidity.
- $d\hat{\sigma}/d\eta$  where  $\eta$  is the Pseudo-rapidity.

We notice that the kinematics variables like  $m_T, p_T, \dots$  etc are defined in the next section.

### Decay rate

Most of the hypothetic particles predicted by BSM models are massive, so they are not stable. Because of that we need to know their decay rates. The decay rate for the processes  $1 \rightarrow 2 + \dots + N$  is defined by,

$$\Gamma = \frac{1}{2m} \int \delta^4(p_1 - \sum_i^n(p_i)) \frac{d^2\vec{p}_2}{(2\pi)^2 2E_2} \cdots \frac{d^3\vec{p}_n}{(2\pi)^2 2E_n} \overline{\sum} |M|^2$$

where  $p$  is the momentum of the decaying particle and  $m$  is its mass,  $p_i$  is the momentum of the produced particles and  $E_i$  are their energies and  $M$  is the amplitude of the process.

We mention that de decay rate is inverse of the particle lifetime which is one of important characteristic of particles.

<sup>1</sup>In the 4FS all the quarks are assumed to be massless except to bottom and the top quarks, and in the 5FS only the top quark which is assumed to be massive.

### 5.1.2 Kinematics

In this subsection, we give some kinematics variables that we will need in this and in the next chapters.

#### Rapidity

Rapidity is commonly used as a measure for relativistic velocity, in the usual convention in accelerator physics is to take the beam axis as the  $z$ -axis and we define a quantity called the rapidity  $y$  [13]. It is given by,

$$y = \frac{1}{2} \ln \left( \frac{E + p_z c}{E - p_z c} \right) \quad (5.3)$$

where  $E$  is the energy of the particle,  $p_z$  is the  $z$ -component of momentum and  $c$  is the speed of light.

#### Pseudo-rapidity

The problem with rapidity is that it can be hard to measure for highly relativistic particles, we need both the energy and the total momentum, and it is hard to get the total momentum in reality, especially when the  $z$ -component of momentum is large, in this case there is a quantity that is almost the same thing as the rapidity which is much easier to measure than  $y$  for highly energetic particles. This leads to the concept of pseudo-rapidity  $\eta$  [13], we define it as :

$$\eta = -\ln[\tan(\theta/2)] \quad (5.4)$$

where  $\theta$  is the angle made by the particle trajectory with  $z$ -axis (in general case), where  $\cos \theta = \frac{p_z}{p}$ .

#### Transverse mass, transverse energy and transverse momentum

The transverse quantities are very important in particle and experimental physics especially when we study collision processes and results of the reactions, in absence of information about the longitudinal components of the four-vectors, useful information on the decay can still be extracted by restricting our attention to the accessible quantities, that are in general energies and momenta measured in the transverse plane [14].

We start with the transverse mass. This quantity is very important since it is invariant under Lorentz boosts along the  $z$  direction (as a convention in general), it is defined by:

$$m_T = m^2 + p_x^2 + p_y^2 = E^2 - p_z^2 \quad (5.5)$$

where the  $z$ -direction is the direction of motion.

This definition of the transverse mass is used in conjunction with the definition of the transverse energy,

$$E_T = E \cdot \frac{p_T}{|p|} = \frac{E}{\sqrt{E^2 - m^2}} \cdot p_T \quad (5.6)$$

with the transverse momentum  $p_T = \begin{pmatrix} p_x \\ p_y \\ 0 \end{pmatrix}$ .

It is easy to see that for vanishing mass ( $m = 0$ ) the three quantities are the same  $E_T = p_T = m_T$ . The transverse mass is used together with the rapidity, transverse momentum and polar angle in the parameterisation of the four-momentum of a single particle as follows,

$$(E, p_x, p_y, p_z) = (m_T \cosh y, p_T \cos \phi, p_T \sin \phi, m_T \sinh y). \quad (5.7)$$

### 5.1.3 Tools of automatic calculations

#### HIP package

The HIP program is a set of packages written in mathematica language. It allows to calculate the amplitudes and the squares of amplitudes of Feynman diagrams symbolically [4]. Here are some basic commands of this code :

- `PrepareIndex[ ]`: to declare the Lorentz indices ( $\mu, \nu \dots$ )
- `SetMass[ ]`: to declare the momenta and masses of particles ( $m_1, m_2 \dots$ )
- `SetReal[ ]`: to declare the real variables
- `SetMandelstam[ ]`: to express the amplitude in term of Mandelstam variables ( $S, U, T$ )
- `DiracGamma[ ]`: Dirac matrix ( $\gamma_{\mu \dots}$ )
- `SpinorU (V)[ ]`: Dirac spinor  $u(v)$
- `SpinorUbar (Vbar)[ ]`: Dirac spinor  $\bar{u}(\bar{v})$
- `Contract[ ]`: to contract on the Lorentz indices ( $g_{\mu\nu} p^\mu = p_\nu$ )
- `GammaTrace[ ]`: to calculate the traces of the matrices
- `AbsSquared[ ]`: to calculate the square of the amplitude ( $|M|^2$ )
- `DotProduct[ ]`: to calculate the dot product ( $p \cdot q$ )
- `MasslessVectorPolarisation[ ]`: massless gauge bosons polarization vector ( $\gamma \dots$ )
- `HeaveyVectorPolarisation[ ]`: massive gauge bosons polarization vector ( $W^\pm, Z \dots$ )

One can download this package from the Mathematica website <https://library.wolfram.com/infocenter/Articles/1080/>.

#### MadGraph5\_aMC@NLO program

MadGraph5\_aMC@NLO is a program which allows us to compute the hadronic cross section at the order LO and NLO. To install MadGraph5\_aMC@NLO we follow the next steps [15] :

- download MadGraph5\_aMC@NLO from : [//launchpad.net/madgraph5](http://launchpad.net/madgraph5)
- start the program with the command : `$/bin/mg5_aMC`
- to calculate the cross section at LO, we follow these steps:
  - **Importing the model:** `MG5_aMC>import model` (the Model name).
  - **Process generation:** generate `p p > i j`, in this step, MadGraph5\_aMC@NLO generates all the Feynman diagrams and the associated amplitudes.
  - **Output:** `MG5_aMC>output` to create the code that the cross section calculates (the Model name).
  - **Execution:** In this step, MadGraph5\_aMC@NLO calculates the cross section by the command `MG5_aMC>launch`.
- We can change the external settings like (center mass energy  $\sqrt{S}$ , number of events, mass of particles ...) in the cards inside the generated code.

## 5.2 Charged Current Processes

Let's first start with the process mediated by charged gauge bosons ( $W^\pm$ ) in Heavy Neutrino Model for both Dirac and Majorana types of neutrino, and ( $W_r^\pm$ ) in Left-Right Symmetric Model.

### 5.2.1 Heavy Neutrino Model (Dirac type)

One of the sub-processes of this reaction in this model is  $d(P1) + \bar{u}(P2) \rightarrow e^-(P3) + \bar{N}(P4)$ . The corresponding Feynman diagramme for this proces is,

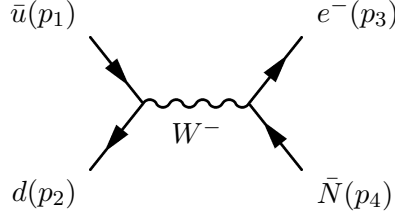


Figure 5.1: Feynman diagram of the charged current proces in HNM (Dirac type of neutrino).

- **The amplitude and its complex conjugate** for this proces are given by:

$$M = \frac{ig^2 \delta_{ij} \cos \theta_c V_{Ni}^*}{8(q^2 - m_W^2)} \left( \bar{v}_i(p_2) \not{3} \gamma^\mu (1 - \gamma_5) u_j(p_1) \bar{u}(p_3) \gamma_\mu (1 - \gamma_5) v(p_4) - \frac{1}{m_W^2} \bar{v}_i(p_2) \not{q} (1 - \gamma_5) u_j(p_2) \bar{u}(p_3) \not{q} (1 - \gamma_5) v(p_4) \right). \quad (5.8)$$

The complex conjugate of  $M$  is,

$$\bar{M} = \frac{-ig^2 \delta_{j'i'} \cos \theta_c V_{Ni}^*}{8(q^2 - m_W^2)} \left( \bar{u}_{j'}(p_1) \not{3} (1 + \gamma_5) \gamma^{\mu'} v_{i'}(p_2) \bar{v}(p_4) (1 + \gamma_5) \gamma_{\mu'} u(p_3) - \frac{1}{m_W^2} \bar{u}_{j'}(p_1) (1 + \gamma_5) \not{q} v_{i'}(p_1) \bar{v}(p_4) (1 + \gamma_5) \not{q} u(p_3) \right) \quad (5.9)$$

now let use some relations to simplify the calculations:

$$\not{p} u(p) = m \quad \not{p} v(p) = -m \quad \bar{u}(p) \not{p} = m \quad \bar{v}(p) \not{p} = -m \quad (5.10)$$

$$\not{p}(1 - \gamma_5) = (1 + \gamma_5) \not{p} \quad (1 - \gamma_5)(1 + \gamma_5) = 0 \quad (1 - \gamma_5)^2 = 2(1 - \gamma_5) \quad (5.11)$$

and we have  $\not{q} = \not{p}_1 + \not{p}_2 = \not{p}_3 + \not{p}_4$ , so:

$$\begin{aligned} \bar{v}_i(p_2) (\not{q}) (1 - \gamma_5) u_j(p_1) &= \bar{v}_i(p_2) (\not{p}_1 + \not{p}_2) (1 - \gamma_5) u_j(p_1) \\ &= -m_u \bar{v}_i(p_2) (1 - \gamma_5) u_j(p_1) + m_d \bar{v}_j(p_2) (1 + \gamma_5) u_j(p_1) \end{aligned} \quad (5.12)$$

$$\begin{aligned} \bar{u}(p_3) (\not{q}) (1 - \gamma_5) v(p_4) &= \bar{u}(p_3) (\not{p}_3 + \not{p}_4) (1 - \gamma_5) v(p_4) \\ &= -m_e \bar{u}(p_3) (1 - \gamma_5) v(p_4) + m_N \bar{u}(p_3) (1 + \gamma_5) v(p_4). \end{aligned} \quad (5.13)$$

But the energy of the experiment is very large (13 TeV at **LHC** and 100 TeV in **the future colliders**), so we can neglect the mass of the quarks and light leptons ( $e^-$  for example), so if we put  $m_u = m_d = m_{e^-} = 0$  and  $m_N \neq 0$  we find :

$$\bar{v}_i(p_2)(\not{q})(1 - \gamma_5)u_j(p_1) = 0 \quad \bar{u}(p_3)(\not{q})(1 - \gamma_5)v(p_4) = 0 \quad (5.14)$$

so the amplitude in this case is,

$$M = \frac{ig^2 \delta_{ij} \cos \theta_c V_{NI}^*}{8(q^2 - m_W^2)} \bar{v}_i(p_2) 3 \gamma^\mu (1 - \gamma_5) u_j(p_1) \bar{u}(p_3) \gamma_\mu (1 - \gamma_5) v(p_4) \quad (5.15)$$

and it's complex conjugate is,

$$\bar{M} = \frac{-ig^2 \delta_{j'i'} \cos \theta_c V_{NI}}{8(q^2 - m_W^2)} \bar{u}_{j'}(p_1) 3 (1 + \gamma_5) \gamma^{\mu'} v_{i'}(p_2) \bar{v}(p_4) (1 + \gamma_5) \gamma^{\mu'} u(p_3). \quad (5.16)$$

- **The amplitude squared:**

To calculate the amplitude squared, we use the following relations on the Dirac spinors:

$$\sum u(p) \bar{u}(p) = \not{p} + m \quad \sum v(p) \bar{v}(p) = \not{p} - m \quad (5.17)$$

$$\sum u_i(p) \bar{u}_j(p) = (\not{p} + m) \delta_{ij} \quad \sum v_i(p) \bar{v}_j(p) = (\not{p} - m) \delta_{ij} \quad (5.18)$$

so

$$\begin{aligned} \sum |M|^2 &= \frac{g^4 \cos^2 \theta_c (V_{NI}^*)^2 \delta_{ij} \delta_{j'i'}}{4N^2 64 (q^2 - m_W^2)^2} \sum_{color} \sum_{spin} \bar{v}_i(p_2) 3 \gamma^\mu (1 - \gamma_5) u_j(p_1) \bar{u}_{j'}(p_1) 3 (1 + \gamma_5) \\ &\quad \gamma^{\mu'} v_{i'}(p_2) \bar{u}(p_3) \gamma_\mu (1 - \gamma_5) v(p_4) \end{aligned} \quad (5.19)$$

$$\begin{aligned} &= \frac{g^4 \cos^2 \theta_c (V_{NI}^*)^2 \delta_{ij} \delta_{j'i'}}{4N^2 64 (q^2 - m_W^2)^2} \sum_{color} \sum_{s_2, s_4} \bar{v}_i(p_2) \gamma^\mu (1 - \gamma_5) \left( \sum_{s_1} u(p_1)_j \bar{u}_{j'}(p_1) 3 \right) \\ &\quad \times \gamma^{\mu'} (1 - \gamma_5) v_{i'}(p_2) \bar{u}(p_3) \gamma_\mu \left( \sum_{s_4} v(p_4) \bar{v}(p_4) \right) (1 + \gamma_5) \gamma^{\mu'} u(p_3) \end{aligned} \quad (5.20)$$

we take into consideration that  $m_u = m_d = m_{e^-} = 0$  and  $m_N \neq 0$ , so we get:

$$\begin{aligned} \sum |M|^2 &= \frac{g^4 \cos^2 \theta_c (V_{NI}^*)^2 \delta_{ij} \delta_{j'i'} \delta_{jj'}}{4N^2 64 (q^2 - m_W^2)^2} \sum_{color} \sum_{s_2, s_4} \bar{v}_i(p_2) \gamma^\mu (1 - \gamma_5) \not{p}_1 \gamma^\mu (1 - \gamma_5) v_{i'}(p_2) \bar{u}(p_3) \gamma_\mu \\ &\quad \times (\not{p}_4 - m_N) (1 + \gamma_5) \gamma^{\mu'} u(p_3) \end{aligned} \quad (5.21)$$

$$\begin{aligned} &= \frac{g^4 \cos^2 \theta_c (V_{NI}^*)^2 \delta_{ij} \delta_{j'i'} \delta_{jj'} \delta_{ii'}}{4N^2 64 (q^2 - m_W^2)^2} \text{Tr}[\not{p}_2 \gamma^\mu (1 - \gamma_5) \not{p}_1 (1 + \gamma_5) \gamma^{\mu'}] \\ &\quad \times \text{Tr}[\not{p}_3 \gamma_\mu (1 - \gamma_5) (\not{p}_4 - m_N) (1 + \gamma_5) \gamma_{\mu'}] \end{aligned} \quad (5.22)$$

to simplify it, we use the relation  $\delta_{ij} \delta_{j'i'} \delta_{jj'} \delta_{ii'} = \delta_{ii} = N = 3$  (3 colors for quarks) and some trace relations and  $\gamma_5$  properties, we find:

$$\begin{aligned} \text{Tr}[\gamma^\alpha \gamma^\beta \gamma^\mu \gamma^{\mu'}] &= 4(g^{\alpha\beta} g^{\mu\mu'} - g^{\alpha\mu} g^{\beta\mu'} + g^{\alpha\mu'} g^{\beta\mu}) \\ \text{Tr}[\gamma_5 \gamma_\alpha \gamma_\beta \gamma_\mu \gamma_{\mu'}] &= 4i \xi \gamma_\alpha \gamma_\beta \gamma_\mu \gamma_{\mu'} \end{aligned} \quad (5.23)$$



so,

$$\begin{aligned}
\text{Tr}[\not{p}_2 \gamma^\mu (1 - \gamma_5) \not{p}_1 \gamma^{\mu'}] &= \text{Tr}[\not{p}_2 \gamma^\mu \not{p}_1 \gamma^{\mu'}] - \text{Tr}[\gamma_5 \not{p}_1 \gamma^{\mu'} \not{p}_2 \gamma^\mu] \\
&= 4p_2^\beta p_1^\alpha (g^{\beta\mu} g^{\alpha\mu'} - g^{\beta\alpha} g^{\mu\mu'} + g^{\beta\mu'} g^{\alpha\mu}) - 4i\xi^{\not{p}_1 \gamma^{\mu'} \not{p}_2 \gamma^\mu} \\
&= 4(p_2^\mu p_1^{\mu'} - p_1 \cdot p_2 g^{\mu\mu'} + p_2^{\mu'} p_1^\mu) - 4i\xi^{\not{p}_1 \gamma^{\mu'} \not{p}_2 \gamma^\mu} \quad (5.24)
\end{aligned}$$

$$\begin{aligned}
\text{Tr}[\not{p}_3 \gamma_\mu (1 - \gamma_5) \not{p}_4 \gamma_{\mu'}] &= \text{Tr}[\not{p}_3 \gamma_\mu \not{p}_4 \gamma_{\mu'}] - \text{Tr}[\gamma_5 \not{p}_4 \gamma_{\mu'} \not{p}_3 \gamma_\mu] \\
&= 4p_3^\beta p_4^\alpha (g_{\beta\mu} g_{\alpha\mu'} - g_{\beta\alpha} g_{\mu\mu'} + g_{\beta\mu'} g_{\mu\alpha}) - 4i\xi_{\not{p}_4 \gamma_{\mu'} \not{p}_3 \gamma_\mu} \\
&= 4(p_3^\mu p_4^{\mu'} - p_4 \cdot p_3 g_{\mu\mu'} + p_3^{\mu'} p_4^\mu) - 4i\xi_{\not{p}_4 \gamma_{\mu'} \not{p}_3 \gamma_\mu} \quad (5.25)
\end{aligned}$$

The amplitude squared is:

$$\begin{aligned}
\sum |M|^2 &= \frac{g^4 \cos^2 \theta_c (V^{*2} Nl)}{12(q^2 - m_W^2)^2} \left( 4(p_2^\mu p_1^{\mu'} - p_1 \cdot p_2 g^{\mu\mu'} + p_2^{\mu'} p_1^\mu) - 4i\xi^{\not{p}_1 \gamma^{\mu'} \not{p}_2 \gamma^\mu} \right) \\
&\times \left( 4(p_3^\mu p_4^{\mu'} - p_4 \cdot p_3 g_{\mu\mu'} + p_3^{\mu'} p_4^\mu) - 4i\xi_{\not{p}_4 \gamma_{\mu'} \not{p}_3 \gamma_\mu} \right) \\
&= \frac{g^4 \cos^2 \theta_c (V^{*2} Nl)}{12(q^2 - m_W^2)^2} \left[ \left( (p_2^\mu p_1^{\mu'} - p_1 \cdot p_2 g^{\mu\mu'} + p_2^{\mu'} p_1^\mu) (p_3^\mu p_4^{\mu'} - p_4 \cdot p_3 g_{\mu\mu'} + p_3^{\mu'} p_4^\mu) \right) \right. \\
&- i \left( (p_2^\mu p_1^{\mu'} - p_1 \cdot p_2 g^{\mu\mu'} + p_2^{\mu'} p_1^\mu) \xi_{\not{p}_4 \gamma_{\mu'} \not{p}_3 \gamma_\mu} \right) - i \left( \xi^{\not{p}_1 \gamma^{\mu'} \not{p}_2 \gamma^\mu} (p_3^\mu p_4^{\mu'} - p_4 \cdot p_3 g_{\mu\mu'} + p_3^{\mu'} p_4^\mu) \right) \\
&\left. - \left( \xi^{\not{p}_1 \gamma^{\mu'} \not{p}_2 \gamma^\mu} \xi_{\not{p}_4 \gamma_{\mu'} \not{p}_3 \gamma_\mu} \right) \right] \quad (5.26)
\end{aligned}$$

$$\begin{aligned}
\sum |M|^2 &= \frac{g^4 \cos^2 \theta_c (V^{*2} Nl)}{12(q^2 - m_W^2)^2} \left[ \left( p_1 \cdot p_4 p_2 \cdot p_3 - p_1 \cdot p_2 p_3 \cdot p_4 - p_1 \cdot p_2 p_3 \cdot p_4 + 4p_1 \cdot p_2 p_3 \cdot p_4 - p_1 \cdot p_2 p_3 \cdot p_4 \right. \right. \\
&\left. \left. + p_1 \cdot p_3 p_2 \cdot p_4 - p_1 \cdot p_2 p_3 \cdot p_4 + p_1 \cdot p_4 p_2 \cdot p_3 \right) - i \left( \overbrace{(p_2^\mu p_1^{\mu'} - p_1 \cdot p_2 g^{\mu\mu'} + p_2^{\mu'} p_1^\mu) \xi_{\not{p}_4 \gamma_{\mu'} \not{p}_3 \gamma_\mu}}^{\text{sym} \times \text{anti-sym} = 0} \right) \right. \\
&\left. - i \left( \overbrace{\xi^{\not{p}_1 \gamma^{\mu'} \not{p}_2 \gamma^\mu} (p_3^\mu p_4^{\mu'} - p_4 \cdot p_3 g_{\mu\mu'} + p_3^{\mu'} p_4^\mu)}^{\text{sym} \times \text{anti-sym} = 0} \right) - \left( \xi^{\not{p}_1 \gamma^{\mu'} \not{p}_2 \gamma^\mu} \xi_{\not{p}_4 \gamma_{\mu'} \not{p}_3 \gamma_\mu} \right) \right] \quad (5.27)
\end{aligned}$$

if we used antisymmetric properties of the tensor  $\xi$  and the property:

$\xi^{\gamma^\alpha \gamma^\beta \gamma^\mu \gamma^\nu} \xi_{\gamma^\alpha \gamma^\beta \gamma^\delta \gamma^\sigma} = -2(g_\delta^\mu g_\sigma^\nu - g_\sigma^\mu g_\delta^\nu)$ , we get:

$$\begin{aligned}
\sum |M|^2 &= \frac{g^4 \cos^2 \theta_c (V^{*2} Nl)}{12(q^2 - m_W^2)^2} \left( 2p_1 \cdot p_4 p_2 \cdot p_3 + 2p_1 \cdot p_3 p_2 \cdot p_4 + \xi^{\gamma^\mu \gamma^{\mu'} \not{p}_1 \not{p}_2} \xi_{\gamma^\mu \gamma^{\mu'} \not{p}_3 \not{p}_4} \right) \\
&= \frac{g^4 \cos^2 \theta_c (V^{*2} Nl)}{12(q^2 - m_W^2)^2} \left( 2p_1 \cdot p_4 p_2 \cdot p_3 + 2p_1 \cdot p_3 p_2 \cdot p_4 - 2p_{1\alpha} p_{2\beta} p_3^\delta p_4^\sigma (g_\delta^\alpha g_\sigma^\beta - g_\sigma^\alpha g_\delta^\beta) \right) \quad (5.28)
\end{aligned}$$

$$\sum |M|^2 = \frac{g^4 \cos^2 \theta_c (V^{*2} Nl)}{3(q^2 - m_W^2)^2} p_1 \cdot p_4 p_2 \cdot p_3. \quad (5.29)$$

- The amplitude squared as a function of MandelStam variables:

The Mandelstam variables are:

$$s = (p_1 + p_2)^2 = (p_3 + p_4)^2 \quad t = (p_1 - p_3)^2 = (p_2 - p_4)^2 \quad u = (p_1 - p_4)^2 = (p_2 - p_3)^2 \quad (5.30)$$

$$\begin{aligned}
s &= p_1^2 + p_2^2 + 2p_1 \cdot p_2 = p_3^2 + p_2^2 + 2p_3 \cdot p_4 \Rightarrow s = 2p_1 p_2 = m_N^2 + 2p_3 \cdot p_4 \\
t &= p_1^2 + p_3^2 - p_1 \cdot p_3 = p_2^2 + p_4^2 - 2p_2 \cdot p_4 \Rightarrow t = -2p_1 p_3 = m_N^2 - 2p_2 \cdot p_4 \\
u &= p_1^2 + p_4^2 - 2p_1 \cdot p_4 = p_2^2 + p_3^2 - 2p_2 \cdot p_3 \Rightarrow u = m_N^2 - 2p_1 p_4 = -2p_2 \cdot p_3
\end{aligned} \tag{5.31}$$

so

$$\left\{ \begin{array}{l} p_1 \cdot p_2 = \frac{s}{2} \\ p_3 \cdot p_4 = \frac{s - m_N^2}{2} \end{array} \right. \quad \left\{ \begin{array}{l} p_1 \cdot p_3 = \frac{-t}{2} \\ p_2 \cdot p_4 = \frac{m_N^2 - s}{2} \end{array} \right. \quad \left\{ \begin{array}{l} p_1 \cdot p_4 = \frac{m_N^2 - u}{2} \\ p_2 \cdot p_3 = \frac{-u}{2} \end{array} \right.$$

the amplitude squared become:

$$\sum |M|^2 = \frac{g^4 \cos^2 \theta_c (V_{Nl}^{*2})}{12(2p_1 \cdot p_2 - m_W^2)^2} \left( (u - m_N^2) u \right) \tag{5.32}$$

• **The amplitude squared in center of mass rference (CM):**

To calculate the cross section we need to write the amplitude squared in CM frame. The 4-momunta of the external particles in this frame are:

$$p_1 = \frac{\sqrt{s}}{2} \begin{pmatrix} 1 \\ 0 \\ 0 \\ 1 \end{pmatrix} \quad p_2 = \frac{\sqrt{s}}{2} \begin{pmatrix} 1 \\ 0 \\ 0 \\ -1 \end{pmatrix} \quad p_3 = \begin{pmatrix} E_3 \\ \rho \sin \theta \\ 0 \\ \rho \cos \theta \end{pmatrix} \quad p_4 = \begin{pmatrix} E_4 \\ -\rho \sin \theta \\ 0 \\ -\rho \cos \theta \end{pmatrix} \tag{5.33}$$

to find  $\rho$  we use the general formula of energies, where we find in our case:

$$\left\{ \begin{array}{l} E_3 = \frac{s + m_3^2 - m_4^2}{2\sqrt{s}} \\ E_4 = \frac{s + m_4^2 - m_3^2}{2\sqrt{s}} \end{array} \right. \Rightarrow \left\{ \begin{array}{l} E_3 = \frac{s - m_N^2}{2\sqrt{s}} \\ E_4 = \frac{s + m_N^2}{2\sqrt{s}} \end{array} \right. \tag{5.34}$$

and we have,

$$\begin{aligned}
p_3^2 &= E_3^2 - \rho^2 = 0 \Rightarrow \rho = E_3 \\
p_4^2 &= E_4^2 - \rho^2 = m_N^2 \Rightarrow \rho = \sqrt{E_4^2 - m_N^2}.
\end{aligned} \tag{5.35}$$

So,

$$\rho = \frac{s - m_N^2}{2\sqrt{s}} = \frac{\sqrt{s}}{2} \left( 1 - \frac{m_N^2}{s} \right) \tag{5.36}$$

The MandelStam variables  $u$  and  $t$  are written as :

$$u = (p_1 - p_4)^2 = \begin{pmatrix} \frac{-m_N^2}{2\sqrt{s}} \\ \rho \sin \theta \\ 0 \\ 1 + \rho \cos \theta \end{pmatrix} \cdot \begin{pmatrix} \frac{-m_N^2}{2\sqrt{s}} & \rho \sin \theta & 0 & 1 + \rho \cos \theta \end{pmatrix} \tag{5.37}$$

$$\begin{aligned}
u &= \frac{m_N^4}{4s} - \rho^2 \sin^2 \theta - (1 - \rho \cos \theta)^2 = \frac{m_N^4}{4s} - 1 - \rho^2 - 2 \cos \theta \\
&= \frac{m_N^4}{4s} - 1 - \frac{s}{4} \left(1 - \frac{m_N^2}{s}\right)^2 - \sqrt{s} \left(1 - \frac{m_N^2}{s}\right) \cos \theta \\
&= \frac{m_N^4}{4s} - 1 - \frac{s}{4} \left(1 + \frac{m_N^4}{s^2} - \frac{2m_N^2}{s}\right) - \sqrt{s} \left(1 - \frac{m_N^2}{s}\right) \cos \theta
\end{aligned} \tag{5.38}$$

$$u = \frac{m_N^2}{2} - \frac{s}{4} - 1 - \sqrt{s} \left(1 - \frac{m_N^2}{s}\right) \cos \theta \tag{5.39}$$

$$t = (p_1 - p_3)^2 = \begin{pmatrix} \frac{-m_N^2}{2\sqrt{s}} \\ \rho \sin \theta \\ 0 \\ 1 + \rho \cos \theta \end{pmatrix} \cdot \begin{pmatrix} \frac{-m_N^2}{2\sqrt{s}} & \rho \sin \theta & 0 & 1 + \rho \cos \theta \end{pmatrix} \tag{5.40}$$

$$\begin{aligned}
t &= \frac{m_N^4}{4s} - \rho^2 \sin^2 \theta - (1 - \rho \cos \theta)^2 = \frac{m_N^4}{4s} - 1 - \rho^2 - 2 \cos \theta \\
&= \frac{m_N^4}{4s} - 1 - \frac{s}{4} \left(1 + \frac{m_N^4}{s^2} - \frac{2m_N^2}{s}\right) - \sqrt{s} \left(1 - \frac{m_N^2}{s}\right) \cos \theta
\end{aligned} \tag{5.41}$$

$$t = \frac{m_N^2}{2} - \frac{s}{4} - 1 - \sqrt{s} \left(1 - \frac{m_N^2}{s}\right) \cos \theta \tag{5.42}$$

if we put the value of  $t$  in the expression of the amplitude, we get:

$$\begin{aligned}
\sum |M|^2 &= \frac{g^4 \cos^2 \theta_c (V^{*2}{}_{Nl})}{12(s - m_W^2)^2} \left[ \left( \frac{m_N^2}{2} - \frac{s}{4} - 1 - \sqrt{s} \left(1 - \frac{m_N^2}{s}\right) \cos \theta \right)^2 \right. \\
&\quad \left. - m_N^2 \left( \frac{m_N^2}{2} - \frac{s}{4} - 1 - \sqrt{s} \left(1 - \frac{m_N^2}{s}\right) \cos \theta \right) \right]
\end{aligned} \tag{5.43}$$

$$\begin{aligned}
\Rightarrow \sum |M|^2 &= \frac{g^4 \cos^2 \theta_c (V^{*2}{}_{Nl})}{12(s - m_W^2)^2} \left[ \left( \frac{m_N^2}{2} - \frac{s}{4} - 1 \right)^2 + s \left(1 - \frac{m_N^2}{s}\right)^2 \cos^2 \theta \right. \\
&\quad \left. + \left( 2 \left( \frac{m_N^2}{2} - \frac{s}{4} - 1 \right) \sqrt{s} \left( \frac{m_N^2}{s} - 1 \right) + m_N^2 \left( \frac{m_N^2}{2} - \frac{s}{4} - 1 - \sqrt{s} \left(1 - \frac{m_N^2}{s}\right) \cos \theta \right) \right) \cos \theta \right].
\end{aligned} \tag{5.44}$$

• **Partonic cross section:**

Now we calculate the partonic cross section,

$$\hat{\sigma} = \frac{1}{4 \sqrt{(p_1 \cdot p_2)^2 - m_1^2 m_2^2}} \frac{1}{(2\pi)^2} \int \delta^4(p_1 + p_2 - p_3 - p_4) \frac{d^3 \vec{p}_3}{2E_3} \frac{d^3 \vec{p}_4}{2E_4} \overline{\sum} |M|^2 \tag{5.45}$$

but  $m_u = m_d = me^- = 0$  and  $m_N \neq 0$ , so

$$\begin{aligned}\hat{\sigma} &= \frac{1}{4\sqrt{(p_1 \cdot p_2)^2}} \frac{1}{(2\pi)^2} \int \delta^4(p_1 + p_2 - p_3 - p_4) \frac{d^3\vec{p}_3}{2E_3} \frac{d^3\vec{p}_4}{2E_4} \overline{\sum} |M|^2 \\ &= \frac{1}{2s(2\pi)^2} \int \delta^4(p_1 + p_2 - p_3 - p_4) \frac{d^3\vec{p}_3}{2E_3} \frac{d^3\vec{p}_4}{2E_4} \overline{\sum} |M|^2\end{aligned}\quad (5.46)$$

we use the relation  $\int \frac{d^3\vec{p}_4}{2E_4} = \int d^4p_4 \delta^+(p_4^2 - m_N^2)$ , so

$$\hat{\sigma} = \frac{1}{2s(2\pi)^2} \int \frac{d^3\vec{p}_3}{2E_3} \delta^+((p_1 + p_2 - p_3)^2 - m_N^2) \overline{\sum} |M|^2 \quad (5.47)$$

in CM frame we have that:

$$\begin{aligned}(p_1 + p_2 + p_3)^2 &= (p_1 + p_2)^2 + p_3^2 + 2p_3 \cdot (p_1 + p_2) \\ &= s^2 - 2(E_3 - \vec{p}_3) \cdot \begin{pmatrix} \sqrt{s} \\ \vec{p}_3 \end{pmatrix} = s^2 - 2E_3\sqrt{s}\end{aligned}\quad (5.48)$$

but  $p_3^2 = 0 = E_3^2 - |\vec{p}_3|^2 \Rightarrow E_3 = |\vec{p}_3|$  so  $(p_1 + p_2 + p_3)^2 = (s - 2|\vec{p}_3|\sqrt{s})$  so from it we get

$$\delta^+((p_1 + p_2 + p_3)^2 - m_N^2) = \delta^+(s - 2|\vec{p}_3|\sqrt{s} - m_N^2) \quad (5.49)$$

now we use the following relation:

$$\delta(g(x)) = \frac{\delta(x - x_i)}{|g'(x_i)|} \quad (5.50)$$

with  $g(x_i) = 0$ . So,

$$g(x) \rightarrow s - 2|\vec{p}_3|\sqrt{s} - m_N^2 \Rightarrow \begin{cases} g(x_i) = 0 \rightarrow s - 2|\vec{p}_3|\sqrt{s} - m_N^2 = 0 \\ |\vec{p}_3|_i = \frac{s - m_N^2}{2\sqrt{s}} \end{cases} \quad (5.51)$$

and

$$g'(x_i) \Rightarrow -2\sqrt{s} \quad (5.52)$$

we get:

$$\delta(g(x_i)) \Rightarrow \frac{|\vec{p}_3| - \left(\frac{s - m_N^2}{2\sqrt{s}}\right)}{2\sqrt{s}}. \quad (5.53)$$

In the the spherical coordinates, we have  $\int d^3\vec{p}_3 = \int_0^{2\pi} \int_0^\pi |\vec{p}_3|^2 d|\vec{p}_3| \sin\theta d\theta d\phi$  to simplify the calculations, we get:

$$\begin{aligned}\Rightarrow \hat{\sigma} &= \frac{1}{8s\pi} \int_0^\pi \int_0^\pi |\vec{p}_3| d|\vec{p}_3| \frac{\left(|\vec{p}_3| - \frac{s - m_N^2}{2\sqrt{s}}\right)}{2\sqrt{s}} \sin\theta d\theta \overline{\sum} |M|^2 \\ &= \frac{1}{8s\pi} \int_0^\pi \frac{(s - m_N^2)}{4s} \sin\theta d\theta \overline{\sum} |M|^2\end{aligned}\quad (5.54)$$

puting expression of the amplitude  $\overline{\sum}|M|^2$  in the previous relation, gives us:

$$\hat{\sigma} = \frac{g^4 \cos^2 \theta_c (V^{*2}_{NI})}{384s^2 (s - m_W^2)^2} (s - m_N^2) \int_0^\pi \left[ \left( \frac{m_N^2}{2} - \frac{s}{4} - 1 \right)^2 + s \left( 1 - \frac{m_N^2}{s} \right)^2 \cos^2 \theta \right. \\ \left. + \left( 2 \left( \frac{m_N^2}{2} - \frac{s}{4} - 1 \right) \sqrt{s} \left( \frac{m_N^2}{s} - 1 \right) + m_N^2 \left( \frac{m_N^2}{2} - \frac{s}{4} - 1 - \sqrt{s} \left( 1 - \frac{m_N^2}{s} \right) \right) \cos \theta \right) \sin \theta d\theta \right] \quad (5.55)$$

now we change the variable,

$$\cos \theta = X \quad \Rightarrow \quad dX = -\sin \theta d\theta \quad \text{and} \quad \begin{cases} \theta = 0 \\ \theta = \pi \end{cases} \quad \Rightarrow \quad \begin{cases} X = 1 \\ X = -1 \end{cases} \quad (5.56)$$

$$\Rightarrow \hat{\sigma} = \frac{g^4 \cos^2 \theta_c (V^{*2}_{NI})}{384s^2 (s - m_W^2)^2} (s - m_N^2) \int_{-1}^1 \left[ \left( \frac{m_N^2}{2} - \frac{s}{4} - 1 \right)^2 + s \left( 1 - \frac{m_N^2}{s} \right)^2 X^2 + \right. \\ \left. \left( 2 \left( \frac{m_N^2}{2} - \frac{s}{4} - 1 \right) \sqrt{s} \left( \frac{m_N^2}{s} - 1 \right) + m_N^2 \left( \frac{m_N^2}{2} - \frac{s}{4} - 1 - \sqrt{s} \left( 1 - \frac{m_N^2}{s} \right) \right) X \right) \right] dX \quad (5.57)$$

$$= \frac{g^4 \cos^2 \theta_c (V^{*2}_{NI})}{384s^2 (s - m_W^2)^2} (s - m_N^2) \left[ \left( \frac{m_N^2}{2} - \frac{s}{4} - 1 \right)^2 X + \frac{s}{3} \left( 1 - \frac{m_N^2}{s} \right)^2 X^3 + \right. \\ \left. \frac{1}{2} \left( 2 \left( \frac{m_N^2}{2} - \frac{s}{4} - 1 \right) \sqrt{s} \left( \frac{m_N^2}{s} - 1 \right) + m_N^2 \left( \frac{m_N^2}{2} - \frac{s}{4} - 1 - \sqrt{s} \left( 1 - \frac{m_N^2}{s} \right) \right) X^2 \right) \right]_{-1}^1 \quad (5.58)$$

$$(5.59)$$

$$\hat{\sigma} = \frac{g^4 \cos^2 \theta_c (V^{*2}_{NI})}{192s^2 (s - m_W^2)^2} (s - m_N^2) \left[ \left( \frac{m_N^2}{2} - \frac{s}{4} - 1 \right)^2 + \frac{s}{3} \left( 1 - \frac{m_N^2}{s} \right)^2 \right]. \quad (5.60)$$

### 5.2.2 Heavy Neutrino Model (Majorana type)

We do the same calculations in the HNM (Majorana type), but in this case we do not calculate analytically, instead of that we use some programs of calculation as **Mathematic**, **Hip**, **FeynRules**, and **MadGraph5\_aMC@NLO** to calculate the amplitudes, cross sections and decay rate numerically. The charged current process in this model is:  $d(P1) + \bar{u}(P2) \rightarrow e^-(P3) + N(P4)$ , the Feynman diagramme is:

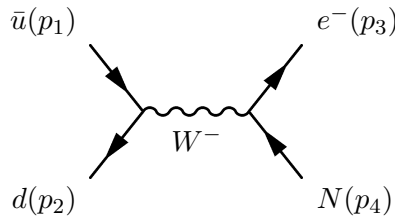


Figure 5.2: Feynman diagram of the charged current process in HNM (Majorana type of neutrino).

**The amplitude of this process is given by:**

$$M = \frac{ig^2 \delta_{ij} \cos \theta_c V_{NI}^*}{8(q^2 - m_W^2)} \left( \bar{v}_i(p_2) \not{3} \gamma^\mu (1 - \gamma_5) u_j(p_1) \bar{u}(p_3) \gamma_\mu (1 - \gamma_5) v(p_4) - \frac{1}{m_W^2} \bar{v}_i(p_2) \not{q} (1 - \gamma_5) u_j(p_2) \right. \\ \left. \times \bar{u}(p_3) \not{q} (1 - \gamma_5) v(p_4) \right) \quad (5.61)$$

it should be noted that the vertices in Feynman diagram in this model are the same of the previous model. Therefore, the results will be the same. The only difference is in the type of neutrino which is Majorana in this case, but this does not affect on the results. To calculate the **amplitude squared**, we use **Hip** according to the following steps:

- After installing Hip, we called it on Mathematica and putting the following commands:

```
Exit[ ]
<< /home/yassin/master/hip/work.m
```

- we put the information about the Particles that will participate in process

```
PrepareIndex[mu, mup, nu, nup, mu1, mu2]
SetMass[p1, 0, p2, 0, p3, 0, p4, mN]
(*SetMandelstam[p1, p2, p3, p4, 0, 0, 0, mN, S, T, U]*)
SetReal[mN, Mw, V, cos, ct, gg]
k = p1 + p2
```

- putting the amplitude value in the programe

```
M = (gg^2*cos*V)*SpinorVbar[p2]**g[mu]**(1-g5)**SpinorU[p1]**(G[mu, nu] - k[mu]*
*k[nu]/Mw^2)**
SpinorUbar[p3]**g[nu]**(1-g5)**SpinorV[p4]/8/(p[k, k] - Mw^2)
The amplitude squared:
```

- now we put this commands to calculate the amplitude squared

```
sqM = Simplify[Contract[Simplify[Contract[AbsSquared[M]/12, {mu, nu, Conjugate[mu],
Conjugate[nu]}]], {mu, nu, Conjugate[mu], Conjugate[nu]}]]
after we clicking on evaluate cell on all commands, we get the result
```

$$\frac{(\cos^2 g g^4 V^2 \text{DotProduct}[p1, p4] \text{DotProduct}[p2, p3])}{(3(Mw^2 - 2\text{DotProduct}[p1, p2])^2)} \quad (5.62)$$

so the result of the amplitude squared in this case is the same of the Dirac case,

$$\sum |M|^2 = \frac{g^4 \cos^2 \theta_c (V^{*2}_{NI})}{3(2p_1 \cdot p_2 - m_W^2)^2} p_1 \cdot p_4 p_2 \cdot p_3 \quad (5.63)$$

- **The amplitude squared as a function of MandelStam variables**

- To calculate it, we put the commands:

```
SetMandelstam[p1, p2, p3, p4, 0, 0, 0, mN, S, T, U]
sqMstu = Simplify[sqM]
we get the result
```

$$\frac{-(\cos^2 g g^4 (mN^2 - U) UV^2)}{(12(Mw^2 - S)^2)} \quad (5.64)$$

so,

$$\sum |M|^2 = \frac{g^4 \cos^2 \theta_c (V^{*2}_{NI})}{12(s - m_W^2)^2} \left( (u - m_N^2) u \right) \quad (5.65)$$

**The amplitude squared in CM frame:**

- We must put the value of Mandelstam variables in mass center frame (to calculate the amplitude squared) by putting the following commands

```
sqMthe = Simplify[sqMstu /. {T -> ((mN^2)/2) - (S/4) - 1 - Sqrt[S] * (1 - mN^2/S) *
cos theta, U -> ((mN^2)/2) - (S/4) - 1 - Sqrt[S] * (1 - mN^2/S) * cos theta}
```

we get the result

$$\frac{1}{(192(Mw^2 - S)^2 S)} \cos^2 g g^4 (-4ct(mN^2 - S) + Sqrt[S](4 - 2mN^2 + S))(-4ct(mN^2 - S) + Sqrt[S](4 + 2mN^2 + S))V^2$$

so after simplifying, we get:

$$\begin{aligned} \sum |M|^2 = & \frac{g^4 \cos^2 \theta_c (V^{*2}_{Nl})}{12(s - m_W^2)^2} \left[ \left( \frac{m_N^2}{2} - \frac{s}{4} - 1 \right)^2 + s \left( 1 - \frac{m_N^2}{s} \right)^2 \cos^2 \theta \right. \\ & \left. + \left( 2 \left( \frac{m_N^2}{2} - \frac{s}{4} - 1 \right) \sqrt{s} \left( \frac{m_N^2}{s} - 1 \right) + m_N^2 \left( \frac{m_N^2}{2} - \frac{s}{4} - 1 - \sqrt{s} \left( 1 - \frac{m_N^2}{s} \right) \right) \right) \cos \theta \right]. \end{aligned} \quad (5.66)$$

- **Partonic cross section:**

We calculated the partonic cross section analytically as in the previous model, and since the amplitude and it's squared is the same of Dirac case, we get the same result :

$$\hat{\sigma} = \frac{g^4 \cos^2 \theta_c (V^{*2}_{Nl})}{192s^2 (s - m_W^2)^2} (s - m_N^2) \left[ \left( \frac{m_N^2}{2} - \frac{s}{4} - 1 \right)^2 + \frac{s}{3} \left( 1 - \frac{m_N^2}{s} \right)^2 \right] \quad (5.67)$$

### 5.2.3 Left-Right Symmetric Model

Now we want to see the same process (charged current) and studying it in LRSM, therefore to know the diffrens between the propriety of the produced heavy neutino in this model and the previous models, to do that we going to calculate numerically. We use the same computational steps as we calculated in HNM, Majorana case and the same tools (Mathematica, Hip, FeynRules and MadGraph).

The charged current process in this model is:  $d(P1) + \bar{u}(P2) \rightarrow e^-(P3) + N(P4)$ , and Feynman diagramme is:

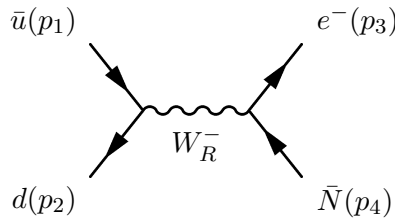


Figure 5.3: Feynman diagram of the charged current process in LRSM (Majorana type of neutrino).

**The amplitude:**

$$\begin{aligned} M = & \frac{ig^2 \delta_{ij} (K_r^q)^2 V_{ij}^{CKM} Y_{lm}}{8(q^2 - m_{W_r}^2)} \left( \bar{v}_i(p_2) \not{3} \gamma^\mu (1 + \gamma_5) u_j(p_1) \bar{u}(p_3) \gamma_\mu (1 - \gamma_5) v(p_4) \right. \\ & \left. - \frac{1}{m_{W_r}^2} \bar{v}_i(p_2) \not{q} (1 + \gamma_5) u_j(p_2) \times \bar{u}(p_3) \not{q} (1 - \gamma_5) v(p_4) \right) \end{aligned} \quad (5.68)$$

We going now to use the same commands that we used in Majorana type With a difference in some points in the commands, this is due to the difference in the process on `MadGraph`, and therefore the location of the file on the computer differs and some names in constants and bosons. But in general the method is the same. So after the computational steps, we get :

- **The amplitude squared:**

$$\sum |M|^2 = \frac{g^4(K_r^q)^4(V_{ij}^{CKM})^2(Y_{lm})^2}{3(2p_1 \cdot p_2 - m_{W_r}^2)^2} p_1 \cdot p_4 p_2 \cdot p_3 \quad (5.69)$$

- **The amplitude squared as a function of MandelStam variables:**

$$\sum |M|^2 = \frac{g^4(K_r^q)^4(V_{ij}^{CKM})^2(Y_{lm})^2}{12(s - m_{W_r}^2)^2} \left( (u - m_N^2)u \right) \quad (5.70)$$

- **Amplitude square in CM frame:**

$$\begin{aligned} \sum |M|^2 = & \frac{g^4(K_r^q)^4(V_{ij}^{CKM})^2(Y_{lm})^2}{12(s - m_{W_r}^2)^2} \left[ \left( \frac{m_N^2}{2} - \frac{s}{4} - 1 \right)^2 + s \left( 1 - \frac{m_N^2}{s} \right)^2 \cos^2 \theta \right. \\ & \left. + \left( 2 \left( \frac{m_N^2}{2} - \frac{s}{4} - 1 \right) \sqrt{s} \left( \frac{m_N^2}{s} - 1 \right) + m_N^2 \left( \frac{m_N^2}{2} - \frac{s}{4} - 1 - \sqrt{s} \left( 1 - \frac{m_N^2}{s} \right) \right) \cos \theta \right) \right] \end{aligned} \quad (5.71)$$

- **Partonic cross section:** We calculated the cross section analytically as in the previous models, we got the result:

$$\hat{\sigma} = \frac{g^4(K_r^q)^4(V_{ij}^{CKM})^2(Y_{lm})^2}{192s^2(s - m_{W_r}^2)^2} (s - m_N^2) \left[ \left( \frac{m_N^2}{2} - \frac{s}{4} - 1 \right)^2 + \frac{s}{3} \left( 1 - \frac{m_N^2}{s} \right)^2 \right] \quad (5.72)$$

#### 5.2.4 Variation of the Cross Section in Term of Heavy Neutrino Mass

In this section we going to study the variation of the hadronic cross section as a function of the mass of the produced heavy neutrino  $\bar{N}$  (Dirac case), ( $N$ ) (Majorana case). We remind that the numerical calculation is performed by `MadGraph5`, where we have created the codes that enable us to compute the hadronic cross section numerically for different masses and parameters for each model.

- Here's the directories that contain those codes:

```
cd master/MG5_aMC_v2_5_4/pp_en1_Dirac_lo/ [in Heavy Neutrino Model (Dirac type)]
cd master/MG5_aMC_v2_5_4/pp_en1_lo/ [in Heavy Neutrino Model (Majorana type)]
cd master/MG5_aMC_v2_5_4/pp_en1_LR_lo/ [in LR-Symmetric Model]
```

- To change the masses, one has to go to the file `param_card.dat` inside the directory `Cards`:

```
cd Cards/
gedit param_card.dat
```

- The `param card.dat` looks like the following:

we get a different result for the hadronic cross section every time we change the value of mass, the values that we choose and the hadronic cross section results that we got in charged current processes are summarized in the following tables:



```

#####
#####
## INFORMATION FOR LOOP
#####
Block Loop
  1 9.118800e+01 # MU_R

#####
## INFORMATION FOR MASS
#####
Block mass
  5 4.700000e+00 # MB
  6 1.733000e+02 # MT
 15 1.777000e+00 # MTA
 23 9.118760e+01 # MZ
 25 1.257000e+02 # MH
9990012 5.000000e+02 # mN1
9990014 5.000000e+02 # mN2
9990016 1.000000e+03 # mN3
## Dependent parameters, given by model restrictions.
## Those values should be edited following the
## analytical expression. MG5 ignores those values
## but they are important for interfacing the output of MG5
## to external program such as Pythia.
 1 0.000000 # d : 0.0
 2 0.000000 # u : 0.0
 3 0.000000 # s : 0.0
 4 0.000000 # c : 0.0
11 0.000000 # e- : 0.0
12 0.000000 # ve : 0.0
13 0.000000 # mu- : 0.0
14 0.000000 # vm : 0.0
16 0.000000 # vt : 0.0
21 0.000000 # g : 0.0
22 0.000000 # a : 0.0
24 79.951230 # w+ : cmath.sqrt(MZ__exp__2/2. + cmath.sqrt(MZ__exp__4/4. - (aEW*cmath.pi*MZ__exp__2)/(Gf*sqrt__2)))
9000002 91.187600 # ghz : MZ
9000003 79.951230 # ghwp : MW

```

Figure 5.4: param card.dat

$m_{N(\bar{N})}$ (GeV)	$\sigma^H(pb)$ in HNM (Dirac type)	$\sigma^H(pb)$ in HNM (Majorana type)
200	$0.3764 \pm 3.4 \times 10^{-03}$	$0.3847 \pm 1.1 \times 10^{-03}$
400	$0.02684 \pm 2.5 \times 10^{-05}$	$0.02722 \pm 7.3 \times 10^{-05}$
600	$0.005189 \pm 4.3 \times 10^{-06}$	$0.005238 \pm 1.3 \times 10^{-05}$
800	$0.00148 \pm 4.2 \times 10^{-06}$	$0.001491 \pm 4.2 \times 10^{-06}$
1000	$0.0005163 \pm 1.2 \times 10^{-06}$	$0.0005194 \pm 1.2 \times 10^{-06}$

Table 5.1: Hadronic cross section as a function of  $m_N$  in HNM (Dirac and Majorana cases).

$m_{N(\bar{N})}$ (Gev)	$\sigma^H(pb)$ ( $m_{W_R}=3$ TeV)	$\sigma^H(pb)$ ( $m_{W_R}=W$ TeV)	$\sigma^H(pb)$ ( $m_{W_R}=1.5$ TeV)
200	$0.002941 \pm 4.8 \times 10^{-06}$	$0.5802 \pm 1.6 \times 10^{-03}$	$0.09377 \pm 2.7 \times 10^{-04}$
400	$0.002944 \pm 3.8 \times 10^{-06}$	$0.04007 \pm 1.1 \times 10^{-04}$	$0.08372 \pm 2.3 \times 10^{-04}$
600	$0.002602 \pm 5.5 \times 10^{-06}$	$0.00768 \pm 2.1 \times 10^{-05}$	$0.06903 \pm 1.9 \times 10^{-04}$
800	$0.002418 \pm 4.6 \times 10^{-06}$	$0.002143 \pm 6.2 \times 10^{-06}$	$0.05141 \pm 1.1 \times 10^{-04}$
1000	$0.002219 \pm 3.4 \times 10^{-06}$	$0.0007492 \pm 2.1 \times 10^{-06}$	$0.03227 \pm 8.5 \times 10^{-05}$

Table 5.2: Hadronic cross section as a function of  $m_N$  in LRSM for  $m_{W_R} = 3$  TeV,  $m_{W_R} = m_W$  and  $m_{W_R} = 1.5$  TeV.

The variation of the hadronic cross section in terms of the mass of the heavy neutrinos in the three different models are displayed in Fig.(5.5).

#### Remarks and comments:

- We observe that the variation of the hadronic cross section in the HNM in both cases (Dirac and Majorana) strongly depends on the mass of the produced heavy neutrino  $m_N$ . We have seen from the theoretical calculations that the Feynman Diagrams and the couplings in Dirac type HNM and Majorana type HNM are almost the same. The slight differences in the curves are due to the errors in the numerical calculations by MadGraph5 especially since we used just 10000 of events in our calculations. We observe also that the hadronic cross section decrease when the mass of the heavy neutrino increase (and vice versa), this is due to the fact the phase space is reduced for heavy particles in the final state since one needs more energy to produce them. We deduce that this process cannot help us to know if the hypothetical heavy neutrinos are Dirac, Majorana or they might exist in both cases (since the hadronic cross are almost the same at this level), so one has to go the higher order corrections and look for the decay

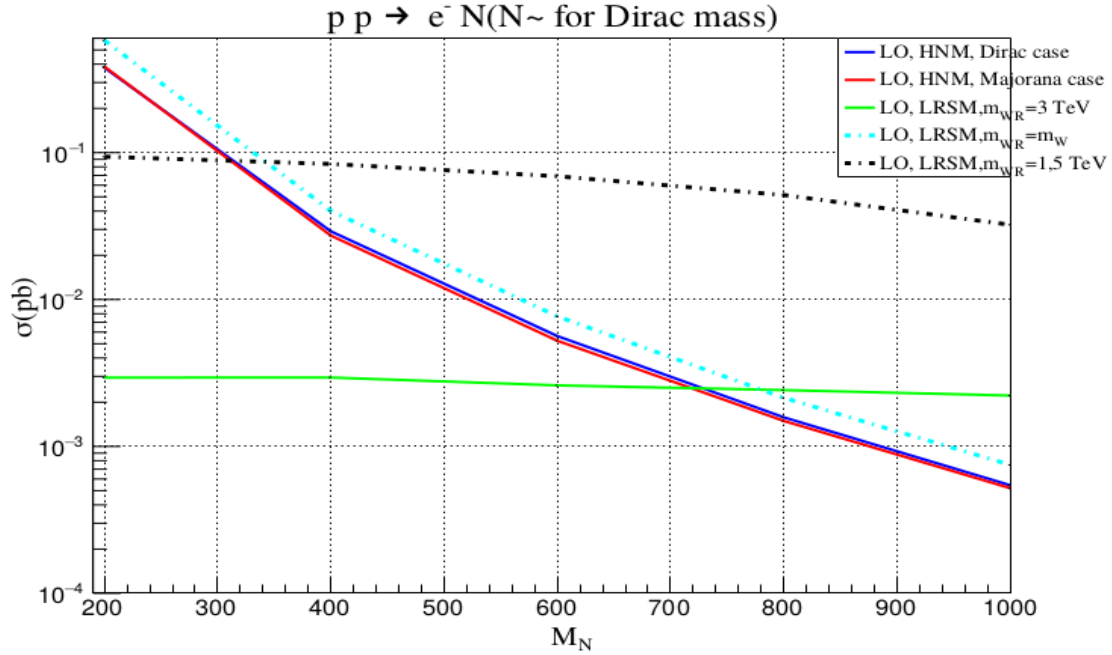


Figure 5.5: Variation of the hadronic cross section as a function of  $m_N$  at  $\sqrt{S} = 13$  TeV.

product of the heavy neutrinos which will be done in the next chapter. We notice that the values of  $V_{lN}$  are model dependant, so we just give them the same values for simplicity.

- Regarding the LRSM, we observe that the behaviours of the hadronic cross section is completely different compared to the previous tow models, see the green curve in Fig. (5.5). For very high mass of the new heavy gauge boson  $W_R$  (around 3000 GeV), we see that the hadronic cross section is small and depends very weakly on the mass of the heavy neutrino. This is due to the fact that the virtuality of the mediator gauge boson is very large which restrict the phase space and the hadronic cross section of the production of the heavy neutrino. Which supports this explanation, is that if we changed the mass of the right charged gauge boson  $m_{W_R}$  and put it equal to  $m_W$  we note that the hadronic cross section is strongly depends on the mass of the produced heavy neutrino  $m_N$  almos as in HNM cases (see the dashed blue curve in Fig. (5.5)). For a high mass of the new heavy gauge boson  $W_R$  (we put it for example around 1500 GeV), we see that the hadronic cross section is dependent weakly on the mass of the heavy neutrino  $N$  then the case of  $m_{W_R} = m_W$ , but its change remains greater than the case where the right charge gauge boson mass  $m_{W_R} = 3000$  GeV (see the dashed black curve in Fig. (5.5)).

### 5.3 Neutral Current Processes

In this part, division will not be triplet as we did in the previous section but rather binary, we will study the process  $p + p \rightarrow Z \rightarrow \bar{\nu}_{e^-} + N$  in HNM where the process is the same in Dirac and Majorana types. The only difference is the type of neutrino and this has no impact on results. The second process is  $p + p \rightarrow Z_r \rightarrow N + N$  in LRSM.

#### 5.3.1 Heavy Neutrino Model

The neutral current process in HNM, with their two case is  $u(p_1) + \bar{u}(p_2) \rightarrow \bar{\nu}_{e^-}(p_3) + N(p_4)$ , and the **Feynman diagram** in the two models is:

The calculation will be numerically as we did in the previous section, so we just going to give a brief reminder to the computational steps:

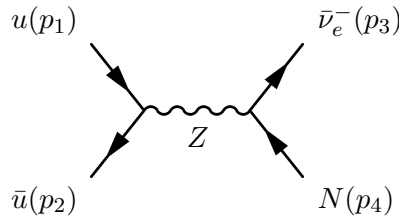


Figure 5.6: Feynman diagram of the neutral current process in HNM, Dirac and Majorana type of neutrino.

- **Amplitude is:**

$$M = \frac{ieg\delta_{ij}V_{lm}^*}{8(q^2 - m_W^2) \sin\theta_w \cos^2\theta_w} \left( \bar{v}_i(p_2)\gamma^\mu \left[ \frac{1}{2} - \frac{2\sin^2\theta_w}{3}(1 - \gamma_5) - \frac{2\sin^2\theta_w}{3}(1 + \gamma_5) \right] \right) \times \left( u_j(p_1) \left[ g^{\mu\nu} - \frac{q^\mu q^\nu}{m_Z} \right] \bar{u}(p_3)\gamma^\nu(1 - \gamma_5)v(p_4) \right) \quad (5.73)$$

The amplitude is the same in the two models. To get the results we following the next steps:

- we called Hip on `Matematica` ase we do before,
- we put the information about the Particles that will participate in process,
- puting the amplitude value in the programe,  
`M = (gg * ee * V) * SpinorVbar[p2] * *g[mu] * *(((1/2) - (2/3) * sin^2) * (1 - g5) - (2/3) * sin^2 * (1 + g5)) * *`  
`SpinorU[p1] * *(G[mu, nu] - k[mu] * *k[nu]/Mz^2) * *SpinorUbar[p3] * *g[nu] * *(1 - g5)`  
`**SpinorV[p4]/8 * sin * cos^2/(p[k, k] - Mz^2)`

- **The amplitude squared:**

- now we following this commands to calculate the amplitude squared:

```
sqM = Simplify[Contract[Simplify[Contract[AbsSquared[M]/12,
{mu, nu, Conjugate[mu], Conjugate[nu]}]], {mu, nu, Conjugate[mu], Conjugate[nu]}]]]
after we clicking on evaluate cell on all commands, we get the result:
```

$$\sum |M|^2 = \frac{e^2 g^2 (V_{lm}^*)^2 \cos^4\theta_w \sin^2\theta_w}{216m_Z^4 (m_N^2 - m_Z^2 + 2p_3 \cdot 4)} \left( 24 \sin^2\theta_w - 32 \sin^4\theta_w - g \right) p_1 \cdot p_2 p_4 \cdot p_4 \times \left( m_N^2 - 2m_N^2 m_Z^2 - 2m_Z^4 + 2m_N^2 p_3 \cdot p_4 \right) \quad (5.74)$$

- **The amplitude squared as a function of MandelStam variables:**

- To calculate it, we put the command:  
`SetMandelstam[p1, p2, p3, p4, 0, 0, 0, mN, S, T, U]`  
`sqMstu = Simplify[sqM]`  
we get the result

$$\sum |M|^2 = \frac{e^2 g^2 (V_{lm}^*)^2 \cos^4\theta_w \sin^2\theta_w}{864m_Z^4} s(m_N^2 - s)(m_N^2(s - 2m_Z^2) - 2m_Z^4) \times (9 - 24 \sin^2\theta_w + 32 \sin^4\theta_w) \quad (5.75)$$

- **The amplitude square in CM frame:**

The result rest the same.

- **Partonic cross section:**

We calculated the partonic cross section analytically as in the previous section, we do the same steps:

$$\hat{\sigma} = \frac{(s - m_N^2)}{32\pi s^2} \int_0^\pi \sin \theta \sum \overline{|M|^2} \quad (5.76)$$

$$(5.77)$$

the amplitude squar is independent of  $\theta$  so:

$$\hat{\sigma} = \frac{(s - m_N^2)}{16\pi s^2} \sum \overline{|M|^2} = \frac{(s - m_N^2)}{16\pi s^2} \frac{e^2 g^2 (V_{lm}^*)^2 \cos^4 \theta_w \sin^2 \theta_w}{864 m_Z^4} s (m_N^2 - s) \times (m_N^2 (s - 2m_Z^2) - 2m_Z^4) (9 - 24 \sin^2 \theta_w + 32 \sin^4 \theta_w). \quad (5.78)$$

### 5.3.2 Left Right Symmetric Model

The neutral gauge boson in this case is  $Z_r$  and neutral current process is  $u(p_1) + \bar{u}(p_2) \rightarrow N(p_3) + N(p_4)$ . **Feynman diagramme is:**

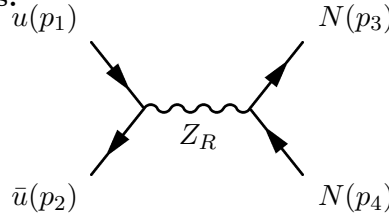


Figure 5.7: Feynman diagram of the neutral current process in LRSM.

we following the same way. The results are:

- **The amplitude is:**

$$\begin{aligned} M &= \bar{v}_i(p_2) \left[ \frac{-i K_r^f g \delta_{ij}}{\sqrt{1 - \frac{\tan^2 \theta_w}{(K_r^f g)^2}}} \gamma^\mu \left( g_l^{Z_r, f} \left( \frac{1 - \gamma_5}{2} \right) + g_r^{Z_r, f} \left( \frac{1 + \gamma_5}{2} \right) \right) \right] u_j(p_1) \left[ \frac{-i}{q^2 - m_{Z_l}^2} (g^{\mu\nu} - \frac{q^\mu q^\nu}{m_{Z_r}}) \right] \\ &\times \bar{u}_i(p_3) \left[ \frac{-i K_r^f g}{\sqrt{1 - \frac{\tan^2 \theta_w}{(K_r^f g)^2}}} \gamma^\nu \left( g_l^{Z_r, f} \left( \frac{1 - \gamma_5}{2} \right) + g_r^{Z_r, f} \left( \frac{1 + \gamma_5}{2} \right) \right) \right] v(p_4) \\ &= \frac{i (K_r^f)^2 g^2 \delta_{ij}}{4 (q^2 - m_{Z_r}^2) (1 - \frac{\tan^2 \theta_w}{(K_r^f g)^2})} \bar{v}_i(p_2) \left[ \gamma^\mu \left( g_l^{Z_r, f} \left( \frac{1 - \gamma_5}{2} \right) + g_r^{Z_r, f} \left( \frac{1 + \gamma_5}{2} \right) \right) \right] u_j(p_1) \left[ (g^{\mu\nu} - \frac{q^\mu q^\nu}{m_{Z_r}}) \right] \\ &\times \bar{u}_i(p_3) \left[ \gamma^\nu \left( g_l^{Z_r, f} \left( \frac{1 - \gamma_5}{2} \right) + g_r^{Z_r, f} \left( \frac{1 + \gamma_5}{2} \right) \right) \right] v(p_4) \end{aligned} \quad (5.79)$$

- **The amplitude squared is:**

$$\sum |M|^2 = \frac{(K_r^f)^8 g^4}{3 m_{Z_r}^4 (K_r^f - \tan \theta_w) (m_{Z_r}^2 + 2 p_1 \cdot p_2)} \left[ ((g^{Z_r, f})_l^4 + (g_r^{Z_r, f})^4) p_1 \cdot p_4 p_2 \cdot p_3 + (g_l^{Z_r, f})^2 (g_r^{Z_r, f})^2 p_1 \cdot p_3 p_2 \cdot p_4 \right] \quad (5.80)$$

- **The amplitude squared as a function of MandelStam variables:**

$$\sum |M|^2 = \frac{4(K_r^f)^8 g^4}{3(m_{Z_r}^2 - s)^2 ((K_r^f)^2 - \tan \theta_w)^2} \left[ \frac{-1}{2} (g_l^{Z_r, f})^2 (g_r^{Z_r, f})^2 (m_N^2 - t) - \frac{1}{4} ((g_l^{Z_r, f})^4 + (g_r^{Z_r, f})^4) (m_N^2 - u) u \right] \quad (5.81)$$

- **The amplitude squared in CM frame** After we putting the values of Mandelstam variables in CM frame we get:

$$\sum |M|^2 = \frac{(K_r^f)^8 g^4 ((g_l^{Z_r, f})^2 + (g_r^{Z_r, f})^2)}{48s (m_{Z_r}^2 - s)^2 ((K_r^f)^2 - \tan \theta_w)^2} \left[ -4 \cos \theta (m_N^2 - s) - \sqrt{s} (4 - 2m_N^2 - s) \right]^2 \quad (5.82)$$

- **Partonic cross section:** We calculated the cross section analytically as we did in the previous cases, we do the same steps,

$$\begin{aligned} \hat{\sigma} &= \frac{(s - m_N^2)}{32\pi s^2} \int_0^\pi \sin \theta \sum |M|^2 \\ &= \frac{(K_r^f)^8 g^4 ((g_l^{Z_r, f})^2 + (g_r^{Z_r, f})^2)}{48s (m_{Z_r}^2 - s)^2 ((K_r^f)^2 - \tan \theta_w)^2} \frac{(s - m_N^2)}{32\pi s^2} \int_0^\pi \sin \theta \left[ 4 \cos \theta (m_N^2 - s) + \sqrt{s} (4 - 2m_N^2 - s) \right]^2 d\theta \end{aligned} \quad (5.83)$$

After using **Mathematica** to calculate the integral we find:

$$\hat{\sigma} = \frac{(K_r^f)^8 g^4 ((g_l^{Z_r, f})^2 + (g_r^{Z_r, f})^2)}{768\pi s^3 ((K_r^f)^2 - \tan \theta_w)^2} \frac{(m_{Z_r}^2 - s)^2}{(s - m_N^2)} \sqrt{s} (-4 + 2m_N + s)^2 \quad (5.84)$$

### 5.3.3 Variation of the Cross Section in Term of Heavy Neutrino Mass

In this section we, study the variation of the cross section in neutral current process as a function of the produced heavy neutrino  $N$  ( $\bar{N}$ ) in the three models: HNM Dirac type, HNM Majoran type and LRSM. We follow the same steps as in the case of charged current processes.

- First, we generate the codes which allow us the compute the cross section by **MadGraph5**:

```
cd master/MG5_aMC_v2_5_4/pp_veñ1_Dirac_lo/ [in Heavy Neutrino Model (Dirac type)]
cd master/MG5_aMC_v2_5_4/pp_veñ1m_lo/ [in Heavy Neutrino Model (Majorana type)]
cd master/MG5_aMC_v2_5_4/pp_n1n1_LR_lo/ [in LR-Symmetric Model]
```

- We variate the masses in the **param\_card.dat** for every model.

The variation of the cross section in term of the masses of the heavy neutrinos, for the three model, are given in the following tables:

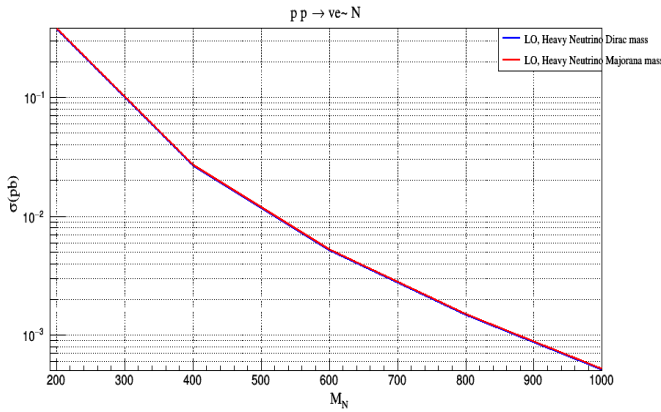
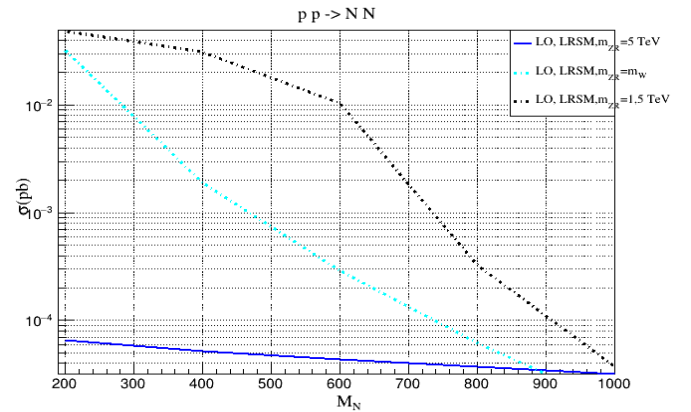
The variation of the cross section, the three models, are displayed in Fig.(5.9).

**Remarks and comments:**

$m_{N(\bar{N})}(Gev)$	$\hat{\sigma}^H(pb)$ in $HNM$ -Dirac mass-	$\hat{\sigma}^H(pb)$ in $HNM$ -Majorana mass-
200	$0.3764 \pm 1.1 \times 10^{-03}$	$0.3847 \pm 1.0 \times 10^{-03}$
400	$0.02684 \pm 7.4 \times 10^{-05}$	$0.02722 \pm 6.9 \times 10^{-05}$
600	$0.005189 \pm 1.7 \times 10^{-06}$	$0.005238 \pm 1.7 \times 10^{-06}$
800	$0.00148 \pm 4.2 \times 10^{-06}$	$0.001491 \pm 4.4 \times 10^{-06}$
1000	$0.0005163 \pm 1.8 \times 10^{-06}$	$0.0005194 \pm 1.9 \times 10^{-06}$

Table 5.3: Variation of the hadronic cross section as a function of  $m_N$  in HNM.

$m_{N(\bar{N})}(Gev)$	$\sigma^H(pb)$ ( $m_{Z_R} = 5$ TeV)	$\sigma^H(pb)$ ( $m_{Z_R}=Z$ TeV)	$\sigma^H(pb)$ ( $m_{Z_R} = 1.5$ TeV)
200	$0.00006549 \pm 1.2 \times 10^{-07}$	$0.03211 \pm 1.3 \times 10^{-04}$	$0.0489 \pm 1.9 \times 10^{-04}$
400	$0.00006544 \pm 1.8 \times 10^{-07}$	$0.001912 \pm 7.5 \times 10^{-06}$	$0.03094 \pm 1.2 \times 10^{-04}$
600	$0.00004314 \pm 1.1 \times 10^{-07}$	$0.0002891 \pm 1.1 \times 10^{-06}$	$0.01044 \pm 4.0 \times 10^{-05}$
800	$0.00003691 \pm 7.4 \times 10^{-08}$	$0.00006237 \pm 2.3 \times 10^{-07}$	$0.0003246 \pm 1.1 \times 10^{-06}$
1000	$0.00003165 \pm 5.8 \times 10^{-08}$	$0.00001622 \pm 6.4 \times 10^{-07}$	$0.00003758 \pm 1.5 \times 10^{-07}$

Table 5.4: Hadronic cross section as a function of  $m_N$  in LRSM for  $m_{Z_R} = 3$  TeV,  $m_{Z_R} = m_Z$  and  $m_{Z_R} = 1.5$  TeVFigure 5.8: The variation of the hadronic section as a function of produced heavy neutrino mass ( $\bar{N}$ ) (in Dirac case) and  $N$  (in Majorana case) with  $\sqrt{S} = 13TeV$ .Figure 5.9: The variation of the hadronic cross section as a function of produced heavy neutrino mass  $N$  in LRSM with  $\sqrt{S} = 13TeV$  for  $m_{Z_R} = 5$  TeV,  $m_{Z_R} = m_Z$  and  $m_{W_R} = 1.5$  TeV .

- We observe that the variation of the hadronic cross section in the HNM in both cases (Dirac and Majorana) strongly depends on the mass of the produced heavy neutrino  $m_N$ . We have seen from the theoretical calculations that the Feynman Diagrams and the couplings in Dirac type HNM and Majorana type HNM are almost the same. The slight differences in the curves are due to the errors in the numerical calculations by MadGraph5 especially since we used just 10000 of events in our calculations. We observe also that the hadronic cross section decrease when the mass of the heavy neutrino increase (and vice versa), this is due to the fact that the phase space is reduced for heavy particles in the final state since one needs more energy to produce them. We deduce that this process cannot help us to know if the hypothetical heavy neutrinos are Dirac, Majorana or they might exist in both cases (since the hadronic cross sections are almost the same at this level), so one has to go to higher order corrections and look for the decay products of the heavy neutrinos which will be done in the next chapter. We notice that the values of  $V_{lN}$  are model dependent, in this we just give them the same values for simplicity.

- Regarding the LRSM, we observe that the behaviours of the hadronic cross section is completely different compared to the previous tow models, see the blue curve in Fig. (5.8). For very high mass of the new heavy gauge boson  $Z_R$  (around 5000 GeV), we see that the hadronci cross section is very small and depends very weakly on the mass of the heavy neutrino. This is due to the fact that the virtuality of the mediator gauge boson is very large which restrict the phase space and the hadronic cross section of the production of the heavy neutrino. Which supports this explanation, is that if we changed the mass of the right charged gauge boson  $m_{Z_R}$  and put it equal to  $m_Z$  we note that the hadronic cross section is strongly depends on the mass of the produced heavy neutrino  $m_N$  almos as in HNM cases (see the dashed blue curve in Fig. (5.9)). For a high mass of the new heavy gauge boson  $Z_R$  (we put it for example around 1500 GeV), we see that the hadronic cross section is dependent weakly on the mass of the heavy neutrino  $N$  then the case of  $m_{Z_R} = m_Z$ , but its change remains greater than the case where the right charge gauge boson mass  $m_{Z_R} = 5000$  GeV (see the dashed black curve in Fig.(5.9)).

## 5.4 Main Differences Between the Two Models

In this section, we summarise and discuss the main results and differences between the different our models.

### 5.4.1 Differences in decay modes and rates

- **HNM, Dirac type:**

The produced particle that we interested with their decaying is the anti-heavy neutrino  $\bar{N}$  in this process . We get the types of decays and the decay rates from *Hip* program automatically, we just putting this commands to called it on Mathematica, It gives us the result of the decay rate for any particle in our model

- We first call FeynRules in Mthematica by the command

```
FeynRulesPath = SetDirectory["/home/sadek/research/feynrules/feynrules-2-3/
feynrules-2.3"]; << FeynRules'
```

```
SetDirectory["/home/sadek/research/feynrules/feynrules-2-3/feynrules-2.3/Models/
heavyNmajorananlo"];
```

- now we calling the package of our model by this command

```
LoadModel["SM.fr", "heavyN.fr"]; LoadRestriction["DiagonalCKM.rst", "Massless.rst"];
FeynmanGauge = True;
```

after we clicking on evaluate cell on all commands, we get the decay rate of the anti-heavy neutino  $N$ :

$$\bar{N}_i \rightarrow H + \nu_l \quad \Gamma = \frac{em_{N_i} V_{lN_i} P}{2m_W \sin \theta_W} \quad (5.85)$$

$$\bar{N}_i \rightarrow W^- + l^+ \quad \Gamma = \frac{em_{N_i} V_{lN_i} P}{\sqrt{2}m_W \sin \theta_W} \quad (5.86)$$

$$\bar{N}_i \rightarrow Z + \nu_l \quad \Gamma = \frac{em_{N_i} V_{lN_i} P}{2m_W \sin \theta_W} \quad (5.87)$$

- **HNM, Majoran type:**

The produced particle that we interested with their decaying in this model is the heavy neutrino  $N$ . We get the types of decays and the decay rates from *Hip* program automatically by following the same steps of the previous model:

- we first call `FeynRules` in `Mthematica` by the command

```
FeynRulesPath = SetDirectory["/home/sadek/research/feynrules/feynrules-2-3/
feynrules-2.3"]; << FeynRules
```

```
SetDirectory["/home/sadek/research/feynrules/feynrules-2-3/feynrules-2.3/Models/
heavyNmajorananlo"];
```

- now we calling the package of our model by this command

```
LoadModel["SM.fr", "heavyN.fr"]; LoadRestriction["DiagonalCKM.rst", "Massless.rst"];
FeynmanGauge = True;
```

after we clicking on evaluate cell on all commands, we get the decay rate of the heavy neutrino  $N$ :

$$N \rightarrow H + \nu_l \quad \Gamma = -\frac{i e m_{N_i} V_{lN_i} P}{2m_W \sin \theta_W} \quad (5.88)$$

$$N \rightarrow H + \bar{\nu}_l \quad \Gamma = -\frac{i e m_{N_i} V_{lN_i} P}{2m_W \sin \theta_W} \quad (5.89)$$

$$N_i \rightarrow W^- + \bar{l} \quad \Gamma = \frac{e m_{N_i} V_{lN_i} P}{\sqrt{2} m_W \sin \theta_W} \quad (5.90)$$

$$N_i \rightarrow W^+ + l \quad \Gamma = \frac{e m_{N_i} V_{lN_i} P}{\sqrt{2} m_W \sin \theta_W} \quad (5.91)$$

$$N \rightarrow Z + \nu_l \quad \Gamma = \frac{e m_{N_i} V_{lN_i} P}{2m_W \sin \theta_W} \quad (5.92)$$

$$N \rightarrow Z + \bar{\nu}_l \quad \Gamma = \frac{e m_{N_i} V_{lN_i} P}{2m_W \sin \theta_W} \quad (5.93)$$

- **LRSM:**

We get the decay rate by following the same previous computational steps:

$$N \rightarrow W_R^+ + e^-(\mu^-) \rightarrow t + \bar{b} + e^- \bar{\tau} \text{ or } N \rightarrow W_R^+ + e^-(\mu^-) \rightarrow \nu_\tau + \bar{\tau} + e^- \text{ (if } m_{W_R} < m_N)$$

$$\text{the decay rate is: } \Gamma = \frac{(e^2 K_R^q)(m_N - m_{W_R})(m_N + 2m_{W_R})Y_{eN}X_e^2}{64 m_R^2 \pi \sin^2 \theta_W m_N^3} \quad (5.94)$$

$$N \rightarrow W_R^- + e^+(\mu^+) \rightarrow b + \bar{t} + e^+ \bar{\tau} \text{ or } N \rightarrow W_R^- + e^+(\mu^+) \rightarrow \tau + \bar{\nu}_\tau + e^+ \text{ (if } m_{W_R} < m_N)$$

$$\text{the decay rate is: } \Gamma = \frac{(e^2 K_R^q)(m_N - m_{W_R})(m_N + 2m_{W_R})Y_{eN}X_e^2}{64 m_R^2 \pi \sin^2 \theta_W m_N^3} \quad (5.95)$$



$$N \rightarrow W_R^+ + \tau^-(\mu^-) \rightarrow t + \bar{b} + e^- \bar{\tau} \text{ or } N \rightarrow W_R^+ + \tau^-(\mu^-) \rightarrow \nu_\tau + \bar{\tau} + e^- \text{ (if } m_{W_R} < m_N \text{)} \quad (5.96)$$

$$\begin{aligned} \text{the decay rate is: } \Gamma = & \frac{(e^2 K_R^q)[m_N^2 + m_\tau^4 - 2m_{w_R}^4 + m_N^2(-2m_\tau^2 + m_{W_R}^2)]}{64 m_R^2 \pi \sin^2 \theta_W m_N^3} \\ & \times \sqrt{[m_N^4 + (m_\tau^2 - m_{W_R}^2)^2 - 2m_N^2(m_\tau^2 + m_{W_R}^2)Y_{eN}X_e^2]} \end{aligned} \quad (5.97)$$

$$N \rightarrow W_R^- + \tau^+ \rightarrow b + \bar{t} + e^+ \bar{\tau} \text{ or } N \rightarrow W_R^- + \tau^+(\mu^+) \rightarrow \tau + \bar{\nu}_\tau + e^+ \text{ (if } m_{W_R} < m_N \text{)} \quad (5.98)$$

$$\begin{aligned} \text{the decay rate is: } \Gamma = & \frac{(e^2 K_R^q)[m_N^2 + m_\tau^4 - 2m_{w_R}^4 + m_N^2(-2m_\tau^2 + m_{W_R}^2)]}{64 m_R^2 \pi \sin^2 \theta_W m_N^3} \\ & \times \sqrt{[m_N^4 + (m_\tau^2 - m_{W_R}^2)^2 - 2m_N^2(m_\tau^2 + m_{W_R}^2)Y_{eN}X_e^2]} \end{aligned} \quad (5.99)$$

#### 5.4.2 Differences between HNM and LRSM models

We observe that the hadronic cross section and decay rates in these two models are very different. We can summarise the main differences between these two models in three points:

- There are new weak mediators in LRSM ( $W_R$  and  $Z_R$ ) which are absent in HNM. These gauge bosons come from the extra gauge group  $SU_R(2)$  after the first step of symmetry breaking. We notice that the ordinary weak gauge bosons ( $W$  and  $Z$ ), in this model, cannot interact with the heavy neutrinos since they belong to different groups, i.e. the  $W$  and  $Z$  are charged under  $SU_L(2)$  and the heavy neutrinos are charged under  $SU_R(2)$ .
- The values of some constants and the structure of the vertices in these two models are different, because of the appearance of new right weak mediators in LRSM, therefore leads to different results.
- In neutral current processes, we notice that in HNM the produced particles are ordinary antineutrino and heavy neutrino while in LRSM the produced particles are pair of heavy neutrinos.

#### 5.4.3 Differences between Dirac and Majorana types of neutrino

To find out the difference between the Dirac type of neutrino and Majorana, we studied HNM in the two cases. The results were the same, but we have several points that can be distinguished between the two cases:

- We conclude that in the processes where the type is a Dirac, the leptonic number is conserved, but if it is violated, the type of neutrino is a Majorana type.
- In the first charged current process, the produced heavy particle is an anti-heavy neutrino in Dirac case while the produced heavy particle in Majorana case is a heavy neutrino.

These were some of differences between the two models and the type of mass that can be compared with the experimental results. In the next chapter, we study these processes in many high order approximations: **fLO**, **fNLO**, **LO+PS** and **NLO+PS**.



# Production of Heavy Neutrino at Higher Perturbative Orders

In this chapter, we study the production of heavy neutrinos in the three BSM models discussed in the previous chapters at NLO order and in the parton shower approximation. We start this part by giving the definition of the hadronic cross section at NLO order with more details, then we discuss the organisation of an NLO calculation matched (or not) to parton shower. We study the same processes studied in chapter 5, where we will discuss the variation of the total cross section in terms of the mass of the heavy neutrino, in terms of the scale (renormalisation and factorisation scales) and some differential distributions. Finally, we conclude this chapter by giving the main differences between the three different models and the types of neutrino at higher order corrections.

## 6.1 Hadronic Cross Section and Factorization Theorem

We already have defined the hadronic cross section in the previous chapter within the framework of the parton model. It was first pointed out by Drell and Yan that the parton model idea for deep inelastic scattering could be extended to processes in hadron-hadron collisions. They claimed that the hadronic cross section  $\sigma^H$  could be obtained by weighting the partonic cross section of the sub-processes  $\hat{\sigma}^{ij \rightarrow k+l+X}$  with the parton distribution functions (*PDF*'s) [16] as:

$$\sigma^H = \sum_{i,j} \int dx_1 dx_2 \mathcal{F}_i^{H^1}(x_1, \mu_F^2) \mathcal{F}_j^{H^2}(x_2, \mu_F^2) \hat{\sigma}^{ij \rightarrow k+l+X}(p_1, p_2, \mu_F^2, \mu_R^2) \quad (6.1)$$

where  $\mu_F$  and  $\mu_R$  are, respectively, the factorisation and renormalisation scales. The description of a collision between two protons (or hadrons) using the factorization approach is shown schematically as in Fig.(6.3.1):

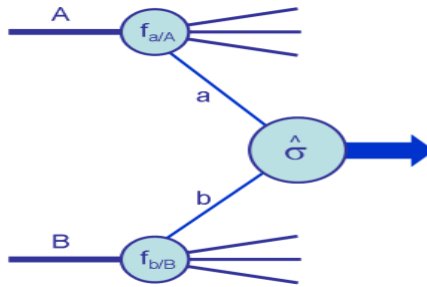


Figure 6.1: Diagrammatic structure of a generic hard scattering process [18].

We notice that the interaction between two partons is subject to two behaviors:

- **The perturbative regime:** which describes the short distance or high energy interactions (the partonic cross section  $\hat{\sigma}^{ij \rightarrow k+l+X}$ ).
- **The non-perturbative regime:** which describes the interactions of large distances or low energy (the parton distribution functions  $\mathcal{F}_i^{H^1}(x_1, \mu_F^2)$ ,  $\mathcal{F}_j^{H^2}(x_2, \mu_F^2)$ ).

The factorization of short- and long-range physics is the cause of the name "**factorization theorem**". We define the parton distribution functions at NLO order, in the  $\overline{MS}$  scheme, by:

$$\begin{aligned} \mathcal{F}(x_1, Q^2) = & x \sum_{q\bar{q}} e_q^2 \int_x^1 \frac{dy}{y} q(y, Q^2) \left[ \delta\left(1 - \frac{y}{x}\right) + \frac{\alpha_s}{2\pi} C_q^{MS} \frac{x}{y} \right] \\ & + x \sum_{q\bar{q}} e_q^2 \int_x^1 \frac{dy}{y} g(y, Q^2) \left[ \frac{\alpha_s}{2\pi} C_g^{MS} \frac{x}{y} \right] \end{aligned} \quad (6.2)$$

with  $\alpha_s$  is the strong coupling constant,  $q$  are the structure function of quarks,  $g$  are the structure function of gluons and  $C_{q,g}$  are some IR divergent coefficients, i.e. the IR divergences of the initial state are adsorbed in those coefficients.

The parton distributions which used in these hard-scattering calculations are the solutions of the **DGLAP** equations:

$$\frac{\partial q_i(x, \mu^2)}{\partial \log \mu^2} = \frac{\alpha_s}{2\pi} \int_x^1 \frac{dz}{z} \left[ P_{q_i q_j}(z, \alpha_s) q_j\left(\frac{x}{z}, \mu^2\right) + P_{q_i g}(z, \alpha_s) g\left(\frac{x}{z}, \mu^2\right) \right] \quad (6.3)$$

$$\frac{\partial g(x, \mu^2)}{\partial \log \mu^2} = \frac{\alpha_s}{2\pi} \int_x^1 \frac{dz}{z} \left[ P_{g q_j}(z, \alpha_s) q_j\left(\frac{x}{z}, \mu^2\right) + P_{g g}(z, \alpha_s) g\left(\frac{x}{z}, \mu^2\right) \right] \quad (6.4)$$

- where  $P_{ab}(z, \alpha_s)$  are the regularized Altarelli-Parisi splitting functions. They describe the collinear splitting of parton  $b$  into parton  $a$ . At one loop order, they are given by:

$$\begin{aligned} P_{q_i q_j}(z) &= C_F \left[ \frac{(1+z^2)}{(1-z)} + \frac{1}{3} \delta(1-z) \right] \\ P_{q_i g}(z) &= C_F \left[ \frac{1+(1-z)^2}{z} \right] \\ P_{g q_i}(z) &= T_R \left[ z^2 + (1-z)^2 \right] \\ P_{g g}(z) &= 2C_A \left[ \frac{z}{(1-z)} + \frac{(1-z)}{z} + z(1-z) \right] + \delta(1-z) \left[ \frac{11}{6} C_A - \frac{2}{3} n_f T_R \right] \end{aligned} \quad (6.5)$$

The DGLAP equations determine the hard scattering scale  $Q^2$  dependence of the *PDF*'s. The  $x$  dependence, on the other hand, has to be obtained from fitting deep inelastic scattering and other hard-scattering data.

The production of heavy neutrino  $N$  at NLO order, in hadronic colliders is described by the theory of perturbative QCD, since it is produced in collisions of hadrons. The soft and collinear divergences of the final state are compensated by combining the loop correction and the real emission. But there are still collinear divergences from the initial state. The latter are absorbed in *PDF*'s according to the factorization theorem [18].

## 6.2 NLO Corrections and Parton Shower

NLO calculations are corrections we make by entering an extra factor of  $\alpha_s$  into the hadronic cross section, this requires consideration of all diagrams beyond the LO which they are:

- The virtual correction: interfacing the one-loop diagrams with the Born diagrams.
- The real emission: obtained by emitting one extra parton from the Born diagrams, they might be soft and collinear divergent.

The strong coupling constant ( $\alpha_s = g_s^2/4\pi$ ) becomes small at large energies ( $Q^2$ ), so we can calculate  $\hat{\sigma}$  perturbatively by keeping only the first and the second order and neglecting the remaining contributions:

$$\begin{aligned}\hat{\sigma}^{ij \rightarrow k+l+X}(p_1, p_2, \mu_F^2, \mu_R^2) &= \alpha_s^k \sum_{m=0}^{\infty} \alpha_s^m \hat{\sigma}_m^{ij \rightarrow k+l+X} \\ &= \alpha_s^k \hat{\sigma}_0^{ij \rightarrow k+l+X} + \alpha_s^{k+1} \hat{\sigma}_1^{ij \rightarrow k+l+X} + \mathcal{O}(\alpha_s^{k+2}).\end{aligned}\quad (6.6)$$

- $m = 0$ : Leading Order (*LO*) or Born level, it includes contributions proportional to  $\alpha_s^k$ .
- $m = 1$ : Next to Leading Order (*NLO*), it includes contribution proportional to  $\alpha_s^{k+1}$ .
- $m = 2$ : Next to Next to Leading Order (*NNLO*), it includes contribution proportional to  $\alpha_s^{k+2}$  and so on.

We can give the general form of the NLO calculations when we consider only the QCD corrections by the following structure in the 4-flavor scheme (4*F*). In this scheme all the quarks are assumed to be of zero mass except the  $b$  and  $t$  [17]. The general structure of a QCD cross section in NLO is:

$$\hat{\sigma}^{NLO} = \hat{\sigma}^{LO}(\alpha_s, \mu_R, \mu_L) + \hat{\sigma}^{HO}(\alpha_s^2, \mu_R, \mu_L) \quad (6.7)$$

In the following, we will discuss in details each contribution alone.

### 6.2.1 Born contribution

The Born contribution is given by,

$$\hat{\sigma}^{LO} = \int_2 d\hat{\sigma}_{Born} = \int_2 |M|^2 \quad (6.8)$$

The Feynman diagrams that contribute to Born order for the production of heavy neutrino is pictured in Fig.(6.2) (this is one diagram from a process in LRSM as an example).

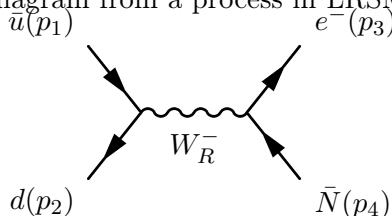


Figure 6.2: Feynman diagram at Born's order.

### 6.2.2 Higher Order (HO) corrections

When we talk about the contribution of higher order, we mean two types of complementary contributions: the virtual and the real emission contributions to avoid the problem. The higher order cross section is given by,

$$\hat{\sigma}^{HO} = \int_2 d\hat{\sigma}_V + \int_3 d\hat{\sigma}_R \quad (6.9)$$

where

- $\hat{\sigma}_V$  is the cross section of the virtual part.
- $\hat{\sigma}_R$  is the cross section of the real part.

Before we talk about these two types of higher order corrections, we should discuss the types of divergences that will face us in the HO calculations, which are:

- **Ultraviolet divergences (UV):** ultraviolet divergences appear in the loop-diagrams when the 4-momuntum running on loop goes to infinity (high energies).
- **Infrared divergences (IR):** infrared divergences (soft or collinear) appear in the loop diagram and the real emission diagrams, they happen when the energy of the emitted massless parton becomes vey small.

**Virtual One-Loop corrections**

The virtual correction is obtained by interfacing the one-loop diagrams with the Born diagrams, the calculation of the one-loop integral leads to ultraviolet, soft and collinear divergences. The ultraviolet divergences can be handled in a simple way within the loop corrections by carrying out the renormalization procedure by redefinition of the coupling constant which must eliminate the possible infinites. To do so, we have to add a new term  $\delta\mathcal{L}$ , called lagrangian of counterterms, to the lagrangian of the model:

$$\mathcal{L}_R = \mathcal{L} + \delta\mathcal{L} \tag{6.10}$$

We notice that in our case, the renormalisation of the BSM models is done automatically by `FeynRules`.

The Feynman diagrams of virtual contribution is for example, like the one in fig.(6.3).

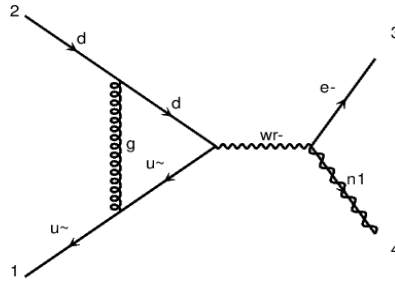
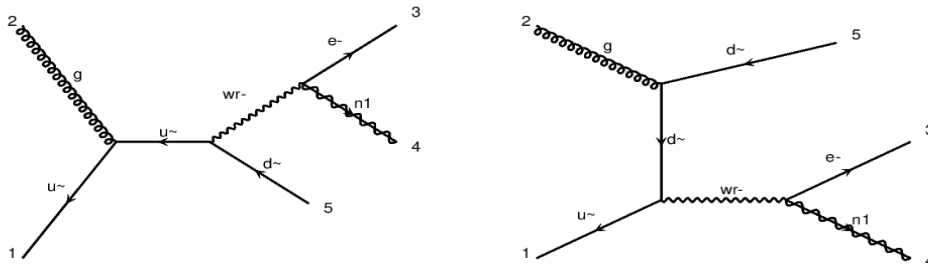


Figure 6.3: Feynman diagrams of virtual contribution.

Soft and collinear divergences instead lead to another problem. These divergences do not cancel within  $\hat{\sigma}_V$ , we must accompanied them with analogous divergences arising from the integration of the real cross section  $\hat{\sigma}_R$ .

**Real emission**

As we said before there are tow types of real emission, soft and collinear. Feynman diagrams of the real emission is for example, like the one in the fig.(6.4).



We can write the soft and collinear propagator in the Feynman diagram as follows:

$$\frac{1}{(p_1 + p_2)^2} = \frac{1}{2E_1 E_2 (1 - \cos \theta)} \quad p_1^2 = 0 \quad p_2^2 = 0 \tag{6.11}$$

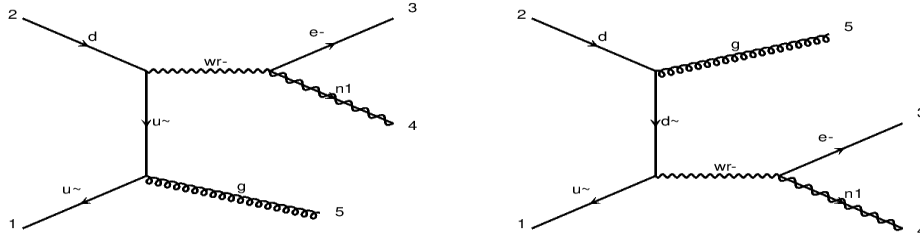


Figure 6.4: Feynman diagrams of real emission.

where the particle with 4-momenta  $p_1$  and  $p_2$  must be massless. We observe that:

- If  $E_{1,2} \rightarrow 0$ , we have a soft divergence.
- If  $\theta \rightarrow 0$ , we have a collinear divergence.

Real emission diagrams are needed to make a complete NLO calculation, they are essential to compensate the infrared divergences. However, this mechanism of cancellation is not trivial because it does not take place at the integrand level. The two integrals on (6.9) are separately divergent, so we must use a gauge-invariant and Lorentz-invariant regularization to any order of the QCD perturbative expansion, we do that by means of analytic continuation in a number of space-time dimensions  $d = 4 - 2\varepsilon$  different from four. Using **dimensional regularization** allowed us to replace the divergences (arising out of the integration) by double  $1/\varepsilon^2$  and single  $1/\varepsilon$  (soft and collinear) poles [19], where  $\varepsilon \rightarrow 0$ .

After making some complicated calculations (this is not the place for it), we get the result of accompanying the soft and collinear divergences from the virtual and real corrections:

$$\hat{\sigma}_V = A \hat{\sigma}^{LO} \left[ \frac{a}{\varepsilon^2} + \frac{b}{\varepsilon} + c \right]_{\varepsilon \rightarrow 0} \quad \hat{\sigma}_R = A \hat{\sigma}^{LO} \left[ -\frac{a}{\varepsilon^2} - \frac{b}{\varepsilon} + c' \right]_{\varepsilon \rightarrow 0} \quad (6.12)$$

$$\Rightarrow \hat{\sigma}_{HO} = \hat{\sigma}_V + \hat{\sigma}_R = A \hat{\sigma}^{LO} [c + c'] \quad (6.13)$$

In fact, this is not enough to eliminate all divergences, some of it still comes from the real emission in elementary entangled particles. We eliminate these divergences by absorbing them inside the *PDF*'s. In this way, we have eliminated all divergences.

In principle this computation procedure does not pose any problems, but in reality, this is not the case. Because in general, we have hundreds of Feynman diagrams, so, analytic calculations are impossible for all. On the other side, when we use numerical methods, we can't do the computation because real and virtual contributions have to be integrated separately, that's why we use an innovative method to perform numerical computations, which is implemented in **MadGraph5**. It is **the subtraction method**.

### 6.2.3 Subtraction method

The idea of this method is to add and subtract the same term  $d\hat{\sigma}_A$  that removes infrared divergences from both real and virtual emission [19]:

$$\hat{\sigma}^{HO} = \int_2 d\hat{\sigma}_V + d\hat{\sigma}_A + \int_3 d\hat{\sigma}_R - d\hat{\sigma}_A \quad (6.14)$$

the cross section contribution  $d\hat{\sigma}_A$  has to fulfil two main properties:

- $d\hat{\sigma}_A$  must be a proper approximation of  $d\hat{\sigma}_R$  such as to have the same "pointwise" singular behaviour (in  $d$  dimensions) as  $d\hat{\sigma}_R$  itself.

- $d\hat{\sigma}_A$  is its analytic integrability (in  $d$  dimensions) over the one-parton subspace leading to the soft and collinear divergences, so we can rewrite the last two terms :

$$\int_3 d\hat{\sigma}_R - d\hat{\sigma}_A = \int_2 \left[ d\hat{\sigma}_R - \int d\hat{\sigma}_A \right]_{\varepsilon=0} \quad (6.15)$$

Performing the integration  $d\hat{\sigma}_A$ , we obtain  $\varepsilon$ -pole contributions that can be combined with those in  $d\hat{\sigma}_V$ , thus, cancelling all the divergences.

The subtraction is automated at `MadGraph5` program thanks to the `MadFKS` [27] program. To calculate loops, we use the package `Madloop`[28]. The latter is a package to calculate the one-loop QCD corrections.

#### 6.2.4 Why NLO?

We can summarize some of the advantages of NLO on LO calculations in several points [20], we mention for example:

- LO uncertainty becomes larger for multijet production, where Born approximation starts at high power of  $\alpha_s$ , it takes NLO corrections to get more accurate results.
- The hadronic cross section at NLO order is bigger than LO order because the corrections that comes from the NLO calculations. As we did in chapter 5, we study the variation of the hadronic cross section in the charged and the neutral current processes in the two models. We have chosen the energy in center mass frame  $\sqrt{S} = 13$  TeV and the number 100000 of events. The numerical results are in the next tables. The results are more accurate and better predictive of the presence of  $N$  as shown at figures (6.6), (6.7) and (6.8), the results are :

##### Charged current processes:

$m_{N,(\bar{N})}(Gev)$	$\hat{\sigma}^{LO}(pb)$	$\hat{\sigma}^{NLO}(pb)$
200	$0.5585 \pm 1.5 \times 10^{-03}$	$0.6622 \pm 2.0 \times 10^{-03}$
400	$0.04077 \pm 1.1 \times 10^{-04}$	$0.04723 \pm 1.4 \times 10^{-04}$
600	$0.00769 \pm 2.1 \times 10^{-05}$	$0.008854 \pm 2.4 \times 10^{-05}$
800	$0.002117 \pm 5.9 \times 10^{-06}$	$0.002453 \pm 6.7 \times 10^{-06}$
1000	$0.0007244 \pm 2.0 \times 10^{-06}$	$0.0008363 \pm 2.1 \times 10^{-06}$

Table 6.1: LO and NLO Hadronic cross section as a function of  $m_N$  in HNM (Dirac type).

$m_N(Gev)$	$\hat{\sigma}^{LO}(pb)$	$\hat{\sigma}^{NLO}(pb)$
200	$0.5585 \pm 1.5 \times 10^{-03}$	$0.6609 \pm 1.9 \times 10^{-03}$
400	$0.04077 \pm 1.1 \times 10^{-04}$	$0.04695 \pm 1.4 \times 10^{-04}$
600	$0.007667 \pm 2.1 \times 10^{-05}$	$0.008819 \pm 2.5 \times 10^{-05}$
800	$0.002129 \pm 5.9 \times 10^{-06}$	$0.002443 \pm 6.7 \times 10^{-06}$
1000	$0.0007215 \pm 2.0 \times 10^{-06}$	$0.000837 \pm 2.3 \times 10^{-06}$

Table 6.2: LO and NLO Hadronic cross section as a function of  $m_N$  in HNM (Majorana type).



$m_{N(\bar{N})}(GeV)$	$\sigma^{LO}(pb) (m_{W_R} = 3 \text{ TeV})$	$\sigma^{LO}(pb)(m_{W_R}=W \text{ TeV})$	$\sigma^{LO}(pb)(m_{W_R} = 1.5 \text{ TeV})$
200	$0.003853 \pm 1.1 \times 10^{-05}$	$0.5802 \pm 1.6 \times 10^{-03}$	$0.09377 \pm 2.7 \times 10^{-04}$
400	$0.003585 \pm 8.9 \times 10^{-06}$	$0.04007 \pm 1.1 \times 10^{-04}$	$0.08372 \pm 2.3 \times 10^{-04}$
600	$0.003343 \pm 1.0 \times 10^{-05}$	$0.00768 \pm 2.1 \times 10^{-05}$	$0.06903 \pm 1.9 \times 10^{-04}$
800	$0.003075 \pm 8.6 \times 10^{-06}$	$0.002143 \pm 6.2 \times 10^{-06}$	$0.05141 \pm 1.1 \times 10^{-04}$
1000	$0.002807 \pm 7.6 \times 10^{-06}$	$0.0007492 \pm 2.1 \times 10^{-06}$	$0.03227 \pm 8.5 \times 10^{-05}$

Table 6.3: LO Hadronic cross section as a function of  $m_N$  in LRSM for  $m_{W_R} = 3 \text{ TeV}$ ,  $m_{W_R} = m_W$  and  $m_{W_R} = 1.5 \text{ TeV}$ .

$m_{N(\bar{N})}(GeV)$	$\sigma^{NLO}(pb) (m_{W_R} = 3 \text{ TeV})$	$\sigma^{NLO}(pb)(m_{W_R} = W \text{ TeV})$	$\sigma^{NLO}(pb)(m_{W_R} = 1.5 \text{ TeV})$
200	$0.00439 \pm 1.3 \times 10^{-05}$	$0.6641 \pm 2.4 \times 10^{-03}$	$0.1085 \pm 3.0 \times 10^{-04}$
400	$0.004135 \pm 1.4 \times 10^{-05}$	$0.04717 \pm 1.5 \times 10^{-04}$	$0.09577 \pm 2.4 \times 10^{-04}$
600	$0.003862 \pm 9.4 \times 10^{-06}$	$0.008965 \pm 2.4 \times 10^{-05}$	$0.07957 \pm 2.0 \times 10^{-04}$
800	$0.003573 \pm 1.1 \times 10^{-05}$	$0.002501 \pm 7.1 \times 10^{-06}$	$0.0592 \pm 1.4 \times 10^{-04}$
1000	$0.003267 \pm 9.7 \times 10^{-06}$	$0.0008579 \pm 2.6 \times 10^{-06}$	$0.03711 \pm 8.7 \times 10^{-05}$

Table 6.4: NLO Hadronic cross section as a function of  $m_N$  in LRSM for  $m_{W_R} = 3 \text{ TeV}$ ,  $m_{W_R} = m_W$  and  $m_{W_R} = 1.5 \text{ TeV}$ .

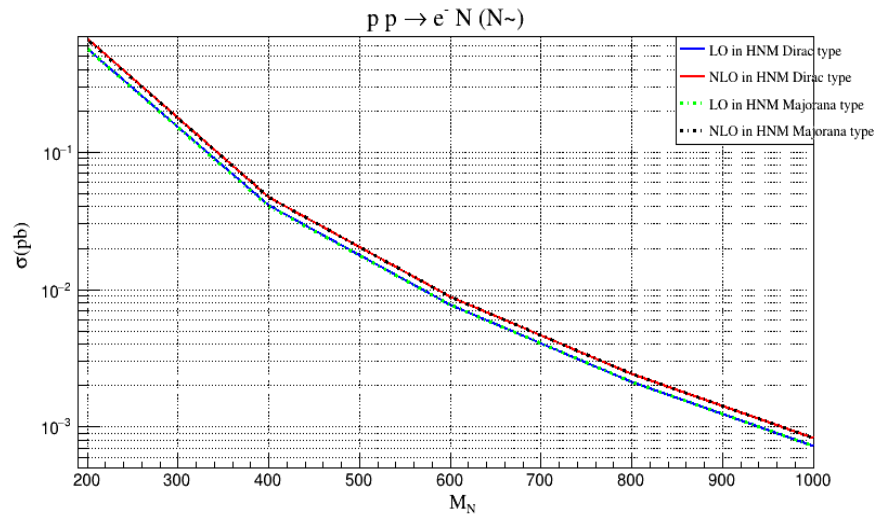


Figure 6.5: The variation of the LO and NLO hadronic cross section as a function of  $m_N$  in HNM with  $\sqrt{S} = 13 \text{ TeV}$  at orders for  $m_{W_R} = 3 \text{ TeV}$ ,  $m_{W_R} = m_W$  and  $m_{W_R} = 1.5 \text{ TeV}$ .

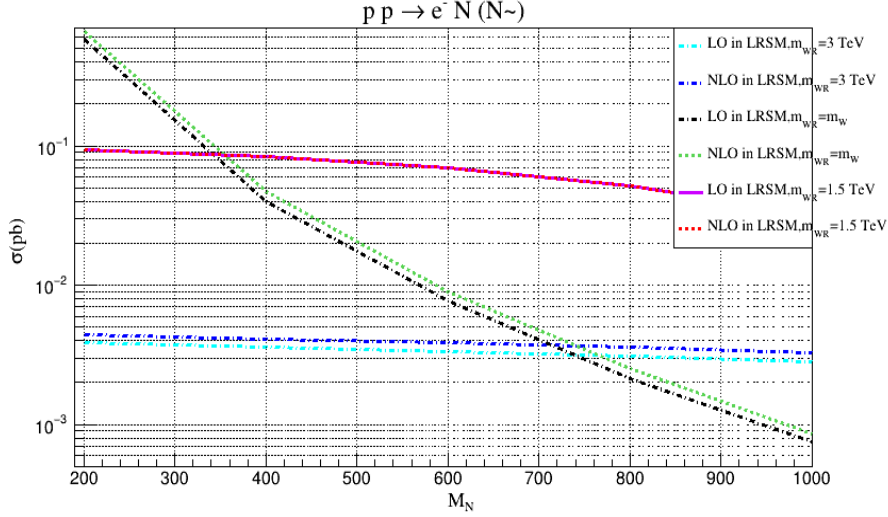


Figure 6.6: The variation of the LO and NLO hadronic cross section as a function of  $m_N$  in LRSM with  $\sqrt{S} = 13$  TeV at orders for  $m_{W_R} = 3$  TeV,  $m_{W_R} = m_W$  and  $m_{W_R} = 1.5$  TeV.

### Neutral current processes:

$m_{N,(\bar{N})}(Gev)$	$\hat{\sigma}^{LO}(pb)$	$\hat{\sigma}^{NLO}(pb)$
200	$0.4143 \pm 1.1 \times 10^{-03}$	$0.4894 \pm 9.8 \times 10^{-04}$
400	$0.0314 \pm 8.6 \times 10^{-05}$	$0.03646 \pm 7.0 \times 10^{-05}$
600	$0.006253 \pm 1.7 \times 10^{-05}$	$0.007252 \pm 1.5 \times 10^{-05}$
800	$0.001808 \pm 5.0 \times 10^{-06}$	$0.002092 \pm 4.1 \times 10^{-06}$
1000	$0.0006386 \pm 1.8 \times 10^{-06}$	$0.0007377 \pm 1.5 \times 10^{-06}$

Table 6.5: LO and NLO Hadronic cross section as a function of  $m_N$  in HNM (Dirac type).

$m_N(Gev)$	$\hat{\sigma}^{LO}(pb)$	$\hat{\sigma}^{NLO}(pb)$
200	$0.4143 \pm 1.1 \times 10^{-03}$	$0.4894 \pm 9.8 \times 10^{-04}$
400	$0.0314 \pm 8.6 \times 10^{-05}$	$0.03646 \pm 7.0 \times 10^{-05}$
600	$0.006253 \pm 1.7 \times 10^{-05}$	$0.007252 \pm 1.5 \times 10^{-05}$
800	$0.001808 \pm 5.0 \times 10^{-06}$	$0.002092 \pm 4.1 \times 10^{-06}$
1000	$0.0006386 \pm 1.8 \times 10^{-06}$	$0.0007377 \pm 1.5 \times 10^{-06}$

Table 6.6: LO and NLO Hadronic cross section as a function of  $m_N$  in HNM (Majorana type).

$m_{N(\bar{N})}(Gev)$	$\sigma^{LO}(pb) (m_{Z_R}=5 \text{ TeV})$	$\sigma^{LO}(pb)(m_{Z_R}=Z \text{ TeV})$	$\sigma^{LO}(pb)(m_{Z_R} = 1.5 \text{ TeV})$
200	$0.00006818 \pm 1.8 \times 10^{-07}$	$0.03211 \pm 1.3 \times 10^{-04}$	$0.05599 \pm 9.6 \times 10^{-05}$
400	$0.0000514 \pm 1.4 \times 10^{-07}$	$0.001912 \pm 7.5 \times 10^{-06}$	$0.03543 \pm 6.1 \times 10^{-05}$
600	$0.00004128 \pm 1.0 \times 10^{-07}$	$0.0002891 \pm 1.1 \times 10^{-06}$	$0.01192 \pm 2.0 \times 10^{-05}$
800	$0.00003427 \pm 8.6 \times 10^{-07}$	$0.00006237 \pm 2.3 \times 10^{-07}$	$0.0003646 \pm 7.7 \times 10^{-07}$
1000	$0.00002855 \pm 7.5 \times 10^{-08}$	$0.00001622 \pm 6.4 \times 10^{-07}$	$0.0000397 \pm 7.1 \times 10^{-07}$

Table 6.7: LO Hadronic cross section as a function of  $m_N$  in LRSM for  $m_{Z_R} = 5$  TeV,  $m_{Z_R} = m_Z$  and  $m_{Z_R} = 1.5$  TeV.

$m_{N(\bar{N})}(GeV)$	$\sigma^{NLO}(pb) (m_{Z_R}=5 \text{ TeV})$	$\sigma^{NLO}(pb)(m_{Z_R}=Z \text{ TeV})$	$\sigma^{NLO}(pb)(m_{Z_R} = 1.5 \text{ TeV})$
200	$0.00008009 \pm 2.6 \times 10^{-07}$	$0.03792 \pm 7.7 \times 10^{-04}$	$0.0489 \pm 1.9 \times 10^{-05}$
400	$0.00006124 \pm 1.7 \times 10^{-07}$	$0.002221 \pm 4.3 \times 10^{-06}$	$0.03094 \pm 1.2 \times 10^{-06}$
600	$0.00005004 \pm 9.4 \times 10^{-07}$	$0.0003267 \pm 6.7 \times 10^{-06}$	$0.01044 \pm 4.0 \times 10^{-07}$
800	$0.00004177 \pm 1.1 \times 10^{-07}$	$0.00006885 \pm 1.4 \times 10^{-07}$	$0.0003246 \pm 1.1 \times 10^{-07}$
1000	$0.00003514 \pm 7.8 \times 10^{-08}$	$0.00001743 \pm 3.8 \times 10^{-07}$	$0.00003758 \pm 1.5 \times 10^{-08}$

Table 6.8: NLO Hadronic cross section as a function of  $m_N$  in LRSM for  $m_{Z_R} = 5 \text{ TeV}$ ,  $m_{Z_R} = m_Z$  and  $m_{Z_R} = 1.5 \text{ TeV}$ .

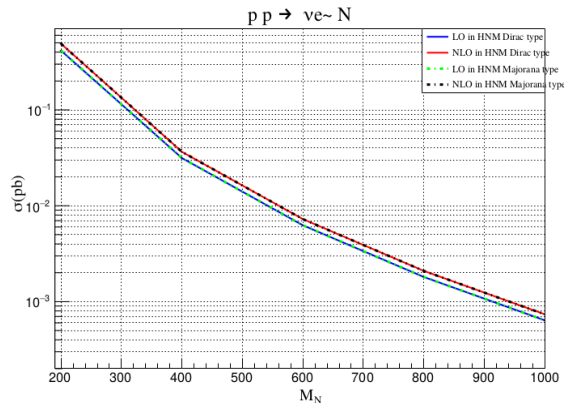


Figure 6.7: The variation of the LO and NLO hadronic cross section as a function of  $m_N$  in HNM and LRSM with  $\sqrt{S} = 13 \text{ TeV}$  at orders for  $m_{Z_R} = 5 \text{ TeV}$ ,  $m_{Z_R} = m_Z$  and  $m_{Z_R} = 1.5 \text{ TeV}$ .

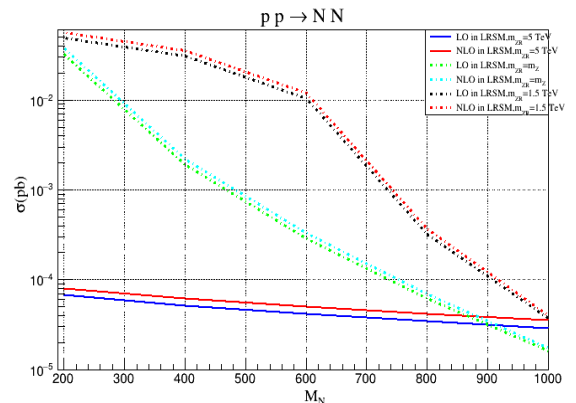


Figure 6.8: The variation of the LO and NLO hadronic cross section as a function of  $m_N$  in HNM and LRSM with  $\sqrt{S} = 13 \text{ TeV}$  at orders for  $m_{Z_R} = 5 \text{ TeV}$ ,  $m_{Z_R} = m_Z$  and  $m_{Z_R} = 1.5 \text{ TeV}$ .

- The numerical results at LO order are compatible with the results in the previous chapter (note figure 6.6 and figure 6.7). At NLO order we notice that the type of neutrino has no impact at the results. In the charged current processes in dirac type the produced neutrino is anti-heavy neutrino where in Majorana case is a heavy neutrino, but the result still exactly the same as at LO order. The smallest value of the hadronic cross section corresponds to the case of production a pair of heavy neutrinos (figure 6.8), since in this case we need more energy to produce the heavy neutrino and the phase space is very restricted.
- In LRSM the cross section at LO and NLO depend with another free parameter which is the mass of the new heavy gauge boson. We observe that for low gauge boson mass ( $m_{Z_R} = m_Z$ ), the cross section is larger and close to the HNM cross sections and for high mass of the new heavy gauge bosons it decreases and becomes mostly independant of the heavy neutrino mass.

The NLO calculation is very important since it has more physics by parton merging as the jets and initial and final state radiation. It is a necessary to use more sophisticated techniques which match NLO with Parton Shower (we will discuss it later). At NLO order, the physical cross section is formally independent of  $\mu_F$  and  $\mu_R$ . Thus, if we plot its change in terms of  $\mu_F$  or  $\mu_R$ , we get a straight horizontal line (as we will note in the following figures). The dashed line represent the physical cross section if we can calculate all the higher corrections. Note in the same figures below that the hadronic cross section variation correlates strongly with  $\mu_F$  scales at LO order (we dont need to  $\mu_R$  at LO since there is no renormalisation), while NLO curve seems near-realistic calculations where it is at least less sensitive to unphysical scales (eg. renormalisation  $\mu_R$  and factorsation  $\mu_F$  scales). This appears clearly in charged current type process (6.11) and neutral current process (6.14) of the LR Symmetric Model.

- We plot the curve of the hadronic cross section in the following figures by setting  $\mu_R = \mu_F$ ,  $m_N = 500$  GeV, we draw it at LO order as a function of  $\mu_F$  and at NLO order as a function of  $\mu_R = \mu_F$  in the three models (HNM Dirac type and Majorana type and LRSM). The numerical results for the charged and the neutral current processes with the curves of the variation of the hadronic cross section,

**Charged current processes:**

$\mu_R = \mu_F (Gev)$	$\hat{\sigma}^{LO}(pb)$	$\hat{\sigma}^{NLO}(pb)$
50	$0.01811 \pm 4.3 \times 10^{-05}$	$0.02088 \pm 6.6 \times 10^{-05}$
100	$0.01756 \pm 4.8 \times 10^{-05}$	$0.02027 \pm 6.1 \times 10^{-05}$
150	$0.01737 \pm 4.8 \times 10^{-05}$	$0.01996 \pm 5.4 \times 10^{-05}$
200	$0.01712 \pm 4.7 \times 10^{-05}$	$0.01964 \pm 5.3 \times 10^{-05}$
250	$0.01694 \pm 4.5 \times 10^{-05}$	$0.01965 \pm 5.2 \times 10^{-05}$
300	$0.01682 \pm 4.6 \times 10^{-05}$	$0.0196 \pm 5.4 \times 10^{-05}$
350	$0.01669 \pm 4.5 \times 10^{-05}$	$0.01942 \pm 5.4 \times 10^{-05}$
400	$0.01658 \pm 4.6 \times 10^{-05}$	$0.01938 \pm 5.4 \times 10^{-05}$
450	$0.01644 \pm 4.6 \times 10^{-05}$	$0.01928 \pm 5.4 \times 10^{-05}$
500	$0.01643 \pm 6.6 \times 10^{-05}$	$0.01929 \pm 4.9 \times 10^{-05}$

Table 6.9: Hadronic cross section results as a function of  $\mu_F$  at LO order,  $\mu_R, \mu_F$  at NLO order in HNM, Dirac type of neutrino.

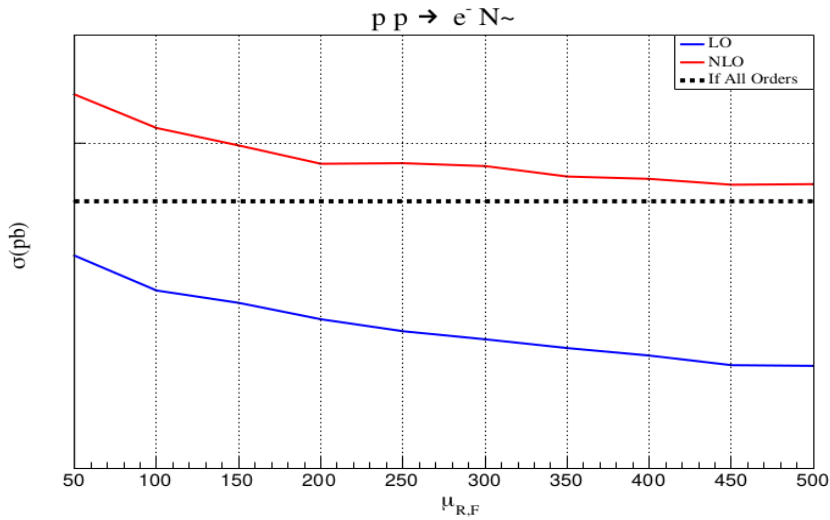


Figure 6.9: Comparison between the variation of the hadronic cross section as a function of  $\mu_F$  at LO order,  $\mu_R, \mu_F$  at NLO order in HNM, Dirac type with the physical cross section *All-orders*.

$\mu_R = \mu_F(\text{Gev})$	$\hat{\sigma}^{LO}(\text{pb})$	$\hat{\sigma}^{NLO}(\text{pb})$
50	$0.01807 \pm 4.9 \times 10^{-05}$	$0.02095 \pm 5.9 \times 10^{-05}$
100	$0.01769 \pm 4.9 \times 10^{-05}$	$0.02022 \pm 5.7 \times 10^{-05}$
150	$0.01735 \pm 4.7 \times 10^{-05}$	$0.02006 \pm 6.0 \times 10^{-05}$
200	$0.01712 \pm 4.7 \times 10^{-05}$	$0.01978 \pm 5.5 \times 10^{-05}$
250	$0.01696 \pm 4.8 \times 10^{-05}$	$0.01964 \pm 5.6 \times 10^{-05}$
300	$0.01681 \pm 4.6 \times 10^{-05}$	$0.01949 \pm 5.6 \times 10^{-05}$
350	$0.01664 \pm 4.7 \times 10^{-05}$	$0.01951 \pm 5.7 \times 10^{-05}$
400	$0.01661 \pm 4.5 \times 10^{-05}$	$0.01929 \pm 5.5 \times 10^{-05}$
450	$0.01642 \pm 4.6 \times 10^{-05}$	$0.01926 \pm 5.3 \times 10^{-05}$
500	$0.01633 \pm 4.7 \times 10^{-05}$	$0.01922 \pm 5.5 \times 10^{-05}$

Table 6.10: Hadronic cross section results as a function of  $\mu_F$  at LO order,  $\mu_R, \mu_F$  at NLO order in HNM, Majorana type.

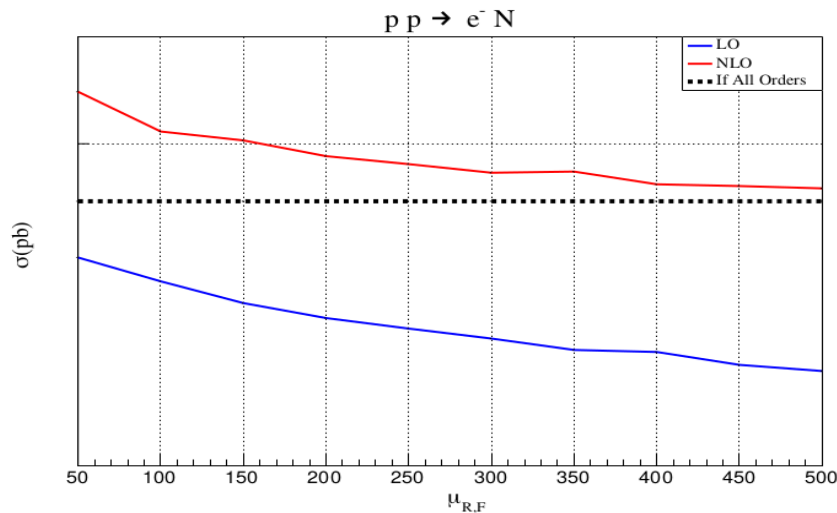


Figure 6.10: Comparison between the variation of the hadronic cross section as a function of  $\mu_F$  at LO order,  $\mu_R, \mu_F$  at NLO order in HNM, Majorana type with the physical cross section *All-orders*.

$\mu_R = \mu_F(\text{Gev})$	$\hat{\sigma}^{LO}(\text{pb})$	$\hat{\sigma}^{NLO}(\text{pb})$
50	$0.006164 \pm 1.8 \times 10^{-05}$	$0.003898 \pm 2.2 \times 10^{-05}$
100	$0.005274 \pm 1.5 \times 10^{-05}$	$0.004149 \pm 1.4 \times 10^{-05}$
150	$0.004911 \pm 1.5 \times 10^{-05}$	$0.004211 \pm 1.4 \times 10^{-05}$
200	$0.004628 \pm 1.4 \times 10^{-05}$	$0.00424 \pm 1.3 \times 10^{-05}$
250	$0.004427 \pm 1.4 \times 10^{-05}$	$0.004237 \pm 1.4 \times 10^{-05}$
300	$0.004289 \pm 1.3 \times 10^{-05}$	$0.004239 \pm 1.0 \times 10^{-05}$
350	$0.004178 \pm 1.2 \times 10^{-05}$	$0.004226 \pm 1.2 \times 10^{-05}$
400	$0.004071 \pm 1.3 \times 10^{-05}$	$0.004212 \pm 1.2 \times 10^{-05}$
450	$0.003965 \pm 1.2 \times 10^{-05}$	$0.004193 \pm 1.1 \times 10^{-05}$
500	$0.003918 \pm 1.2 \times 10^{-05}$	$0.004181 \pm 1.1 \times 10^{-05}$

Table 6.11: Hadronic cross section results as a function of  $\mu_F$  at LO order,  $\mu_R, \mu_F$  at NLO order in LRSM.

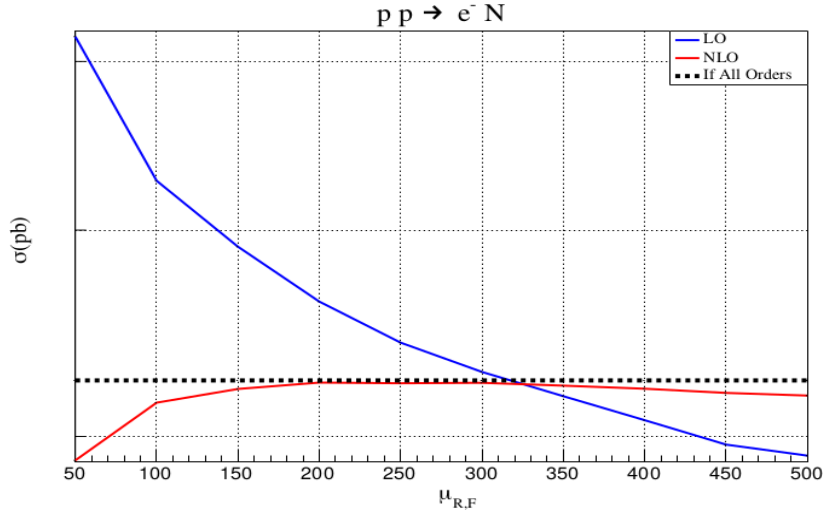


Figure 6.11: Comparison between the variation of the hadronic cross section as a function of  $\mu_F$  at LO order,  $\mu_R, \mu_F$  at NLO order in LRSM. With the physical cross section *All-orders*.

### Neutral current processes:

$\mu_R = \mu_F (Gev)$	$\hat{\sigma}^{LO}(pb)$	$\hat{\sigma}^{NLO}(pb)$
50	$0.01445 \pm 4.0 \times 10^{-05}$	$0.01659 \pm 3.8 \times 10^{-05}$
100	$0.01396 \pm 3.8 \times 10^{-05}$	$0.01612 \pm 3.3 \times 10^{-05}$
150	$0.01382 \pm 3.9 \times 10^{-05}$	$0.01589 \pm 3.1 \times 10^{-05}$
200	$0.01362 \pm 3.8 \times 10^{-05}$	$0.01568 \pm 3.2 \times 10^{-05}$
250	$0.01352 \pm 3.8 \times 10^{-05}$	$0.01564 \pm 3.1 \times 10^{-05}$
300	$0.01339 \pm 3.8 \times 10^{-05}$	$0.01555 \pm 3.2 \times 10^{-05}$
350	$0.0132 \pm 3.6 \times 10^{-05}$	$0.01545 \pm 3.1 \times 10^{-05}$
400	$0.01322 \pm 3.8 \times 10^{-05}$	$0.01543 \pm 3.0 \times 10^{-05}$
450	$0.01308 \pm 3.6 \times 10^{-05}$	$0.0154 \pm 3.0 \times 10^{-05}$
500	$0.01305 \pm 3.6 \times 10^{-05}$	$0.01534 \pm 2.9 \times 10^{-05}$

Table 6.12: Hadronic cross section results as a function of  $\mu_F$  at LO order,  $\mu_R, \mu_F$  at NLO order in HNM, Dirac type of neutrino.

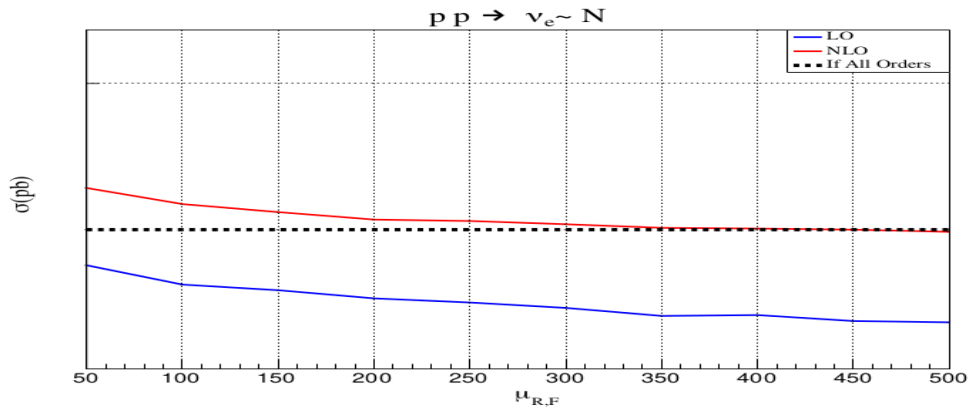


Figure 6.12: Comparison between the variation of the hadronic cross section as a function of  $\mu_F$  at LO order,  $\mu_R, \mu_F$  at NLO order in HNM, Dirac type with the physical cross section *All-orders*.

$\mu_R = \mu_F(\text{Gev})$	$\hat{\sigma}^{LO}(\text{pb})$	$\hat{\sigma}^{NLO}(\text{pb})$
50	$0.01445 \pm 4.0 \times 10^{-05}$	$0.01659 \pm 3.8 \times 10^{-05}$
100	$0.01396 \pm 3.8 \times 10^{-05}$	$0.01612 \pm 3.3 \times 10^{-05}$
150	$0.01382 \pm 3.9 \times 10^{-05}$	$0.01589 \pm 3.1 \times 10^{-05}$
200	$0.01362 \pm 3.8 \times 10^{-05}$	$0.01568 \pm 3.2 \times 10^{-05}$
250	$0.01352 \pm 3.8 \times 10^{-05}$	$0.01564 \pm 3.1 \times 10^{-05}$
300	$0.01339 \pm 3.8 \times 10^{-05}$	$0.01555 \pm 3.2 \times 10^{-05}$
350	$0.0132 \pm 3.6 \times 10^{-05}$	$0.01545 \pm 3.1 \times 10^{-05}$
400	$0.01322 \pm 3.8 \times 10^{-05}$	$0.01543 \pm 3.0 \times 10^{-05}$
450	$0.01312 \pm 3.6 \times 10^{-05}$	$0.0154 \pm 3.0 \times 10^{-05}$
500	$0.01302 \pm 3.6 \times 10^{-05}$	$0.01534 \pm 2.9 \times 10^{-05}$

Table 6.13: Hadronic cross section results as a function of  $\mu_F$  at LO order,  $\mu_R, \mu_F$  at NLO order in HNM, Majorana type.

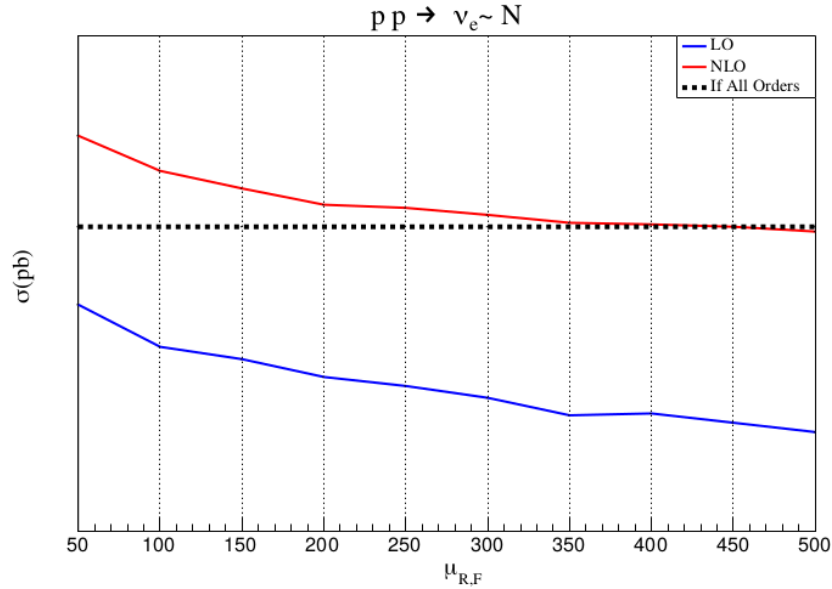


Figure 6.13: Comparison between the variation of the hadronic cross section as a function of  $\mu_F$  at LO order,  $\mu_R, \mu_F$  at NLO order in HNM, Majorana type with the physical cross section *All-orders*.

$\mu_R = \mu_F(\text{Gev})$	$\hat{\sigma}^{LO}(\text{pb})$	$\hat{\sigma}^{NLO}(\text{pb})$
50	$0.0001133 \pm 3.0 \times 10^{-07}$	$0.00003266 \pm 5.8 \times 10^{-07}$
100	$0.00009069 \pm 2.3 \times 10^{-07}$	$0.00004987 \pm 3.3 \times 10^{-07}$
150	$0.00008118 \pm 2.1 \times 10^{-07}$	$0.00005472 \pm 2.7 \times 10^{-07}$
200	$0.00007482 \pm 2.1 \times 10^{-07}$	$0.00005689 \pm 1.7 \times 10^{-07}$
250	$0.00007072 \pm 1.9 \times 10^{-07}$	$0.00005801 \pm 2.1 \times 10^{-07}$
300	$0.0000673 \pm 1.8 \times 10^{-07}$	$0.00005877 \pm 2.3 \times 10^{-07}$
350	$0.00006446 \pm 1.7 \times 10^{-07}$	$0.00005817 \pm 2.0 \times 10^{-07}$
400	$0.00006268 \pm 1.8 \times 10^{-07}$	$0.00005832 \pm 1.7 \times 10^{-07}$
450	$0.00006077 \pm 1.6 \times 10^{-07}$	$0.00005876 \pm 1.6 \times 10^{-07}$
500	$0.00005918 \pm 1.6 \times 10^{-07}$	$0.00005849 \pm 2.7 \times 10^{-07}$

Table 6.14: Hadronic cross section results as a function of  $\mu_F$  at LO order,  $\mu_R, \mu_F$  at NLO order in LRSM.

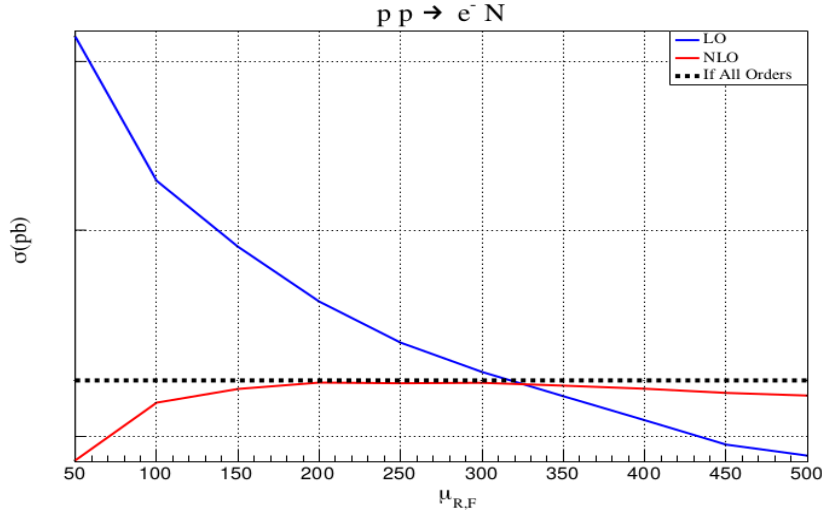


Figure 6.14: Comparison between the variation of the hadronic cross section as a function of  $\mu_F$  at LO order,  $\mu_R, \mu_F$  at NLO order in LRSM. with the physical cross section *All-orders*.

### 6.2.5 Fixed order and non Fixed order

When we generate a process at `MadGraph5`, the type of computation Fixed Order (*FO*) means that the produced particles at the final state are real (physical) or "**on-shell**" ( $p^2 = m^2$  for a particle at the final state). If we not chosen this computation property we get a non physical particles at the final state, in this case we said : the particles are "**off-shell**" ( $p^2 \neq m^2$  for a particle at the final state). Because in our case we will compare the theoretical results with the experimental results, we will chose in the numerical calculations (at next section) the the Fixed Order property.

### 6.2.6 Parton Shower; Why ?

The basic idea leading to Parton Shower comes from the repeated implementation of equations (6.3 and 6.4) leads to arbitrarily many parton splittings, and therefore arbitrarily many particles in the final state and this is the basic idea leading to **Parton shower**. In other words it approximates higher-order real-emission corrections to the hard scattering by simulating the branching of a single external parton into two partons with high energy, each of these partons may either split into two partons with less energy. This partons locally conserve flavor, four momentum, respect unitarity, which simply means that a partons are **off-shell** ( $p^2 \neq m^2$  for a particle at the final state) [18].

At very low energy, the emission of partons stops due to the confinement phenomenon and hadronization begins. Hadronization is the process of forming hadrons from quarks and gluons, this occurs when low energy partons confine themselves to form hadrons which are not stable so they are decays in general. This process is shown in figure (6.15). We can do the numerical computation of Parton Shower automatically by using `pythia8` to simulate the following phenomena:

- Partons emission.
- Hadronization.
- Decays processes.

The Parton Shower is very important for several reasons [15], we mention for example:

- It gives a good simulation for what's happening on detectors. Because in just one collision, we can detect thousands of particles, see figure (6.15).



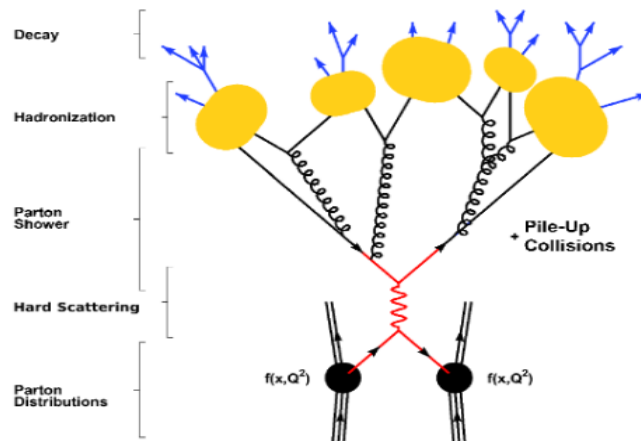


Figure 6.15: Parton Shower, hadronization and decays processes [22].

- In the LO and NLO calculations, one can consider a limited number of particles in the final state. If the number of particles increases, the calculation becomes technically very complicated (impossible to do technically). But the Parton Shower, even if it is just an approximation in the soft and collinear, it allows to consider a very large number of particles in the final state.
- Theoretically, Parton Shower gives a better prediction at low energy than the calculation of LO and NLO which might diverge.

### 6.3 Differential distribution at fixed order and parton shower

In this section we will study, the differential cross sections for the same processes discussed above (the charged current and neutral current processes). We will study the the variation of the hadronic cross section as a function of the kinematics: transverse momentum ( $P_T$ ), rapidity ( $Y$ ) and pseudo-rapidity ( $\eta$ ) at Higher Order (HO) perturbative corections. Then we make a comparison between the obtained results in three BSM models (HNM Dirac type, HNM Majorana type and LRSM). We will consider the following approximations:

- Fixed Leading Order (**FLO**).
- Fixed Next to Leading Order (**FNLO**).
- Leading Order matched to Parton Shower (**LO+PS**).
- Next to Leading Order matched to Parton Shower (**NLO+PS**).

we will discuss too the impact of the type of HO corrections on results and the main differences between them. This is helpful to compare theory with experiment, and to put constraints on the free parameters of the model under consideration.

#### 6.3.1 Charged current process

As we did in chapter (5) the charged current process in HNM is  $(p + p \rightarrow W^- \rightarrow e^- + \bar{N})$  where the type of neutrino is Dirac),  $(p + p \rightarrow W^- \rightarrow e^- + N)$  where the type of neutrino is Majorana) and  $(p + p \rightarrow W_R^- \rightarrow e^- + N)$  in LRSM. Before we discuss and analyse the results, we give the main computational steps that we do to get the differential distribution:

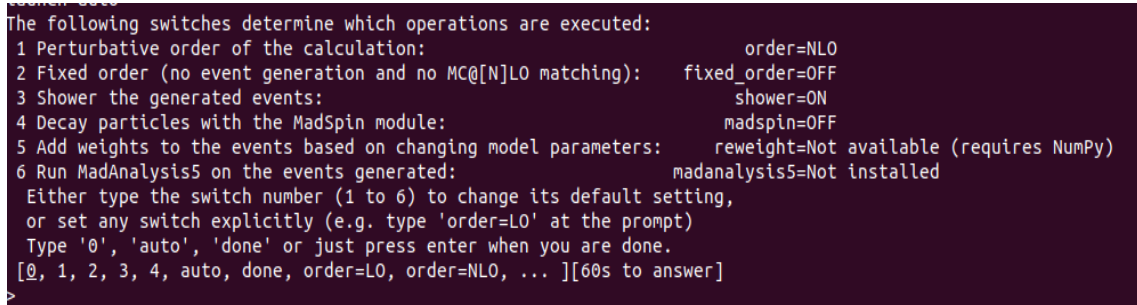
- We start by generating our process at MadGraph on the defferent modeles by the following steps:

```

cd master/MG5_aMC_v2_5_4/./bin/mg5_aMC/ (for starting MadGraph).
MG5_aMC>import model SM_HeavyN_Dirac_NLO/ (to importing the HNM, Dirac type of neu-
trino).
MG5_aMC>import model SM_HeavyN_NLO/ (to importing the HNM, Majorana type of neu-
trino).
MG5_aMC>import model EffLRSM_NLO/ (to importing the LR Symmetric Model).
MG5_aMC>generate p p > e- n1 [QCD] (for generating the process at HO corrections).

```

- After naming our process we do the command `launch` to get a table we can from it choose the type of HO calculation that we need as in fig.(6.16). :



```

The following switches determine which operations are executed:
1 Perturbative order of the calculation:                order=NLO
2 Fixed order (no event generation and no MC@NLO matching):  fixed_order=OFF
3 Shower the generated events:                          shower=ON
4 Decay particles with the MadSpin module:              madspin=OFF
5 Add weights to the events based on changing model parameters:  reweight=Not available (requires NumPy)
6 Run MadAnalysis5 on the events generated:             madanalysis5=Not installed
Either type the switch number (1 to 6) to change its default setting,
or set any switch explicitly (e.g. type 'order=L0' at the prompt)
Type '0', 'auto', 'done' or just press enter when you are done.
[0, 1, 2, 3, 4, auto, done, order=L0, order=NLO, ... ][60s to answer]
>

```

Figure 6.16: HO calculations that we can do on MadGraph.

- Now to get the numerical results that we use to calculate the histograms of differential hadronic cross section variations we use `MadanAllysis`, we follow these steps: `/master/madanalysis5$./bin/ma5` (to run `MadanAllysis`).

```

import /home/yassin/master/MG5_aMC_v2_5_4/pp_en1 _Dirac_NLO/Events/run_01/
events_flo_dirac.lhe.gz (for importing the HO file that madanalysis used to drawing his-
tograms. The command still the same for the other Models and the file in the format .lhe.gz
differs according to the HO calculation and the model that we need).

```

- To plot the distribution, we use:

```

ma5>plot PT(nn1) 20 0 500 [logY].
ma5>plot ETA(nn1) 20 -3 3 [logY].
ma5>plot Y(nn1) 20 -3 3 [logY].

```

to get the variation of hadronic cross section as a function of  $P_T$ ,  $Y$  and  $\eta$ . While when we calculate LO+PS and NLO+PS we use the following commands to plot the histograms before the decay of the heavy neutrino:

```

ma5>plot PT(nn1) 20 0 500 [interstate].
ma5>plot ETA(nn1) 20 -3 3 [interstate].
ma5>plot Y(nn1) 20 -3 3 [interstate].

```

- The final step is using the numerical results that we get by `madanalysis` to draw the histograms of a variation of hadronic cross section as a function  $P_T$ ,  $Y$  or  $\eta$  at LO, NLO, LO+PS and NLO+PS by using `Root`.

We choose in all the calculations the fixed scale scheme, where we set renormalization  $\mu_R$  and factorization  $\mu_F$  scales equal to heavy neutrino mass ( $\mu_R = \mu_F = m_N = 500 \text{ GeV}$ ). The results are displayed below:

**Differential distributions of the hadronic cross section as a function of  $P_T$ :**

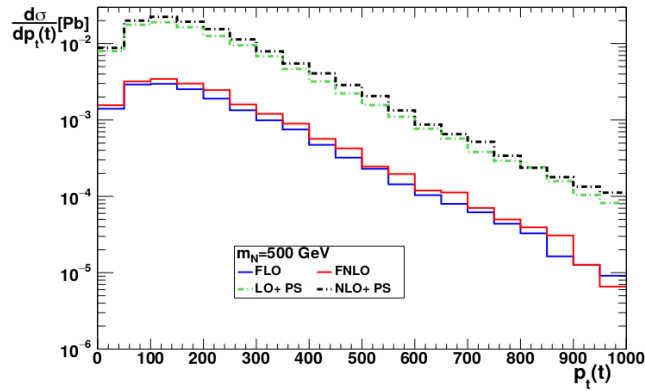


Figure 6.17: Hadronic cross section variation as a function  $P_T$  with  $\sqrt{S} = 13$  TeV in HNM, Dirac neutrino type.

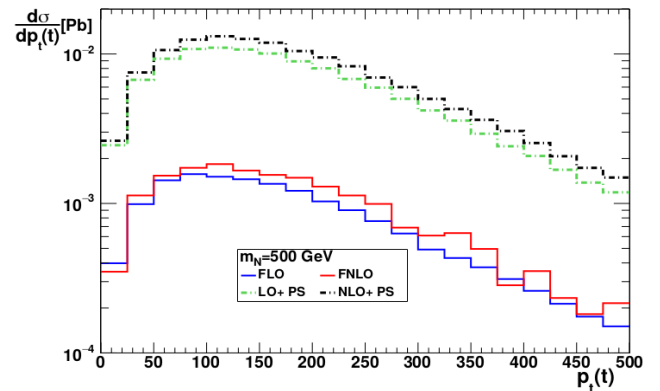


Figure 6.18: Hadronic cross section variation as a function  $P_T$  with  $\sqrt{S} = 13$  TeV in HNM, Majorana neutrino type.

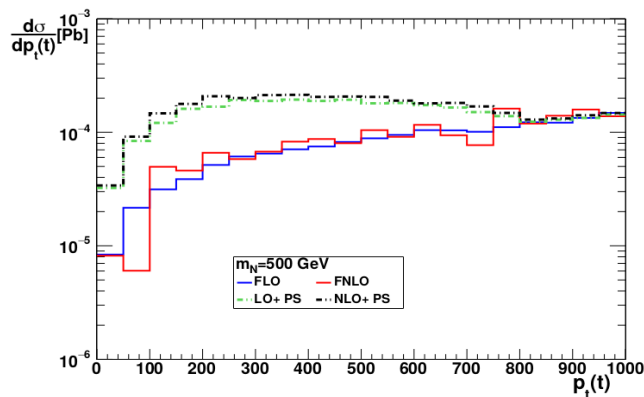


Figure 6.19: Hadronic cross section variation as a function  $P_T$  with  $\sqrt{S} = 13$  TeV in LRSM.

- In the first three figures, we show the differential distributions of the hadronic cross section on the transverse momentum  $P_T$ . We observe that the Parton Shower contributions (LO+PS and NLO+PS) are more important than the fixed order contributions (fLO and fNLO). This appears clearly for relatively small values of  $P_T$  for the tree models. For example, for the bins between 100-150 GeV the cross section is about  $10^{-3}$  pb for fixed order and  $10^{-2}$  pb for parton shower. This is due to initial state radiations which has a dominant contribution in this case since we have only leptons in the final state.
- We observe also, that fLO is very close to the fNLO and the LO+PS is very close to NLO+PS for the three models. This can be interpreted by the fact that the k-factor (which is NLO/LO contribution) is very small for the studied processes.
- In their two types of neutrino (Dirac and Majorana), the differential distributions of the hadronic cross section are large for small values of  $P_T$  and they decrease for large values of  $P_T$ . In the Majorana case, the distribution cancels at the value 500 GeV which is not the case for Dirac case. While in LRSM the differential distributions of the hadronic cross section are small for small values of  $P_T$  and increase with increasing  $P_T$ . In the later model, the distribution in the 4 approximations (fLO, fNLO, LO+PS and NLO+PS) converge to each other to become the same at large  $P_T$ , (see figure 6.19).
- We observe that the distributions in HNM models are larger than the distributions in LRSM since in the later one the processes are mediated by a very heavy gauge bosons which reduce the total cross section and the differential distributions.

- Only for a very low  $P_T$ , significant changes observed between the fixing order of LO and NLO contributions and LO and NLO matched to the Parton Shower (LO+PS and NLO+PS). LO+PS and NLO+PS seems to be more stable at this scale of  $P_T$  [21], we can see that more clearly if we zoom up the variation of the hadronic cross section at the region of  $P_T$  between 0 GeV and 100 GeV (see the figure 6.20). We observe that fNLO is not stable at all (it is going up and down) while the NLO+PS is more stable. This is due to the fact that in fNLO approximation, the low physics contribution is ignored (we put it in the PDFs) while in parton shower it is taken into account by considering emissions of a shower of soft and collinear particles.

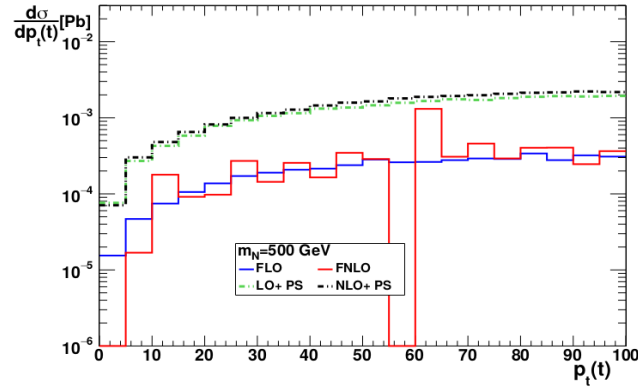


Figure 6.20: Hadronic cross section variation as a function of  $\eta$  with  $\sqrt{S} = 13\text{TeV}$  in HNM, Dirac case as an example.

### Differential distributions of the hadronic cross section as a function of $Y$ :

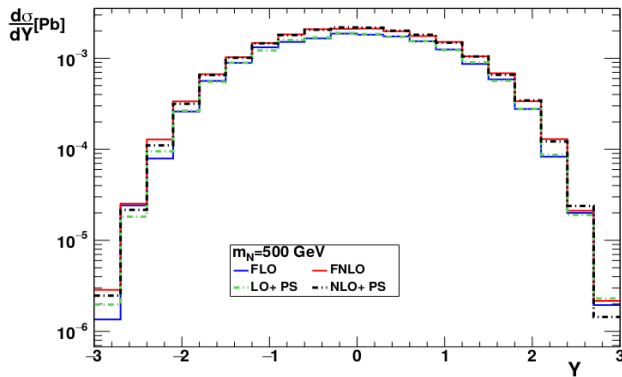


Figure 6.21: Hadronic cross section variation as a function of  $Y$  with  $\sqrt{S} = 13\text{TeV}$  in HNM, Dirac neutrino type.

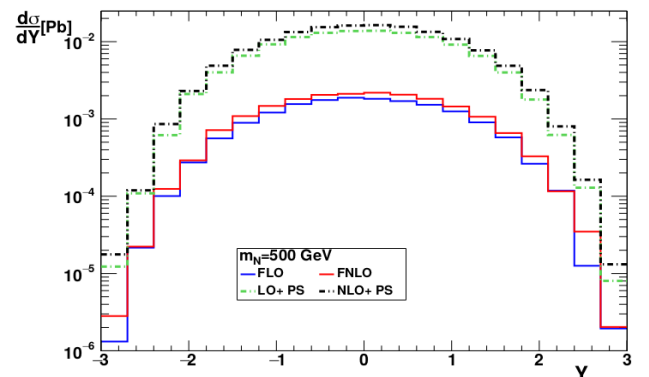


Figure 6.22: Hadronic cross section variation as a function of  $Y$  with  $\sqrt{S} = 13\text{TeV}$  in HNM, Majorana neutrino type.

In general, the differential distributions on the rapidity  $Y$  is helpful to compare theory with experiment. Here's we give some comment on this distribution for the three models.

- The differential distributions of the hadronic cross section on the rapidity  $Y$  seems similar in the three models when its value increase with increasing of  $Y$  and reaches a peak at zero then start decrease with the increasing of  $Y$ .
- We observe that the distributions for LRSM (6.23) are smaller compared to HNM, this can be understood since the processes are mediated by very heavy gauge bosons (of mass around 5000 GeV).

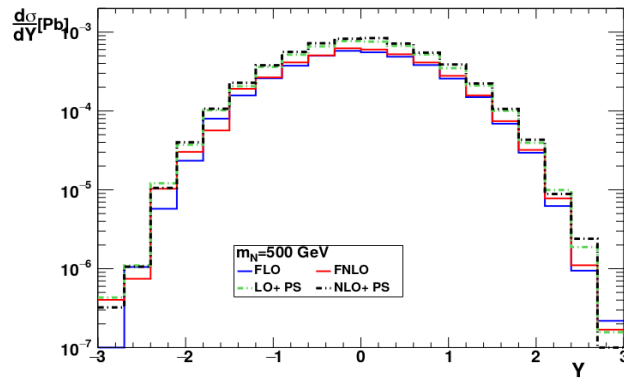


Figure 6.23: Hadronic cross section variation as a function of  $Y$  with  $\sqrt{S} = 13TeV$  in LRSM.

- We observe a discrepancy between NLO+PS and LO+PS for the two classes of HNM which was not expected. We observe that in Majorana case the parton shower distributions are larger than the fixed order contributions which is not the case for Dirac type, see Fig.6.21 and Fig.6.3.1. This point is very important and needs more study since it might help us to know if the heavy neutrinos are of Dirac or Majorana types.

#### Differential distributions of the hadronic cross section as a function of $\eta$ :

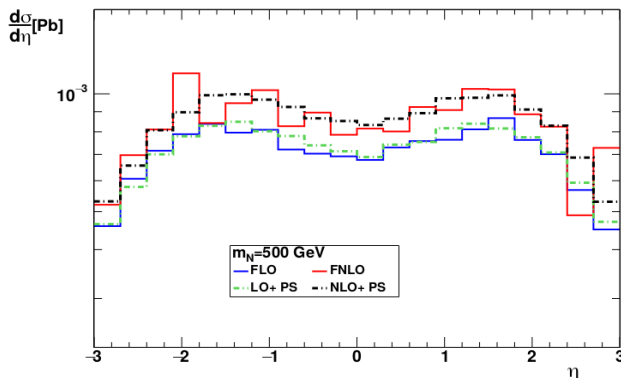


Figure 6.24: Hadronic cross section variation as a function  $\eta$  with  $\sqrt{S} = 13TeV$  in HNM, Dirac neutrino type.

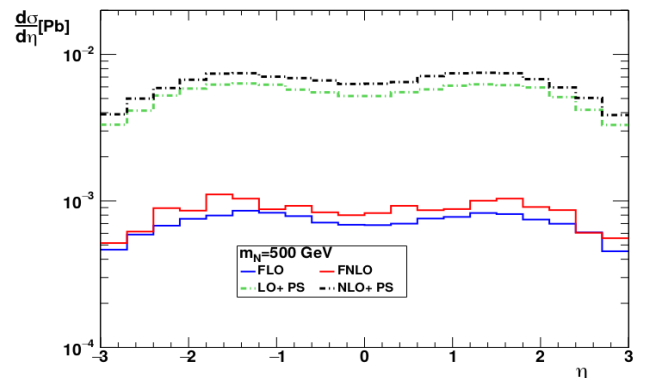


Figure 6.25: Hadronic cross section variation as a function  $\eta$  with  $\sqrt{S} = 13TeV$  in HNM, Majorana neutrino type.

- We observe that the distribution on the pseudo-rapidity  $\eta$  are more different in HNM than in LRSM. The smaller is as usual is the one of LRM for the same reasons claimed above. We observe also that differential distribution in HNM for both classes show two peaks for  $|\eta| = 2$  in the 4 approximation (figure 6.24), while in LRSM there is only one peak at  $\eta = 0$ .
- As we have observed for the rapidity distribution in HNM, parton shower in the Majorana case has a larger distribution than the fixed order approximation which is not the case for Dirac type (figure 6.25).
- In LRSM the behavior of the differential distributions of the hadronic cross section is different from HNM, where we observe only one peak when the value of  $\eta$  was zero (figure 6.26).

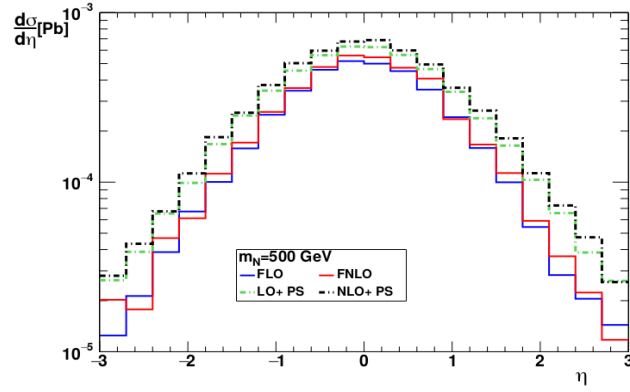


Figure 6.26: Hadronic cross section variation as a function of  $\eta$  with  $\sqrt{S} = 13\text{TeV}$  in LRSM.

### 6.3.2 Neutral current process

In this section, we consider the neutral current process in HNM is  $(p + p \rightarrow Z \rightarrow \bar{\nu}_e - N$  where the type of neutrino is Dirac or Majorana) and  $(p + p \rightarrow Z_R \rightarrow N + N)$  in LR Symmetric Model. We follow the same computational steps as we did with the charged current process in the previous section (6.3.1). The results are:

**Differential distributions of the hadronic cross section as a function of  $P_T$ :**

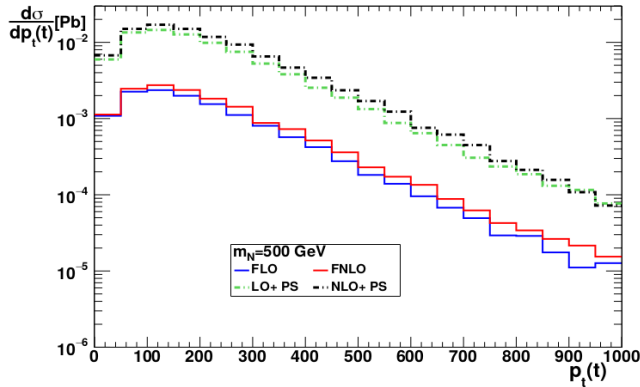


Figure 6.27: Hadronic cross section variation as a function  $P_T$  with  $\sqrt{S} = 13\text{TeV}$  in HNM, Dirac neutrino type.

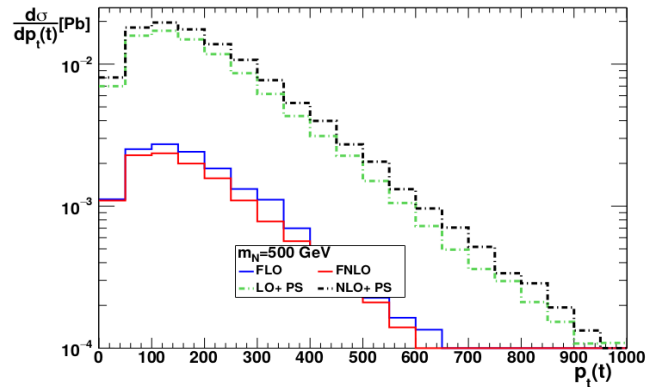


Figure 6.28: Hadronic cross section variation as a function  $P_T$  with  $\sqrt{S} = 13\text{TeV}$  in HNM, Majorana neutrino type.

- We observe that, the distributions in the parton shower approximation (for both LO and NLO) in the 3 models are larger than the distributions in the fixed order approximation (for both LO and NLO).
- We observe that for low  $PT$ , the parton shower is more stable and reliable than the fixed for the same reason stated above (see the zoomed distribution in Fig. 6.30)).
- We observe the two HNM classes have the same distributions for parton shower and fixed order (we can not distinguish between them).
- The second main difference is to note that the values of differential distributions of the hadronic cross section in LRSM (figure 6.29) are very small than the values of HNM and from the values of the charged gauge boson processes, because in this process a pair of heavy neutrinos is produced, and since its mass is large, the possibility of producing two of them is more unlikely.

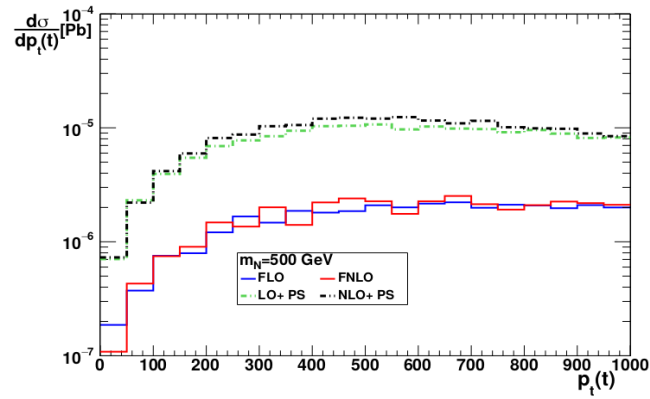


Figure 6.29: Hadronic cross section variation as a function  $P_T$  with  $\sqrt{S} = 13TeV$  in LRSM.

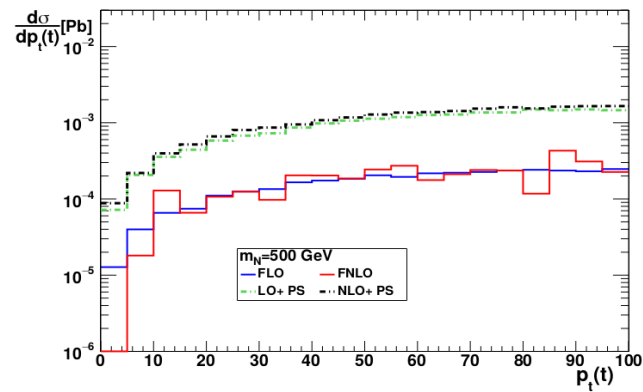


Figure 6.30: Hadronic cross section variation as a function  $\eta$  with  $\sqrt{S} = 13TeV$  in HNM, Dirac case as an example.

### Differential distributions of the hadronic cross section as a function of $Y$ :

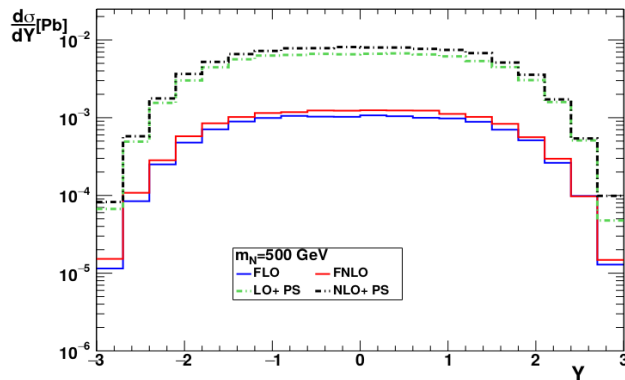


Figure 6.31: Hadronic cross section variation as a function  $Y$  with  $\sqrt{S} = 13TeV$  in HNM, Dirac neutrino type.

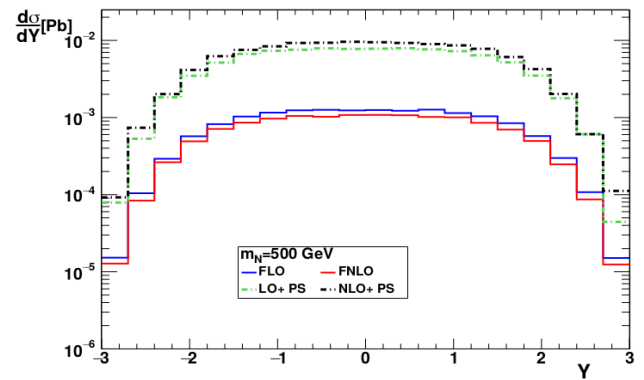


Figure 6.32: Hadronic cross section variation as a function  $Y$  with  $\sqrt{S} = 13TeV$  in HNM, Majorana neutrino type.

- As in section (6.3.1), the differential distributions of the hadronic cross section on the rapidity  $Y$  seems similar in HNM (Dirac and Majorana types) and LRSM where it reaches the highest value at  $Y = -2$ , then it stabilizes until it reaches  $Y = 2$  and starts decreasing again. But, in LRSM the distribution values are smaller.

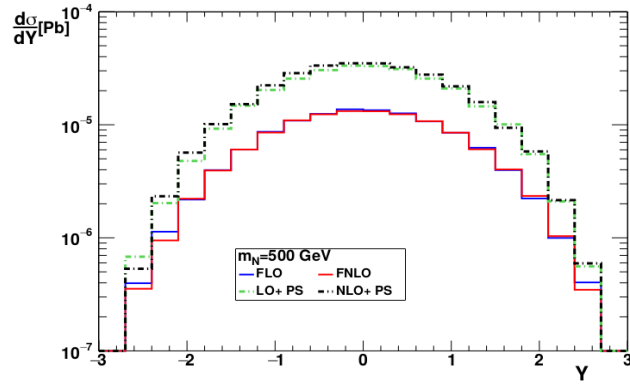


Figure 6.33: Hadronic cross section variation as a function  $Y$  with  $\sqrt{S} = 13TeV$  in LRSM.

- If we compare the fixed order and parton shower approximations, we figure out the parton shower contribution are larger than the fixed order in three models, which means that the parton shower approximation is more important in this case.

Differential distributions of the hadronic cross section as a function of  $\eta$ :

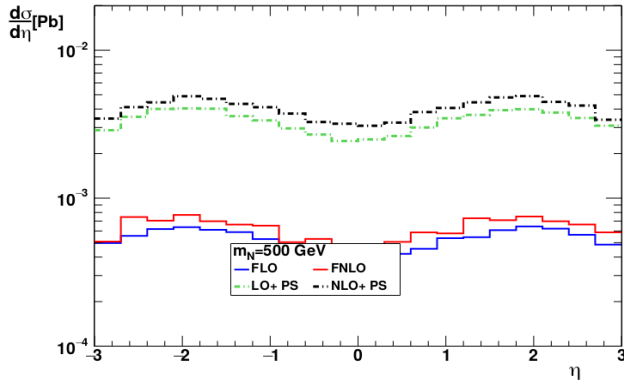


Figure 6.34: Hadronic cross section variation as a function  $\eta$  with  $\sqrt{S} = 13TeV$  in HNM, Dirac neutrino type.

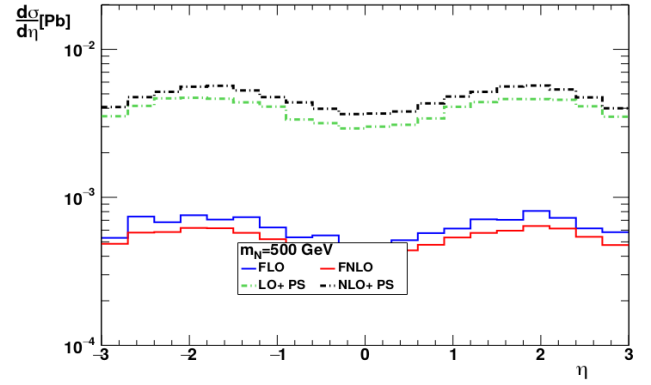


Figure 6.35: Hadronic cross section variation as a function  $\eta$  with  $\sqrt{S} = 13TeV$  in HNM, Majorana neutrino type.

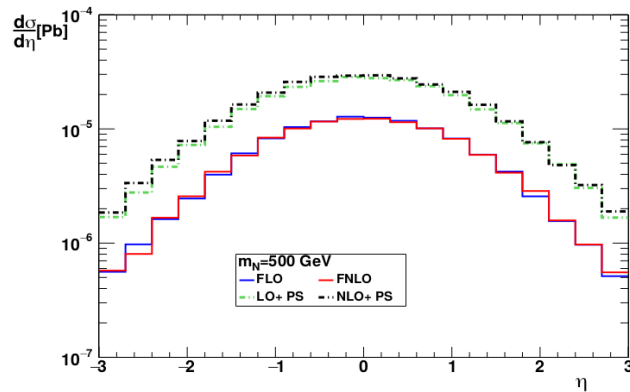


Figure 6.36: Hadronic cross section variation as a function  $\eta$  with  $\sqrt{S} = 13TeV$  in LRSM.

In general, the behavior of the distributions of the hadronic cross section on the pseudo-rapidity  $\eta$



looks as in the previous section (in charge current processes). the main and the important differences are:

- In HNM Dirac case in the previous section (6.3.1 in figure 6.24), the Parton Shower approximation is close to the fixed order, while in this case (figure 6.34) the Parton Shower approximation distributions are larger than the distribution of of Fixed order. We can notice that too in HNM Majorana type of neutrino (figure 6.34).
- The difference between this case and the previous case is that: in charged gauge boson process the produced heavy particle is anti-heavy neutrino  $\bar{N}$  (anti-particle) while in this case the produced is a heavy neutrino  $N$ . In the Majorana type, the output is always a heavy neutrino  $N$  which explains the match between the two cases here (see the figure 6.34 and the figure 6.35).



# General Conclusion

---

The purpose of this master project is the study of heavy neutrinos physics in the BSM models: Heavy neutrino model type Dirac, heavy neutrino model type Majorana and the left right symmetric model in the LHC at NLO and parton shower approximations, using the computations tools `MadGraph`, `Pythia8`, `HIP` and `MadAnalysis` to compute the hadronic cross section and extract the differential distributions.

We dedicated the first part of this work (chapters 2, 3 and 4) to the theoretical part, where in chapter 2, we gave an overview of the Standard Model, we explained how the spontaneous symmetry breaking mechanism (Higgs mechanism) generate the fermions and bosons masses. Also, we discuss some success and failure of the SM. Even with these successes, the SM has many problems, one of it is the absence of the neutrinos masses. Therefore, we mention the necessity of the existence of physics beyond the SM. We have presented two probable models that gives a solution for the absence of the neutrino masses in SM. The first one is the Heavy Neutrino Model, it has been discussed in chapter (3). We notice that in this model we study two type of possible heavy neutrinos Dirac or Majorana where the basic difference is that the Majorana neutrino are the anti-matter of them selves. The second probable Model is the Left Right Symmetric Model which is presented in chapter (4). The common feature in HNM and LRSM is that they predict the existence of new right-chiral type of neutrinos (heavy neutrinos), therefore we have studied the production of the heavy neutrino in those three BSM models.

We dedicated the second part of this work (chapters 5 and 6) to study the production of the heavy neutrinos in three BSM models in proton-proton collision. In chapter (5), We have studied the production of the heavy neutrinos at LO order by studying two types of processes:

- The charged current processes:
  - $p + p \rightarrow W^- \rightarrow e^- + \bar{N}$  (HNM Dirac type).
  - $p + p \rightarrow W^- \rightarrow e^- + N$  (HNM Majorana type).
  - $p + p \rightarrow W_R^- \rightarrow e^- + \bar{N}$  (LRSM).
- The neutral current processes:
  - $p + p \rightarrow Z \rightarrow \bar{\nu}_{e^-} + N$  (HNM Dirac type).
  - $p + p \rightarrow Z \rightarrow \bar{\nu}_{e^-} + N$  (HNM Majorana type).
  - $p + p \rightarrow Z_R \rightarrow \bar{N} + N$  (LRSM).

We have calculated some partonic cross section and decay rates analytically the in charged current processes for HNM Dirac type, the other are almost the same because of that We did not do the calculation. However, We calculated the hadronic cross section for all these processes in the three models for different masses and scales numerically by making use of `MadGraph`. We notices that we have used the UFO model generated by `FeynRules`, and extracted the differential distributions by `MadAnalysis`.

As We mentioned above, one of the purposes of this work is to compare between the heavy neutrinos predicted by three models. We can summarise the main differences in the following points:

- There are new weak mediators in the LRSM ( $W_R$  and  $Z_R$ ) not available in HNM.
- The values of some constants in the vertices between the two models are different.
- In neutral gauge boson processes we note that in HNM the produced particles are antineutrino and heavy neutrino while in LRSM the produced are pair of heavy neutrino.
- If the type of neutrino is a Dirac type, the leptonic number is conserved in all possible processes, but if the type of neutrino is a Majorana type, we should find processes in nature that violate the leptonic number.
- In the first charged gauge boson process, the produced is an anti-heavy neutrino in Dirac case of neutrino while the produced is a heavy neutrino in Majorana case.
- We observe a discrepancy between NLO+PS and LO+PS for the two classes of HNM which was not expected. We observe that in Majorana case the parton shower distributions are larger than the fixed order contributions which is not the case for Dirac type, see Fig. 6.21 and Fig.6.3.1. This point is very important and needs more study since it might help us to know if the heavy neutrinos are of Dirac or Majorana types.

In the final chapter (chapter 6), we have studied the production of the heavy neutrino at HO by studying the same processes at the three models, for the aim of knowing with more details, about the main distinguishing points between HNM and LRSM, and between Dirac type of neutrino and Majorana type. We have discussed first the types of HO corrections from a theoretical perspective. We have given an outlook for the NLO Corrections, Fixed Order and Parton Shower. In the numerical part, we have explained the computational steps that we did with the same previous processes, we studied the differential distributions of the hadronic cross section as a function of transverse momentum  $P_T$ , rapidity  $Y$  and pseudo-rapidity  $\eta$ . We used `madanalysis` to get the numerical results that we use to calculate the histograms of the distributions of the hadronic cross sections, and we used `Root` for plotting the histograms. The comments on histograms it are given in detail. Finally we have given a conclusion about the main differences between our models and the type of neutrino at these higher order computationnelle, and we have given the main differences between FLO, FLO and LO+PS, NLO+PS orders and their impact on the numerical results in our processes at the three models.

# Bibliography

- [1] T. Morii, C. S. Lim and S. N. Mukherjee, *The Physics of the Standard Model and Beyond*, World Scientific Publishing Co. Pte. Ltd (2004)
- [2] Gunion, John F., *Extended Higgs sectors*, 10th International Conference on Supersymmetry and Unification of Fundamental Interactions (SUSY02) 12 (2002) 80-103 [arXiv:hep-ph/0212150]
- [3] T. Morii, C. S. Lim, S. N. Mukherjee, *The Physics of the Standard Model and Beyond*, World Scientific Publishing Co. Pte. Ltd.5 (2004)
- [4] H. Meriem and M. S. Zidi, *Phénoménologie et calcul de précision dans les modèles supersymétriques : production de sleptons au LHC*, Jijel University (2020)
- [5] P. Langacker, *The Standard Model and Beyond*, Series Editors: Brian Foster, Oxford University, UK, (2010) by Taylor and Francis Group, LLC [ISBN 978-1-4200-7906-7]
- [6] D. Parrochia, *Majorana equation and its consequences in physics and philosophy*, History and Philosophy of Physics Publishing (2019) [arXiv:1907.11169v1]
- [7] David o. Caldwell (Ed.), *Current Aspects of Neutrino Physics*, Springer (2001)
- [8] A. Gouvêa, *Neutrino Mass Models*, Ann.Rev.Nucl.Part.Sci.66 (2016) 197-217, <https://www.annualreviews.org/doi/pdf/10.1146/annurev-nucl-102115-044600>
- [9] Atre, Anupama and Han, Tao and Pascoli, Silvia and Zhang, Bin, *The Search for Heavy Majorana Neutrinos*, JHEP 05 (2009) 30 [arXiv:0901.3589]
- [10] Hati, Chandan and Patra et al., *Neutrino Masses and Leptogenesis in Left Right Symmetric Models: A Review From a Model Building Perspective*, Front. in Phys.journal (2018), <https://doi.org/10.3389/fphy.2018.00019>
- [11] J. C. Pati and A. Salam, *Lepton number as the fourth "color"* Phys. Rev. 10 (1974) 275
- [12] Degrande, Celine and Mattelaer et al., *Fully-Automated Precision Predictions for Heavy Neutrino Production Mechanisms at Hadron Colliders*, Phys. Rev. D 94 (2016) 053002 [arXiv:1602.06957]
- [13] E. Daw, *Lecture 7 - Rapidity and Pseudorapidity*, March 23, 2012, [http://www.hep.shef.ac.uk/edaw/PHY206/Site/2012\\_course\\_files/phy206rlec7.pdf](http://www.hep.shef.ac.uk/edaw/PHY206/Site/2012_course_files/phy206rlec7.pdf)
- [14] J.D. Jackson in *High Energy Physics*, Les Houches 1965 Summer School, GORDON AND BREACH Science Publishers (1965), p. 348.
- [15] R. Chahra and M. S. Zidi, *Physique du boson W-prime au LHC: calcul de précision à l'ordre NLO en QCD*, Jijel University (2018)
- [16] K. Ellis, *Precision Perturbative QCD*, lecture in national accelerator laboratory (1973), <https://indico.cern.ch/event/507870/sessions/105735/attachments/1247980/1838806/Precision.pdf>
- [17] Laura Reina, *NLO QCD calculations*, part ICTEQ Summer School (2009), UW-Madison, [https://www.physics.smu.edu/scalise/cteq/schools/summer09/talks/reina/cteq09\\_nlo\\_1.pdf](https://www.physics.smu.edu/scalise/cteq/schools/summer09/talks/reina/cteq09_nlo_1.pdf)
- [18] Campbell, M. John, J. W. Huston and W. J. Stirling, *Hard Interactions of Quarks and Gluons: A Primer for LHC Physics*, Rept. Prog. Phys 70 (2007) 89 [arXiv: hep-ph/0611148]

- [19] S. Catani and M. H. Seymour, *NLO calculations in QCD: A General algorithm*, Nucl. Phys. B Proc. Suppl. 51 (1996) 233-242 [arXiv: hep-ph/9607318]
- [20] Keith Ellis, *QCD for the LHC and the Tevatron*, QCD at the LHC in honor of Bryan Webber September (2010), [https://indico.fnal.gov/event/2444/contributions/76562/attachments/47478/56982/Ellis\\_QCD.pdf](https://indico.fnal.gov/event/2444/contributions/76562/attachments/47478/56982/Ellis_QCD.pdf)
- [21] M. S. Zidi, *NLO QCD corrections to single vector-like top partner production in association with top quark at the LHC*, JHEP 10 (2018) 123, [arXiv: 1805.04972]
- [22] Bauer, Julia, *Prospects for the Observation of Electroweak Top Quark Production with the CMS Experiment*, KIT, Karlsruhe, Dept. Phys.(2010) [doi: 10.5445/IR/1000018393]
- [23] Mattelaer, Olivier and Mitra, Manimala and Ruiz, Richard, *Automated Neutrino Jet and Top Jet Predictions at Next-to-Leading-Order with Parton Shower Matching in Effective Left-Right Symmetric Models*, primary Class hep-ph 10 (2016) [arXiv: 1610.08985]
- [24] FeynRules: <https://feynrules.irmp.ucl.ac.be/wiki/NLOModels>
- [25] J. Alwall and R. Frederix et al, *The automated computation of tree-level and next-to-leading order differential cross sections, and their matching to parton shower simulations*, JHEP 07 (2014) 79 [arXiv: 1405.0301]
- [26] Brdar, Vedran and Helmboldt, Alexander J. and Iwamoto, Sho and Schmitz, Kai, *Type-I Seesaw as the Common Origin of Neutrino Mass, Baryon Asymmetry, and the Electroweak Scale*, PhysRevD 100 (2019)075029 [arXiv: 1905.12634]
- [27] Frederix et al, *Automation of next-to-leading order computations in QCD: The FKS subtraction*, JHEP 10 (2009) 03 [arXiv: 0908.4272]
- [28] rschi, Valentin and Frederix et al *Automation of one-loop QCD corrections*, JHEP 05 (2011) 44 [arXiv: 1103.0621]

---

**Abstract:**

Despite the experimental success of the SM, which predicted the presence of many particles before they were detected in collisions, it is not the ultimate theory since it has many problems like the absence of a neutrinos masses. To solve this problem, many extensions to the Standard Model have been proposed like the Left Right Symmetric Models.

In this work, we focus on two probable models that gives a solution for the absence of the neutrino mass in SM. The first one is the Heavy Neutrino Model and the second one is the Left Right Symmetric Model. The common feature of HNM and LRSM is that they predict the existence of new right-chiral neutrinos of Dirac or Majorana types.

We have studied the production of the heavy neutrino in the three models, where both the charged and neutral current processes have been considered. We computed the variation of hadronic cross section on the heavy neutrino mass and the scales and many differential distributions in the approximations fLO, fNL, LO+PS and NLO+PS by making use of MadGraph and MadAnalysis.

**Keywords:** Standard Model, heavy neutrino, Heavy Neutrino Model, Left Right Symmetric Model, Dirac type of neutrino, Majorana type of neutrino.

---

**Résumé:**

En raison du succès expérimental du modèle standard (SM), c'est l'une des théories les plus importantes de la physique quantique. Il prédit la présence de nombreuses particules avant qu'elles ne soient détectées dans les collisions. Cependant, le modèle standard n'est pas la théorie ultime des particules élémentaires car il a des problèmes fondamentaux comme l'absence d'une masse de neutrinos.

Pour résoudre ce problème, des nombreuses extensions du modèle standard ont été proposées. Nous concentrons sur deux modèles probables qui donnent une solution à l'absence de masse de neutrinos dans le modèle standard, le premier est le modèle de neutrinos lourds (HNM) et le deuxième modèle probable est le modèle symétrique gauche droite (LRSM). La caractéristique commune de HNM et LRSM est qu'ils prédisent l'existence d'un nouveau type de neutrinos de chiralité-droit (neutrinos lourds), c'est pourquoi nous avons étudié la production du neutrino lourd dans les trois modèles.

Nous avons étudié la production du neutrino lourd dans les trois modèles en étudiant deux types de processus (courants neutre et chargé). Nous avons calculé la variation de la section efficace hadronique en fonction de la masse des neutrinos et l'échelle, et les distributions différentielles dans les approximations fLO, fNL, LO+PS and NLO+PS en utilisant MadGraph and MadAnalysis.

**Mots clés:** Modèle standard, neutrino lourd, modèle neutrino lourd, modèle symétrique gauche droite, neutrino de type Dirac, neutrino de type Majorana.

---

**ملخص:**

رغم النجاحات التجريبية للنموذج القياسي (SM) مثل التنبؤ بوجود العديد من الجسيمات قبل اكتشافها في مصادمات الجسيمات، إلا أنه ليس النظرية النهائية فهو يعاني من الكثير من المشاكل مثل غياب كتلة التوتريونات. لحل هذه المشاكل تم اقتراح الكثير من التوسعات لـ SM. في هذا البحث، لقد ركزنا على نموذجين محتملين يقدمان حلاً لغياب كتلة التوتريونات ألا وهما نموذج التوتريونات الثقيلة ونموذج التناظر يمين يسار.

السمة المشتركة لهذين النموذجين هي أنهما يتنبآن بوجود الكثير من التوتريونات الثقيلة. لذلك قمنا بدراسة إنتاج التوتريونات من نوع ديراك ومجورانا عن طريق تفاعلات التيارات المشحونة والمحايدة.

لقد قمنا بدراسة تغير المقطع الفعال الهادروني بدلالة كتلة التوتريون والسلم، كما درسنا العديد من المقاطع الفعالة التفاضلية في التقريبات fLO، fNLO، LO+PS و NLO+PS باستخدام البرامج MadGraph و MadAnalysis.

**كلمات مفتاحية:** النموذج القياسي، التوتريونات الثقيلة، نموذج التوتريونات الثقيلة، نموذج التناظر يمين يسار، توتريونات ديراك ومجورانا.

---